Structural and functional investigation of the phospholipid modulation of KcsA K$^+$ channel (K$^+$ channel of *Streptomyces lividans*)

Dissertation

Zur Erlangung der Würde des Doktors der Naturwissenschaften
des Fachbereichs Biologie, der Fakultät für Mathematik, Informatik und Naturwissenschaften,
der Universität Hamburg

vorgelegt von

Alexander V. Prokofyev

aus St-Petersburg, Russland

Hamburg

2012

Genehmigt vom Fachbereich Biologie
der Fakultät für Mathematik, Informatik und Naturwissenschaften
an der Universität Hamburg
auf Antrag von Professor Dr. O. PONGS
Weiterer Gutachter der Dissertation:
Professor Dr. C. LOHR
Tag der Disputation: 07. Dezember 2012

Hamburg, den 22. November 2012

Professor Dr. J. Fromm
Vorsitzender des Promotionsausschusses
Biologie

Universiteit Utrecht

Lindsay Baker, Ph.D.
Bijvoet Center for Biomolecular Research
Utrecht University, Bloembergen gebouw,
Padualaan 8, 3584 CH, Utrecht, The Netherlands
Telephone: +31(0)-30-253-9929
Fax: +31(0)-30-253-7623
E-mail: L.A.Baker@uu.nl

October 4, 2012
Utrecht, The Netherlands

To whom it may concern:

I, Dr. Lindsay Baker, the undersigned, certify that I am a native English speaker. I have read Alexander Prokofyev's doctoral thesis and have provided the corrections, with respect to English grammar and composition, that should be incorporated into the final thesis. I affirm that the general language of the thesis should be readily understood by any native English speaker.

Sincerely,

Lindsay Baker

Lindsay Baker, Ph.D.

_____

Contents

Contents

_____

Contents

ABSTRACT

Binding of anionic phospholipids to non-annular binding sites of KcsA has been demonstrated with crystallographic and biochemical methods. In my study, I used the combination of electrophysiology, solid-state NMR (ssNMR) spectroscopy and molecular dynamics (MD) simulations to gain further insight into the structural and functional importance of these specific protein-lipid interactions. I observed that single channel properties of KcsA at the steady state conditions strongly depend on the type of anionic phospholipid in the membrane. Both the single channel conductance and open probability (P_O) of the channel were modulated by anionic phospholipids. The single channel conductance was higher in the presence of phosphatidylglycerol (PG) and cardiolipin (CL) in comparison to phosphatidic acid (PA) and phosphatidylserine (PS) at positive voltages, significantly affecting the outward rectification properties of KcsA. This effect correlates with the structure of the phospholipid headgroups rather than their charge. At the same time more negatively charged PA and CL stabilized the open state of KcsA and reduced C-type inactivation of the channel, leading to an increase of overall P_O of KcsA. The maximal P_O of the KcsA was observed for CL, which was the most negatively charged lipid in my study. The ssNMR experiments revealed the structural mechanism of anionic phospholipid modulation of KcsA, suggesting that a strong negative charged anionic phospholipids such as CL stabilize the conductive conformation of the KcsA selectivity filter. Furthermore, in combination with MD simulations the data indicated that extracellular turret region of KcsA plays a significant role in anionic phospholipid – channel interaction. Hence, I propose that interaction of anionic phospholipids with the KcsA turret region induces structural rearrangements within the selectivity filter affecting KcsA function.

1. Introduction

1.1. Ion channels

Ion channels are integral transmembrane (TM) proteins that can open and close to allow ions to cross an impermeable biological lipid membrane along their electrochemical gradient *(Aidley and Stanfield, 1996; Hille, 2001)*. Ion channels play fundamental roles in the functioning of organisms, from bacteria to humans. In excitable cells, ion channels maintain the resting membrane potential and generate the action potential (*Hodgkin and Huxley, 1952*). In non-excitable cells they are involved in many different physiological processes such as cell volume regulation *(Hoffmann, 2011; Niemeyer et al., 2001; Noulin et al., 2001)*, intracellular ionic homeostasis, cell proliferation, intracellular signaling and immune activation (*Cahalan et al., 2001*).

1.2. Potassium channels

Potassium selective channels (K^+ channels) represent the largest and the most diverse group amongst the pore-loop class of ion channels (*Hille, 2001; Kew and Davies, 2010*). In excitable cells, the role of all types K^+ channels are related to stabilization of the resting membrane potential. K^+ channels set the resting potential, keep action potentials short, terminate periods of intense activity, time the interspike intervals during repetitive firing, and generally lower the effectiveness of excitatory inputs on cells *(Hille, 2001; Pongs, 1999)*. K^+ channels are known to modulate neurotransmitter release and to play a role in synaptic plasticity *(Kim and Hoffman, 2008; Watanabe et al., 2002)*. They have an essential role in cardiac excitation-contraction coupling (*Nerbonne, 2000*) and vascular smooth muscle contraction (*Dunn and Nelson, 2010; Longden et al., 2011; Pluger et al., 2000*). K^+ channels are involved in exocytosis (*Kurachi and Ishii, 2004)*, cell proliferation (*Zhang et al., 2012*) and cell volume regulation (*Lang, 2007)*. Malfunction of K^+ channels due to mutations lead to a number of diseases such as long-QT syndromes, episodic ataxia/myokymia, familial convulsions, deafness, Bartter's syndrome, and insulin secretion disorders. In addition, changes in their function have been associated with cardiac hypertrophy and failure, apoptosis and oncogenesis, and various neurodegenerative and neuromuscular disorders (*Huopio et al., 2002; Miller, 2000;*

1

_____

Remedi and Koster, 2010; Sandhiya and Dkhar, 2009; Shieh et al., 2000; Weinreich and Jentsch, 2000). Hence K$^+$ channels are important drug targets.

The diversity of K$^+$ channels is surprisingly large. The genome project revealed over 80 related mammalian genes of subunits of K$^+$ channels, not counting splice variants (*Hille, 2001*). A common underlying structural feature of K$^+$ channels is a so-called pore-lining P-loop containing the highly conserved "signature sequence" TXGYG, which constitutes the K$^+$ selectivity filter *(Heginbotham et al., 1994)*. As K$^+$ channels are tetramers, four copies of the filter motif jointly form the pore (*Hille, 2001; Kew and Davies, 2010).*

The topology of pore-forming K$^+$ channel α-subunits varies from one K$^+$ channel subfamily to another with respect to the number of TM helices (Figure 1.1). There are several broad classes of K$^+$ channels: 2 TM, 4 TM, 6 TM, 7 TM and 8 TM K$^+$ channels *(Alexander et al., 2008; Gutman et al., 2003; Hille, 2001; Kew and Davies, 2010*).

Subunits with two TMs helices connected by a P-loop carrying the "signature sequence" display the simplest architecture within the K$^+$ channel family. This structural core, called the pore-forming region, can be found in all types of K$^+$ channels. 2 TM K$^+$ channel subfamily includes KcsA (*Doyle et al., 1998; Schrempf et al., 1995)* and inward rectifier channels (K$_{ir}$) (*Ho et al., 1993*). 4 TM and 8 TM K$^+$ channels have two pore-forming regions per 4 TM and 8 TM subunit, respectively *(Fink et al., 1996; Ketchum et al., 1995; Lesage et al., 1996a, b; Reid et al., 1996; Wang et al., 1999; Zhou et al., 1995*). Channels with 6 TM domains and one pore-forming region belong to the voltage-gated K$^+$ channel subfamily (K$_v$) (*Armstrong, 2003; Kamb et al., 1987; Noda et al., 1984; Papazian et al., 1987; Pongs, 1999; Pongs et al., 1988; Pongs and Schwarz, 2010*). K$_v$ channels are the predominant class within the K$^+$ channel family. 6 TM K$^+$ channels also include Ca^{2+}-activated potassium channels of small (SK channels) and intermediate (IK channels) conductance *(Alexander et al., 2008; Fanger et al., 1999; Félétou, 2009; Joiner et al., 1997; Xia et al., 1998*). The 7 TM K$^+$ channel subfamily includes Ca^{2+}-activated K$^+$ channels of high conductance (BK channels). These channels have one pore-forming region per 7 TM subunit *(Adelman et al., 1992; Alexander et al., 2008; Atkinson et al., 1991; Félétou, 2009; Latorre and Brauchi, 2006*).
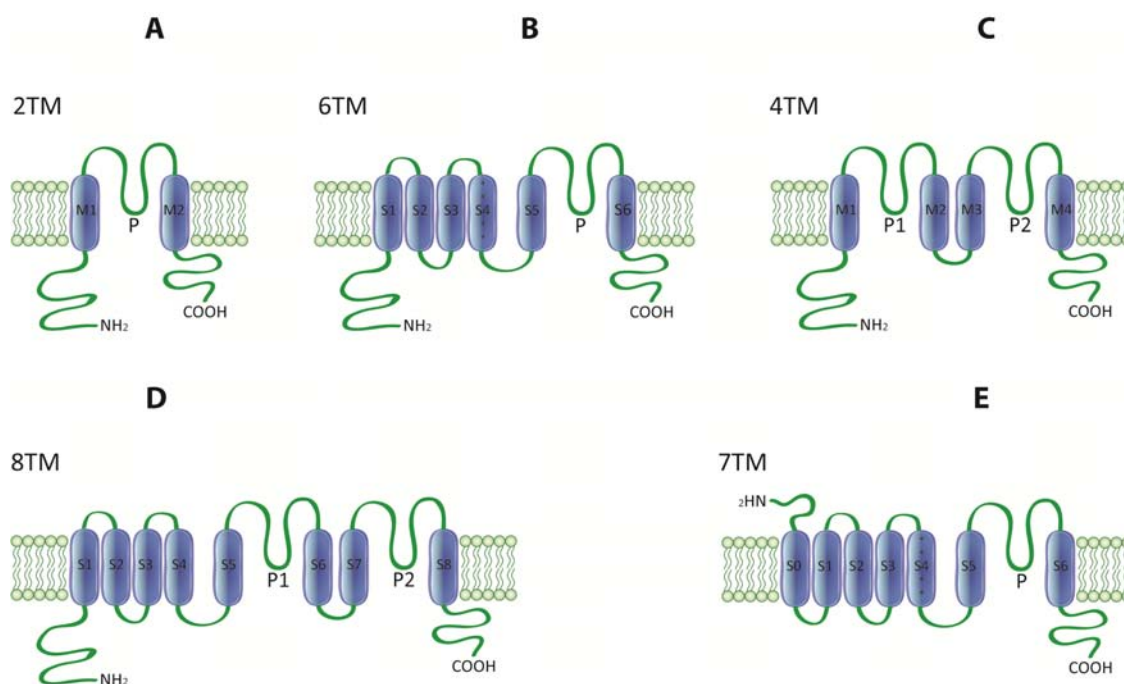
Figure 1.1. Membrane topology and main features of potassium channel subtypes. Schematic representation of the membrane topology of (**A**) 2 TM - KcsA and K_{ir} channels; (**B**) 6 TM - K_v channels, SK_{Ca} and IK_{Ca} channels; (**C**) 4 TM - TWIK, TASK, TREK; (**D**) 8 TM - Yeast TOK channels and (**E**) 7 TM - BK_{Ca} channels. Only one subunit of the tetrameric structure is shown. TM helices are numbered S1-S6 and M1-M4. P - pore loop. The extracellular side is towards the top.

1.3. KcsA potassium channel

KcsA is a proton-activated K^+ potassium channel from *Streptomyces lividians* (*Blunck et al., 2006; Cordero-Morales et al., 2006a; Cordero-Morales et al., 2006b; Cuello et al., 1998; Doyle et al., 1998; Gross et al., 1999; Liu et al., 2001b; Perozo et al., 1998, 1999b; Schrempf et al., 1995; Zhou et al., 2001a; Zhou and MacKinnon, 2003; Zhou et al., 2001b*). The KcsA protein is 160 amino acid residues in length and belongs to the 2 TM K^+ channel family (Figure 1.1 and 1.2). Because KcsA can be expressed in high quantity in *E. coli*, the KcsA channel is an ideal candidate for structural analysis. Indeed, the discovery of KcsA opened a new era in structural investigation of K^+ channels.

_____
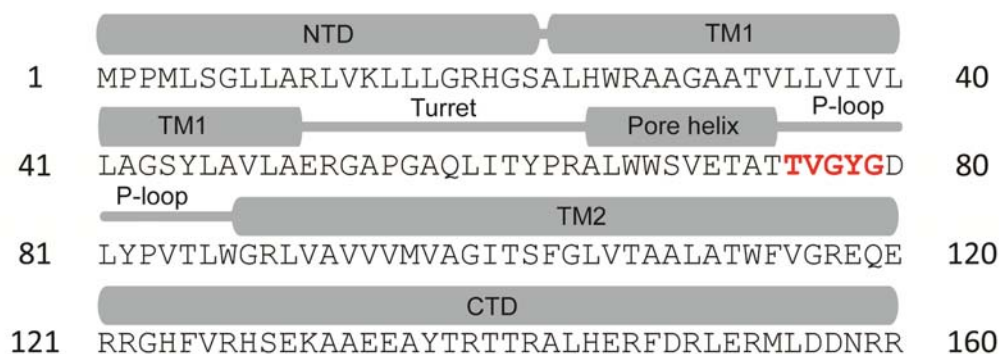
Figure 1.2. Sequence alignment of KcsA potassium channel. Gray boxes and lines above the alignment indicate the membrane topology of the channel. NTD - N-terminal cytoplasmic domain; TM1 - outer helix; P-loop - pore loop; TM2 - inner helix; CTD - C-terminal cytoplasmic domain. Selectivity filter residues corresponding to the K$^+$ channel " signature sequence" are indicated in red.

1.4. KcsA potassium channel structure

1.4.1. Structural basis of ion permeation and selectivity

The last fifteen years have seen remarkable progress in our understanding of K$^+$ channel structure. The first high-resolution atomic structure of a K$^+$ channel was of KcsA, solved by X-ray crystallography in 1998 (*Doyle et al., 1998*). The crystal structure of KcsA at 3.2 Å revealed that four KcsA subunits form an inverted Teepee-like structure with a central ion conduction pathway (Figure 1.3). Each subunit contains two TM α-helices termed the inner (TM2) and outer (TM1) helices. The TM1 outer helix crosses the membrane from inside to outside and is connected to a short extracellular loop (turret), which re-enters the membrane as a short pore helix (P-helix). The P-helix runs half way through the membrane and then tilts and continues as a pore loop (P-loop), that forms the narrow selectivity filter. The pore loop is connected to the TM2 inner helix which crosses the membrane from outside to inside (Figure 1.3) (*Doyle et al., 1998; MacKinnon, 2003, 2004; Zhou et al., 2001b).* It has been found that the overall length of KcsA pore is 45 Å. The diameter of the pore, on the other hand, varies. From inside, the pore begins as a tunnel 18 Å in length (the internal pore) and then opens into a wide cavity (10 Å across) near the middle of the

_____

membrane. Then it narrows again at the selectivity filter (*Doyle et al., 1998*). The X-ray structure revealed that the main chain carbonyl oxygen atoms of the K^+ channel "signature sequence" (TXGYG) line the selectivity filter to form K^+ binding sites, which mimic a K^+ hydration shell to selectively permit the coordination of K^+ ions within the selectivity filter. This interaction provides an explanation for the high selectivity of K^+ channels (*Doyle et al., 1998*).

The K^+ ion coordination within the selectivity filter was not directly visualized, but indirectly inferred by replacing K^+ with Cs^+. A later high-resolution X-ray structure (2 Å) (Zhou et al., 2001b) provided a more detailed view on the mechanism of the ion-coordination chemistry inside the selectivity filter of K^+ channel. It has been shown that within the selectivity filter carbonyl oxygen atoms of K^+ channel "signature sequence" form a very similar square antiprism around each K^+ binding site, so that each binding site is a cage formed by eight oxygen atoms. The cage of carbonyl oxygens perfectly mimick the water molecules of the K^+ hydration shell (*MacKinnon, 2003, 2004; Morais-Cabral et al., 2001; Zhou et al., 2001b)*. The crystal structure of KcsA was a large step forward in our understanding of the structural principles of ion channel biophysics and opened a new era in ion channel research. Figure 1.3 summarizes the structural components of KcsA revealed by high-resolution X-ray crystallography (Figure 1.3).
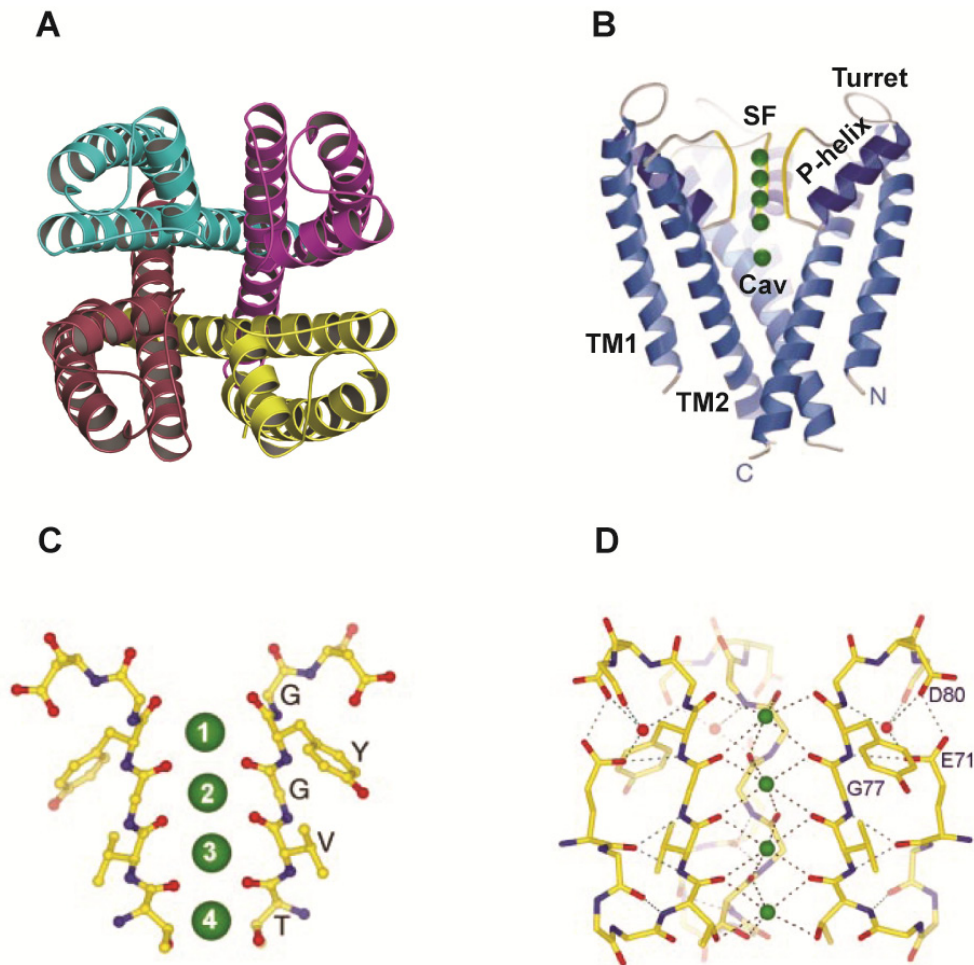
Figure 1.3.Summary of the structural components of KcsA potassium channel. **A** - Tetrameric organization of KcsA. Ribbon representation illustrating the KcsA tetramer viewed from the extracellular side. The four subunits are distinguished by color. **B** - Schematic ribbon diagram of three subunits of KcsA. The forth subunit in the front has been removed. The selectivity filter (SF), outer helix (TM1), inner helix (TM2), pore helix (P-helix), turret and cavity (Cav) are indicated. K$^+$ ions are drawn in green. SF is additionally indicated in yellow **C** - Close-up view of the selectivity filter in ball-and-stick representation, with the front and back subunits removed. The four K$^+$ ions are numbered to indicate the location of binding sites in the selectivity filter; position 1 is closest to the extracellular solution and position 4 is closest to the cavity. Key amino acids forming the selectivity filter are shown (GYGVT). **D** - K$^+$ ion-coordination chemistry inside the selectivity filter. Each K$^+$ ion is located at the centre of eight oxygen atoms. The forth subunit in the front has been removed. This figure is adapted from *Doyle et al., 1998; Morais-Cabral et al., 2001* and *Zhou et al., 2001.*

_____

1.4.2. Structural mechanism of KcsA gating

1.4.2.1. Activation gate and pH sensor

Although X-ray crystallography provided answers to principal questions about the mechanisms of ion permeation and selectivity of K$^+$ channels, the structural basis of channel gating remained unresolved. Using electron paramagnetic resonance (EPR) significant structural rearrangements have been observed within the C-terminal end of the KcsA TM2 helix upon channel activation *(Liu et al., 2001a; Perozo et al., 1999a; Perozo et al., 1998)*. Their data was in good agreement with MacKinnon`s X-ray data, which showed that the inner helix bundle composed of the C-terminal end of TM2 helices of KcsA may serve as the activation gate of the channel. By comparison of the crystal structure of KcsA in its closed conformation with the crystal structure of the MthK potassium channel in the open conformation, it was proposed that the TM2 helix tilts at residue G99, allowing activation gating in the K$^+$ channel pore (*Jiang et al., 2002*). Perozo and coworkers, using EPR spectroscopy, showed that upon activation the inner KcsA helices rotate in a counterclockwise direction away from the permeation pathway, thus opening the conduction pathway *(Liu et al., 2001a; Perozo et al., 1999b)*.

A serious drawback of earlier structural studies was that the KcsA structure was solved without the N-terminal (NTD) and C-terminal (CTD) cytoplasmic domains. NTD and CTD are approximately 23 and 39 amino acid residues in length, respectively (Figure 1.2). These domains are involved in K$^+$ channel regulation (*Goudreau and Stock, 1998; Sheng and Kim, 1996)*. The first structure of full-length KcsA was derived from EPR spectroscopical studies (*Cortes et al., 2001*). Based on these and previous X-ray data obtained by MacKinnon, a three-dimensional (3D) model of full-length KcsA was constructed. According to this model, NTD of KcsA forms an α-helix located at the membrane-water interface, while CTD forms a right-handed four-helix bundle that extends 40–50 Å towards the cytoplasm. Functional analysis suggested that CTD is attached to the activation gate of the channel and is involved in the modulation of the pH-dependent gating mechanism of KcsA (*Cortes et al., 2001*), but CTD plays no essential role in ion permeation properties. Later it was shown that CTD plays an essential role in the tetrameric stabilization of KcsA

_____

(*Kamnesky et al., 2012; Molina et al., 2004; Raja, 2010a*). Finally, the crystal structure of full-length KcsA was solved in its closed and open conformations with resolutions of 3.8 Å and 3.9 Å, respectively (*Uysal et al., 2011; Uysal et al., 2009*). In order to be able to crystallize full-length KcsA, synthetic antigen-binding fragments (Fabs) were used as crystallographic chaperones (*Uysal et al., 2011; Uysal et al., 2009*). The structure of the full-length KcsA reveals a well-defined, 4-helix bundle that projects 70 Å into the cytoplasm in good agreement with previous EPR study (*Cortes et al., 2001*).

Based on the structural data combined with site-directed mutagenesis and single-channel recordings, the molecular mechanism of pH-dependent gating of KcsA was revealed (*Thompson et al., 2008*). It was proposed that a network of ionizable residues (H25, E118, E120, R121 and R122) near the intracellular bundle crossing forms pH-sensitive inter- and intra-subunit interactions to serve as the pH sensor of the KcsA gate. At neutral pH, interaction between these residues stabilizes the closed conformation of the channel (via salt bridges). Lowering the pH disrupts the network of the amino acid side chains and leads to channel opening (*Thompson et al., 2008*). Figure 1.4 summarizes the structural features of KcsA activation gating described in this chapter.
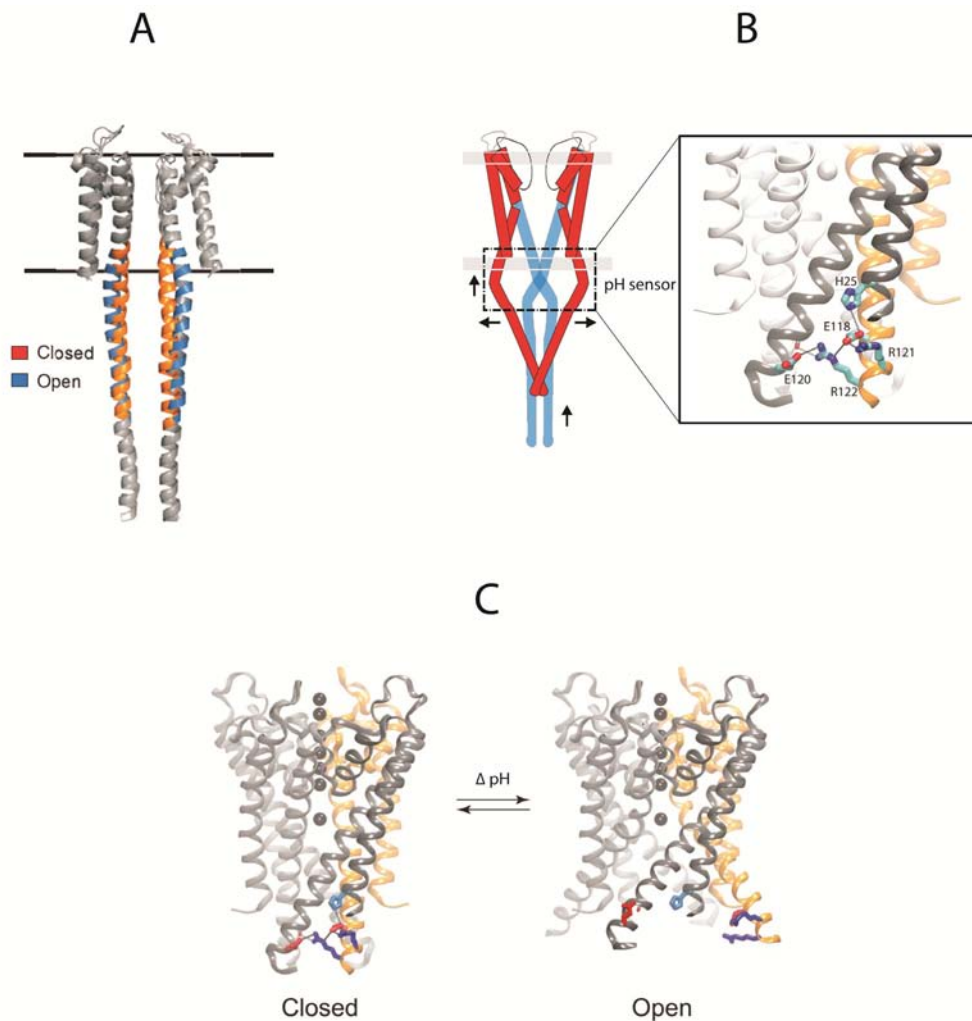
Figure 1.4. The structural mechanism of the pH-dependent KcsA activation. **A** - The crystal structure of full-length KcsA in its closed (orange) and open conformation (blue). The black lines represent the approximate limits of the membrane. **B** - A cartoon model describing the conformational transitions of the activation gate and C-terminal domain in full-length KcsA upon activation. Two KcsA subunits are shown for simplicity. Blue model represents a closed state and red model represents open state. The gray bars demonstrate the approximate limits of the membrane. The network of residues that can be protonated (H25, E118, E120, R121 and R122) involved in the pH sensor of KcsA is shown in the insert. Two adjacent subunits (dark gray and orange) are shown in the foreground with key residues of the pH-sensor indicated: E118, E120, H25, R121 and R122. **C** - 3D model of the transitions between closed and open states during KcsA activation. The closed-to-open transition illustrates that the intersubunit interactions within the pH sensor, which stabilize the closed state at neutral pH (left), are destabilized in acidic pH, allowing key residues (H25, E118, E120, R121 and R122) to move far from each other in the open state (right). Two adjacent subunits (dark gray and orange) are shown in the foreground with key residues highlighted: E118 and E120 (red), H25 (cyan), R121 and R122 (blue). This figure is adapted from *Thompson et al., 2008* and *Uysal et al., 2011*.

_____

1.4.2.2. Coupling of KcsA activation and inactivation

Several structural and functional studies revealed that KcsA activation and inactivation processes are structurally coupled during gating. As mentioned above protonation of particular amino acid residues within the activation gate of the channel leads to channel opening. However electrophysiological recordings at the single channel level demonstrated a low open probability (P_O) at steady state at low pH (*Cuello et al., 1998; Heginbotham et al., 1999; Meuser et al., 1999*). One of the reasons may be due to channel inactivation. Indeed, two types of K^+ channel inactivation are known: fast N-type inactivation, the so-called "ball and chain" inactivation that occurs when the N-terminal domain of the channel blocks the pore domain (*Aldrich, 2001; Armstrong, 1969; Hoshi et al., 1990)* and slow C-type inactivation, which traditionally has been associated with a gate at the selectivity filter (*Hoshi et al., 1991; Kiss et al., 1999; Liu et al., 1996; Lopez-Barneo et al., 1993*).

Electrophysiological recordings at the macroscopic level demonstrated large transient currents upon activation of KcsA by lowering the pH from 7.5 to 4.0 (*Cordero-Morales et al., 2006b*). The transient currents were characterized by a relatively fast activation time course (τ~10-20 ms) followed by a slow exponential decay with a single time constant of approximately 1.5 s. It has been proposed that this slow decay after activation is related to a C-type inactivation process *(Cordero-Morales et al., 2006b*). A detailed structural and functional investigation of KcsA uncovered the molecular mechanism of C-type inactivation of the KscA channel (*Cordero-Morales et al., 2006b; Cordero-Morales et al., 2011; Cuello et al., 2010a; Cuello et al., 2010b)*. It has been shown that the entry into the C-type inactivated state is directly linked to the strength of the hydrogen-bond (H-bond) interaction between residues E71 and D80 behind the selectivity filter, and is allosterically triggered by rearrangement of the inner bundle gate upon KcsA activation. It was also shown that another H-bond pairing between residues W67 and D80 determines the rate and extent of KcsA C-type inactivation. Disruption of this interaction in KcsA also leads to modulation of the inactivation process (*Cordero-Morales et al., 2011*). In summary, KcsA C-type inactivation gating is governed by a multipoint H-bond network formed by the triad W67-E71-D80 (Figure 1.5). This type of H-bond network has been found in other members of the K^+ channel family, such as *Shaker* and Kv1.2 channels (*Kiss et al., 1999; Liu et al., 1996; Loots and Isacoff, 1998*).

_____

Therefore, this H-bond network triad plays a crucial role in the dynamics and conformational stability of the selectivity filter of the K$^+$ channel family (*Cordero-Morales et al., 2011*).
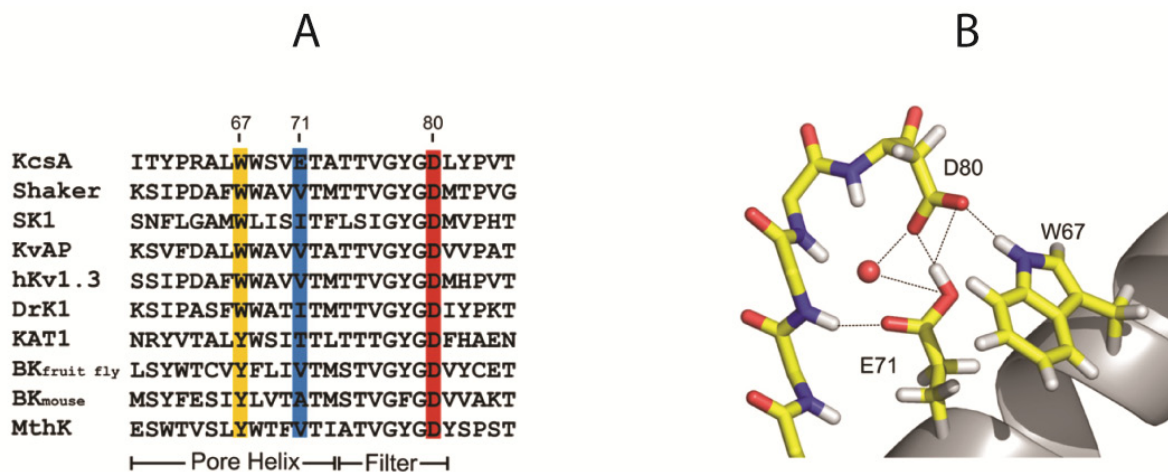
Figure 1.5. The structure of the H-bond network surrounding the K$^+$ channel selectivity filter. **A** - Sequence alignment of KcsA and a series of K$_v$ channels. The key residues of a multipoint hydrogen-bond network triad are indicated (E71-D80-W67). **B** - High-resolution crystal structure of the KcsA selectivity filter and hydrogen-bond network triad. The interactions between E71, D80, W67 and the pore helix of the selectivity filter of KcsA are shown. This figure is adapted from *Cordero-Morales et al., 2011.*

1.5. Solid-state NMR investigation of the KcsA potassium channel

In contrast to X-ray crystallography, solid-state nuclear magnetic resonance (ssNMR) allows further determination of the structure of membrane proteins (MPs) in non-crystalline lipid bilayer environment (*Bertini et al., 2012; Renault et al., 2010*). Furthermore, ssNMR spectroscopy also provides information on protein dynamics (*Ader et al., 2010*). Moreover, this approach gives great flexibility in terms of sample preparation. Many different parameters can be tested such as ionic strength, temperature, pH and lipid composition.

A series of ssNMR spectroscopical studies was conducted on the KcsA-Kv1.3 channel, a chimera between KcsA and Kv1.3 (*Ader et al., 2010; Ader et al., 2009; Ader et al., 2008; Lange et al., 2006a; Lange et al., 2006b; Schneider et al., 2008; Zachariae et al., 2008*). The chimera was constructed by exchanging, within the turret-region of KcsA, 13 amino acid residues by the homologous ones of Kv1.3

(Figure 1.6), corresponding to the scorpion toxin-binding site in the Kv1.3 turret region (*Legros et al., 2000; Legros et al., 2002).* Using ssNMR two-dimensional correlation experiments, the assignments of key residues in the selectivity filter and activation gate of KcsA-Kv1.3 have been obtained. It has been shown that the conformation of the essential structures of this K^+ channel such as selectivity filter, activation gate and turret region can be probed by ssNMR with high resolution (*Ader et al., 2010; Ader et al., 2009; Ader et al., 2008; Lange et al., 2006a; Lange et al., 2006b; Schneider et al., 2008; Zachariae et al., 2008*). It was shown that transition of KcsA-Kv1.3 in proteoliposomes from pH 7.5 to pH 4.0 is associated with distinct structural changes within the pore, corresponding to C-type inactivation. The selectivity filter adopted a nonconductive, collapsed structure while the activation gate was still in its open conformation. Taken together, the ssNMR studies provided a detailed description of the KcsA-Kv1.3 pore domain in a lipid environment for two distinct conformations or channel states, respectively: closed-conductive and open-inactivated (collapsed) (*Ader et al., 2009; Ader et al., 2008*). Structural characteristics of the two channel conformations are illustrated in Figure 1.6.

It is important to note that the conformation of the open-conductive state of the KcsA in lipid bilayer is still unknown. This is most likely due to the very short life time of this channel state during KcsA gating (*Cordero-Morales et al., 2006b*). Determination of the structure of the open-conductive state of a K^+ channel in the lipid environment is, however, crucial for understanding of the molecular mechanism of K^+ channel gating.
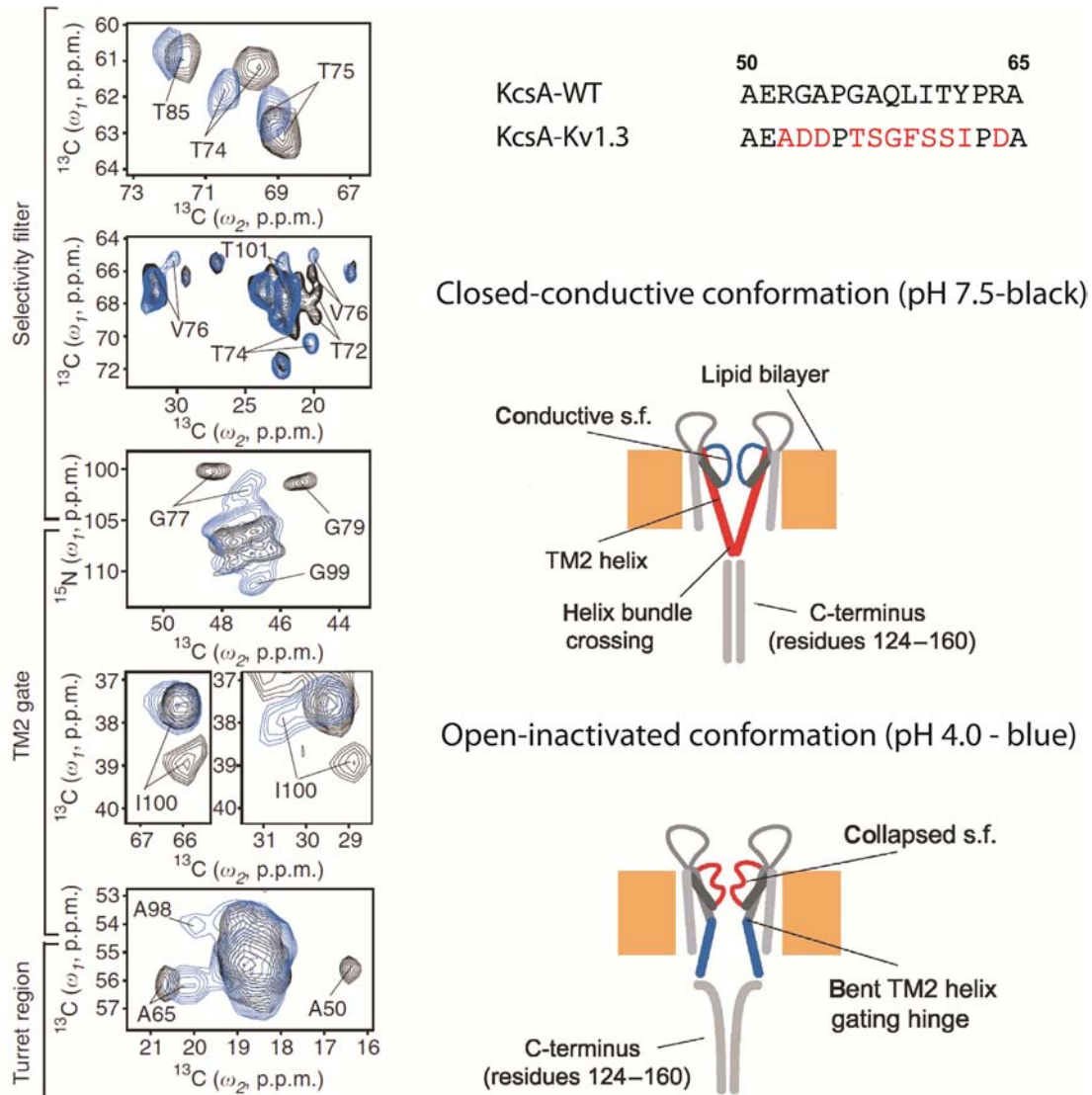
Figure 1.6. The conformation of a K+ channel pore in the lipid bilayer probed by ssNMR spectroscopy. Ss-NMR experiments was conducted on the KcsA-Kv1.3 chimeric potassium channel exposed to pH 7.5 (black spectrum on the left) and pH 4.0 (blue spectrum on the left). The mutations introduced in KcsA to create the chimeric KcsA-K$_v$1.3 channel are indicated in red on the upper panel of figure. The cartoon representation of closed-conductive and open-collapsed conformations on the channel are shown. This figure is adapted from *Ader et al., 2009; Ader et al., 2008.*

1.6. Electrophysiological description of KcsA gating

Functional analysis of KcsA gating by means of electrophysiological approaches has been reported in several studies (*Chakrapani et al., 2011; Chakrapani et al., 2007a, b; Cordero-Morales et al., 2006a; Cordero-Morales et al.,*

2006b; Cuello et al., 1998; Heginbotham et al., 1998; Heginbotham et al., 1999; Irizarry et al., 2002; LeMasurier et al., 2001; Schrempf et al., 1995). In order to detect the currents conducted by KcsA, the channel has to be expressed in _E.coli_, purified and reconstituted into a lipid bilayer. KcsA can be reconstituted into giant liposomes, which are big enough for electrophysiological studies using the patch-clamp technique. Both macroscopic and single channel recording can be performed. Alternatively, KcsA channel activity can be investigated at the single channel level using planar lipid bilayer techniques. For this approach, the protein has to be reconstituted in small unilamellar vesicles (SUV) at a low protein-lipid ratio. Then the SUV is fused with the planar lipid bilayer.

In the planar lipid bilayer studies it has been shown that KcsA is activated by protons (_Cuello et al., 1998_) acting from the intracellular side of the channel (_Heginbotham et al., 1998_). Investigation of KcsA gating properties at the macroscopic level shows that both activation and deactivation gating of KcsA is pH-dependent and voltage-independent (_Chakrapani et al., 2007a_). Upon activation by a rapid shift to acidic pH, KcsA transiently mediates large currents. They activate with a relatively fast time course (τ_{act}~10-20 ms) followed by a slow exponential decay (τ_{inact} ~ 1.5 s). The current decay reflects a C-type inactivation, which, as mentioned above, is associated with structural perturbations in the selectivity filter of the channel. Although KcsA is not a voltage-gated potassium channel, KcsA inactivation is modulated by transmembrane voltage, such that τ_{inact} increases at more negative potentials (_Chakrapani et al., 2007a; Cordero-Morales et al., 2006a)._

At the single channel level KcsA demonstrates a very low P_O at steady-state (from <0.03 to 0.2) _(Cuello et al., 1998; Heginbotham et al., 1999; Meuser et al., 1999)_. EPR measurements indicated that the KcsA-activation gate is open under these conditions (_Perozo et al., 1999b_). Hence, KcsA gating at steady state is controlled by the dynamics of the inactivation gate near or at the selectivity filter. The consequence is that single channel activity of KcsA, measured in lipid bilayer experiments, likely corresponds to an equilibrium between opened and inactivated KcsA channel states (_Chakrapani et al., 2007a, b; Cordero-Morales et al., 2006a; Cordero-Morales et al., 2006b_). Several non-conductive (inactivated) states are observed in single channel recordings obtained in lipid bilayer experiments: two short-lived inactivated states (I_f and I_i) and one long-lived inactivated state (I_s). It was proposed that recovery from inactivation follows a pathway that connects inactivated

_____

states to the closed resting state of the KcsA channel, that comes with an opened inactivation and a closed activation gate. Most likely, the closed-conductive conformation of KcsA at steady state conditions is only detectable at pH-values where the KcsA activation gate becomes effectively deprotonated (*Chakrapani et al., 2007a; Cordero-Morales et al., 2006b*). Figure 1.7 summarizes these conclusions in form of a gating scheme, which combines activation and inactivation gating of the KcsA channel.
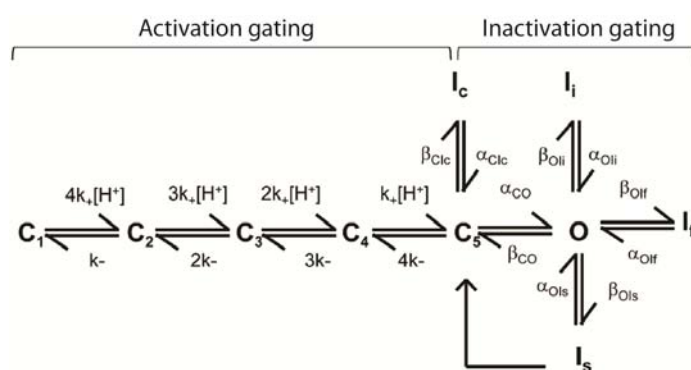
Figure 1.6. The kinetic scheme representing KcsA gating. The discrete closed (**C**), open (**O**) and inactivated (**I**) states are shown. The lines connecting states represent transitions from one state to another with corresponding transition rate constants. This figure is adapted from *Chakrapani et al., 2007b.*

The gating scheme assumes that the KcsA channel enters the opened state from the fully protonated closed state (C_5). It is also assumed that KcsA can enter the inactivated state from C_5 closed state. The gating scheme does not take into account the modal gating behavior of the KcsA channel, which has been demonstrated in electrophysiological studies (*Chakrapani et al., 2011; Chakrapani et al., 2007b*). KcsA modal gating behavior is characterized by existence of three discrete P_O modes: high-P_O, low-P_O and flickery P_O mode. The KcsA channel is able to switch from one mode to another, apparently in a stochastic manner. (*Chakrapani et al., 2011; Chakrapani et al., 2007b*). Modal gating is not unique to KcsA but also has been observed in different K^+ channels, in which time-dependent single-channel activity can switch abruptly between periods of high and low P_O, under fixed experimental conditions (*Cooper and Shrier, 1989; Dreyer et al., 2001; Singer-Lahat et al., 1999; Stuhmer et al., 1988*).

All three P_O-modes of KcsA gating are observed in giant proteoliposomes (GPL) in single channel recordings using the patch-clamp method in the *inside-out*

_____

configuration (*Chakrapani et al., 2011; Chakrapani et al., 2007b*). KcsA channels recorded from planar lipid bilayers appear to gate predominantly in the low-P_O mode (*Heginbotham et al., 1999; LeMasurier et al., 2001; Marius et al., 2012; Marius et al., 2008; Meuser et al., 1999; Rotem et al., 2010; Splitt et al., 2000*). It is likely that preparations for electrophysiological investigations differ in lateral pressure and membrane curvature, factors known to modulate K^+ channel gating and tetramer stability (*Schmidt and MacKinnon, 2008; van den Brink-van der Laan et al., 2004a, b*). Potentially, the lipid environment is another determinant of P_O mode. Indeed, experiments where all three regimes of KcsA gating were detectable have been conducted on KcsA reconstituted in asolectin, while in planar lipid bilayer experiments mixtures of synthetic phospholipids such as PG, PC, PE or native bacterial membranes were used (*Heginbotham et al., 1999; LeMasurier et al., 2001; Marius et al., 2012; Marius et al., 2008; Meuser et al., 1999; Rotem et al., 2010; Splitt et al., 2000*).

Taking into consideration the gating scheme of KcsA described above and the modal gating behavior, steady state P_O of the KcsA channel is defined by the following equation:

$$P_o = \frac{\sum_{i=1}^{n}[O_i]}{\sum_{i=1}^{n}[O_i] + \sum_{j=1}^{n}[I_j] + [C]}$$

Equ. 1.1

O in equation 1.1 is the opened state duration, *i* is the number of opened states, **I** is the non-conductive inactivated state duration, *j* is the number of non-conductive inactivated states, **C** is the non-conductive closed state duration (**C** corresponds to fully protonated **C₅** closed state in the gating scheme).

1.7. Functional and structural aspects of KcsA-lipid interactions

It has become increasingly evident that the lipid bilayer not only provides a medium for transmembrane protein folding and diffusion, but with its dynamic heterogeneity, participates actively in the fine control of membrane protein function (*Escriba et al., 2008; Lee, 2004; Marius et al., 2008; Raja et al., 2007; Tillman and Cascio, 2003; Xu et al., 2008; Zimmerberg and Gawrisch, 2006).* It has been shown that the function of certain membrane proteins depends significantly on the particular lipid environment (*Lee, 2004; Tillman and Cascio, 2003*). It was recently shown that

membrane phospholipids might affect the K^+ channel function (*Heginbotham et al., 1998; Schmidt et al., 2006; Valiyaveetil et al., 2002; Xu et al., 2008*). Membrane lipids are typically divided into two classes: *annular* lipids, which form a shell around the membrane proteins and show relatively weak binding affinity; and *non-annular* lipids which bind to specific site(s) of protein with high affinity (*Lee, 2004; Tillman and Cascio, 2003*). Crystallographic data have shown the presence of co-purified diacylglycerol (DAG)-fragment in KcsA crystals, tightly bound in a shallow groove between adjacent channel-subunits (*Valiyaveetil et al., 2002*). It was proposed that the origin of this co-purified DAG is negatively charged phosphatidylglycerol (PG), which is one component of the lipids of the bacterial membrane. Functional studies with a Rb^+ flux assay showed that negatively charged anionic phospholipids are crucial for KcsA function (*Heginbotham et al., 1998; Valiyaveetil et al., 2002*). Also, anionic phospholipids such as phosphatidylglycerol (PG), phosphatidic acid (PA) and cardiolipin (CL) drastically increase tetrameric stability of KcsA. Moreover, the effect of PA and CL on KcsA tetrameric stability was more pronounced than that of PG (*Raja, 2010b, 2011; Raja et al., 2007; van Dalen et al., 2002*). An electrophysiological study of KcsA in planar lipid bilayers revealed that PG stabilizes the open state of the channel and simultaneously increases single channel conductance (*Marius et al., 2008*). It has been proposed that the effect of negatively charged PG on KcsA is associated with charge-specific interaction of PG with a *non-annular* binding site located between two positively charged Arg - residues: Arg 64 and Arg 89 from adjacent KcsA subunits (*Marius et al., 2012; Marius et al., 2008)* This hypothesis was in good agreement with previous structural and molecular dynamics (MD) simulation studies (*Deol et al., 2006; Valiyaveetil et al., 2002)*. The specific binding of anionic phospholipids with KcsA via *non-annular* binding sites has been shown using fluorescence quenching analysis. However, affinity of anionic phospholipids to the KcsA extracellular *non-annular* lipid binding site shows no correlation to the head group charge (*Marius et al., 2005*). This might indicate that anionic phospholipid interaction with KcsA depends not only on charge-specific interactions as it was proposed (*Deol et al., 2006; Marius et al., 2012; Marius et al., 2008*). Moreover, a recent electrophysiological study showed no effect of PG on KcsA P_O (*Rotem et al., 2010*).

Several studies implicated Arg 64 and Arg 89 in *non-annular lipid* binding. Perozo and co-workers showed that replacement of Arg 64 by aliphatic alanine leads

_____

to an increase in KcsA P_O and reduced C-type inactivation (*Cordero-Morales et al., 2006b*). Marius and co-workers, on the other hand, showed that replacement of Arg 64 by leucine, which has a larger aliphatic side chain than alanine, leads to a decrease in KcsA P_O (*Marius et al., 2012*). The results suggest that lipid – Arg 64 interaction has an important influence on KcsA P_O. Other positively charged restudies might also be involved in lipid modulation of the pore domain, for example Arg 52 in the turret region of the channel. At the intracellular membrane-protein interface of KcsA, N-terminal positively charged amino acid residues as well as a C-terminal Arg - cluster may be engaged in interactions with lipids (*Raja, 2011*).

Although negatively charged anionic phospholipids are crucial for KcsA channel activity, the mechanism of KcsA modulation by anionic phospholipids still remains unresolved, due to a lack of electrophysiological and corresponding structural studies. In particular it is unclear whether head group charge, head group structure, or both play a key role in modulation of KcsA channel activity. Also, it is unclear whether the effects of anionic phospholipids on KcsA gating and single channel conductance share a common mechanism or reflect distinct mechanisms. This can be resolved by a detailed structural analysis of KcsA modulation by different anionic phospholipids in combination with corresponding electrophysiological analysis of single channel activity in different anionic phospholipid environment. Due to the high similarity between the KcsA pore domain and that of other K channel family members, investigation of KcsA modulation by anionic phospholipid will help to understand the role of this modulation for other K^+ channel pores.

Therefore, my work focuses on studying how the KcsA potassium channel, prototype of K^+ channel pore, is modulated by different types of anionic phospholipids at the functional and structural level. In my study using electrophysiological approaches in combination with ssNMR and MD simulations I tried to answer the following questions:

1. How do different anionic phospholipids modulate KcsA function?
2. What is the structural basis of this modulation?
3. Does the KcsA extracellular turret region, which contains positively charged Arg-residues, play a role in anionic phospholipid modulation?

2. Materials and methods

2.1. Chemicals, enzymes and reagents

All chemicals used in this study were purchased from Merck (Germany), Roche (Germany), Roth (Germany), Sigma & Aldrich (Germany). Enzymes, kits and molecular weight standards were obtained from Clontech (France), Invitrogen (Germany), MBI Fermentas (Germany), Stratagene (Agilent technologies, Germany) and Qiagen (Germany).

2.2. Molecular biology

2.2.1. *E. coli* strains, clones and vectors

E. coli strains XL1-Blue and M15 were used for DNA amplification and expression of KcsA and KcsA-Kv1.3 potassium channels, respectively. Detailed descriptions of these bacterial strains are shown in the table below.

	E. coli strain (manufacturer)	Genome Description	Purpose
1	XL1-Blue (Stratagene)	*E. coli* K-12, recA1, endA1, gyrA96, thi-1, hsdR17, supE44, relA1, lac [F'proAB, lacqZΔM15, Tn10 (Tet^r)],	DNA amplification
2	M15 (Qiagen)	Nal^S, Str^S, Rif^S, Thi$^-$, Ara$^+$, Gal$^+$, Mtl$^-$, F$^-$, RecA$^+$, Uvr$^+$, Lon$^+$	Protein expression

Several commercial vectors (Qiagen, Germany) were used for recombinant protein expression. KcsA and KcsA-Kv1.3, which were used in the electrophysiological experiments, were expressed in pQE70 with C-terminal Histidine (His) tags. In order to express KcsA for solid-state NMR (ssNMR) experiments the pQE60 expression vector with C-terminal His-tag was used. This type of expression vector was more efficient for protein expression in M9 minimal media. A description of the expression vectors is provided in the table below.

_____

	Plasmid/Vector (Qiagen)	Marker	Purpose
1	pQE70	Amp^r	Expression of KcsA and KcsA-Kv1.3 for electrophysiological experiments
2	pQE60	Amp^r	Expression of [^{13}C-^{15}N]-labeled KcsA for ssNMR experiments

The DNA constructs based on the pQE70 vector encoding KcsA and KcsA-Kv1.3 potassium channels were previously generated in the Institute for Neural Signal Transduction (Hamburg, Germany). The KcsA pQE60 construct was generated previously in the NMR Spectroscopy Research Group (Utrecht, Netherlands).

2.2.2. Bacterial media and solutions used to grow *E. coli* cells

LB medium:	Tryptone	10 g/l
	Yeast Extract	5 g/l
	NaCl	10 g/l
SB medium:	Peptone	25 g/l
	Yeast Extract	15 g/l
	NaCl	5 g/l
M9 minimal medium:		see Chapter 2.3.2.
LB agar:	Tryptone	10 g/l
	Yeast Extract	5 g/l
	NaCl	10 g/l
	Agar	15 g/l
Kanamycin stock solution:	Kanamycin	50 mg/ml
Ampicillin stock solution:	Ampicillin	100 mg/ml
Tetracycline stock solution:	Tetracycline	25 mg/ml
TFB-1, pH 5.8:	RbCl	100 mM
	$MnCl_2$	50 mM
	CH_3CO_2K	30 mM
	$CaCl_2$	10 mM
	Glycerol	15%
TFB-2, pH 6.8:	MOPS	10 mM
	RbCl	10 mM
	$CaCl_2$	75 mM
	Glycerol	15%

2.2.3. Preparation of competent *E. coli* cells

Commercial strains (XL1-Blue and M15) described above were used to prepare competent cells. The required bacteria cells were spread from a glycerol commercial stock on a LB plate containing a suitable antibiotic (25 µg/ml of kanamycin and tetracycline for M15 and XL1-Blue cells, respectively) and incubated overnight at 37°C. The next morning a single colony was picked up and transferred to 10 ml of LB containing a suitable antibiotic. The culture was grown overnight at 37°C. The overnight grown culture was added to 100 ml pre-warmed LB medium containing

_____

the respective antibiotic in a 250 ml flask. The culture was incubated in the shaker at 37°C until an OD_{600} of 0.5 was reached, following which the culture was cooled down on ice and centrifuged 5 min at 4000 g at 4°C. The supernatant was discarded and pelleted cells were gently resuspended in cold TFB-1 buffer and incubated on ice for 90 min. The suspension was centrifuged for 5 min at 4000 g at 4°C. The supernatant was discarded and pelleted cells were resuspended in cold TFB-2 buffer. The suspension was spread in aliquots of 100 µl in sterile microcentrifuge tubes and frozen via liquid nitrogen. Competent cells were stored at -70°C until usage.

2.2.4. Transformation of competent cells

An aliquot of competent cells was thawed on ice. Cells were gently resuspended and DNA solution (1-10 ng) was added to the cells. The tube with cells was incubated on ice for 20 min and then transferred to 42 °C water bath for 1.5 min. The cells were incubated afterwards another 5 min on ice and then 50-100 µl aliquots were plated out on LB-agar plates containing suitable antibiotics (25 µg/ml kanamycin and 100 µg/ml ampicillin for M15 competent cells and 25 µg/ml tetracycline and 100 µg/ml ampicillin for XL1-Blue competent cells). The LB-agar plates were incubated overnight at 37°C.

2.3. Over expression and purification of KcsA and KcsA-Kv1.3 channels

In this study, two expression approaches have been used: a fermenter expression method to express KcsA and KcsA-Kv1.3 potassium channels, which have been used for electrophysiological experiments, and expression in shake-flask to produce [^{13}C-^{15}N]-labeled KcsA for structural investigations by ssNMR spectroscopy. The conditions of the expression for the fermenter and shake-flask methods had to be optimized separately. Conditions tested included expression temperature, glucose concentration, aeration level, induction time, concentration of the induction substance and duration of the expression.

_____

2.3.1. Over expression KcsA and KcsA-Kv1.3 using the fermenter method

A single colony of transformed M15 competent cells with the appropriate pQE70 construct used to inoculate 500 ml of SB-Amp-Kan medium containing 0.5 % glucose. The preculture was incubated overnight at 25 ºC in the shaker at 120 RPM. The overnight preculture was used to inoculate the fermenter (Biostat-B, B-Braun, Germany) after OD_{600} measurement. 8 L of expression culture in SB-Amp-Kan medium containing 0.5 % of glucose was stirred in the fermenter at 500 RPM and oxygenated by the air flow. The temperature was kept at 30 ºC during the expression by an integrated thermoregulation system. The pH level of the expression culture was kept at 7.5 by adding 1M NaOH with the integrated pH regulation system included pH sensor and peristaltic pump. The fermenter set-up is shown on the Figure 2.1.
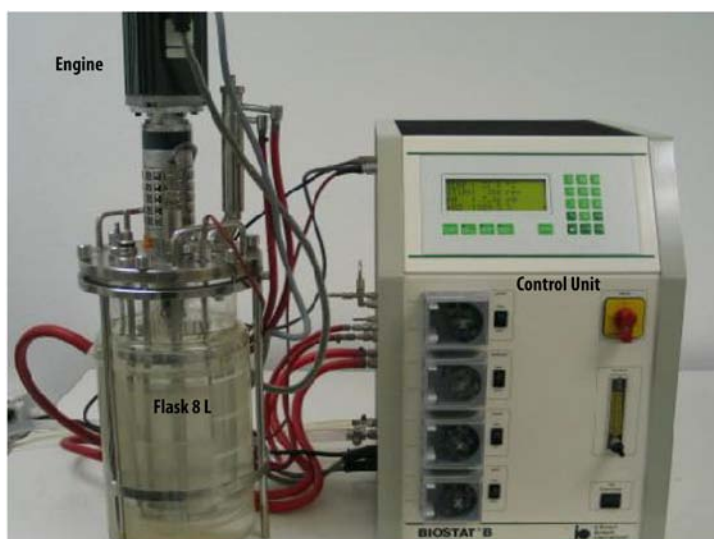
Figure. 2.1. Biostat-B Fermentror (B-Braun, Germany). The main parts are indicated: engine for stirring, 8 L glass flask for the expression culture and control unit containing thermoregulation, air regulation and pH control systems.

The protein expression was induced by the addition of 1 mM isopropyl β-D-1-thiogalactopyranoside (IPTG) at an OD_{600} of 0.8, following which the protein was expressed for 5 h. The final OD_{600} value of the expression culture varied from 9-12 depending on the construct. Cells were harvested by centrifuging at 7000 g for 20 min at 4 ºC and stored at -80 ºC until required.

2.3.2. Over expression of [^{13}C-^{15}N]-KcsA using shake-flask expression

For the ssNMR studies membrane protein samples has to be isotope-labeled and prepared in milligram quantities. In my study, KcsA was uniformly [^{13}C, ^{15}N] - labeled by introducing in the minimal M9 medium containing isotope-enriched sugars and ammonium salts as the exclusive nutrition sources. In order to achieve the required protein yield the type of DNA vector harboring KcsA protein, expression temperature, glucose concentration, aeration level, induction time, IPTG concentration and duration of the expression were optimized.

A single colony of M15 competent cells transformed with pQE60 KcsA was used to inoculate 10 ml LB-Amp-Kan medium containing 0.2 % glucose. After 4-5 h of incubation at 37 $^{\circ}$C 30 µl of this preculture were used to inoculate 500 ml LB-Amp-Kan medium containing 0.2 % glucose. This culture was incubated overnight in the shaker at 250 RPM at 25 $^{\circ}$C. Next morning, when the OD$_{600}$ of ~ 2 was reached, the cells were pelleted at 3000 g for 20 min and resuspended in M9-Amp-Kan minimal medium containing 0.2% of ^{13}C glucose and 0.05% of ^{15}N ammonium chloride. The M9 culture was incubated in the shaker at 250 RPM at 37 $^{\circ}$C for another 30 min. The protein expression was induced by adding of 0.6 mM IPTG. After 6 h of the expression the cells were harvested at 7000 g at 4 $^{\circ}$C and stored at -80 $^{\circ}$C until usage. The composition of M9 minimal medium is shown below.

M9 minimal medium:

Na$_2$HPO$_4$	6 g/l
KH$_2$PO$_4$	3 g/l
NaCl	0.5 g/l
^{15}NH$_4$Cl	0.5 g/l
MgSO$_4$ (1M)	2 ml/l
CaCl$_2$ (0.1M)	100 µl/l
FeSO$_4$ (0.01M)	1 ml/l
^{13}C-Glucose	2 g/l
Thiamine (0.5 mg/ml)	10 ml/l
Kanamycin (50 mg/ml)	0.5 ml/l
Ampicillin (100 mg/ml)	1 ml/l
Micronutrients (1000x)	1 ml/l
Vitamin Supplements (1000x)	1 ml/l

Micronutrients stock (1000x):

Ammonium molibdate	$3 \cdot 10^{-6}$ M
Boric acid	$4 \cdot 10^{-4}$ M
Cobalt chloride	$3 \cdot 10^{-5}$ M
Copper sulphate	$1 \cdot 10^{-5}$ M
Manganese chloride	$8 \cdot 10^{-5}$ M
Zinc chloride	$1 \cdot 10^{-5}$ M

Vitamin Supplements stock (1000x):

D-Biotin	1.0 g/l
Choline Chloride	0.5 g/l
Folic Acid	0.5 g/l
Myoinositol	1.0 g/l
Nicatinamide	0.5 g/l
Panthotenic Acid	0.5 g/l
Pyridoxal HCl	0.5 g/l
Riboflavin	50 mg/l
Thiamine HCl	0.5 g/l

2.3.3. Purification of KcsA, [^{13}C^{15}N]-KcsA and KcsA-Kv1.3

The protein purification strategy for all KcsA potassium channels in this study was similar and included cell lysis by means of French press, solubilization of the membrane fraction in a buffer containing detergent, Ni^{2+}-affinity chromatography, SDS-PAGE and protein concentration measurement.

2.3.3.1. Cell lysis

A cell pellet from -80 ºC with the appropriate type of KcsA potassium channel was gently defrosted on ice. The cell pellet was resuspended in lysis buffer (see page 28) containing a protein inhibitor cocktail (Complete EDTA free, Roche). Lysozyme (BioChemika) and DNAase (Benzonase, Merck) were added to the mixture to make the cell lysis more efficient. The suspension of cells was lysed using a French press (3 cycles at 20,000 psi). The cell lysate was centrifuged at 100,000 g for 3 h at 4 ºC in the ultracentrifuge (Optima L90K, Beckman Coulter, USA). The supernatant was removed and the pellet was resuspended in solubilization buffer (see page 28)

_____

containing 40 mM n-Decyl-β-D-Maltopyranoside (DM). The mixture was placed in two 50 ml tubes and incubated with stirring overnight in the cold room. Next morning, the solubilized solution was centrifuged at 68,000 g for 40 min at 4 °C in the ultracentrifuge to spin down the unsolubilized membrane fraction. The supernatant fraction containing solubilized protein was kept until use in a protein purification procedure.

2.3.3.2. Protein purification using Ni^{2+}-affinity chromatography

The protein purification strategy in this study is based on the presence of C-terminal hexahistidine (6xHis) tag on the protein which binds with high affinity to the Ni^{2+}-NTA resin (Figure 2.2.A).
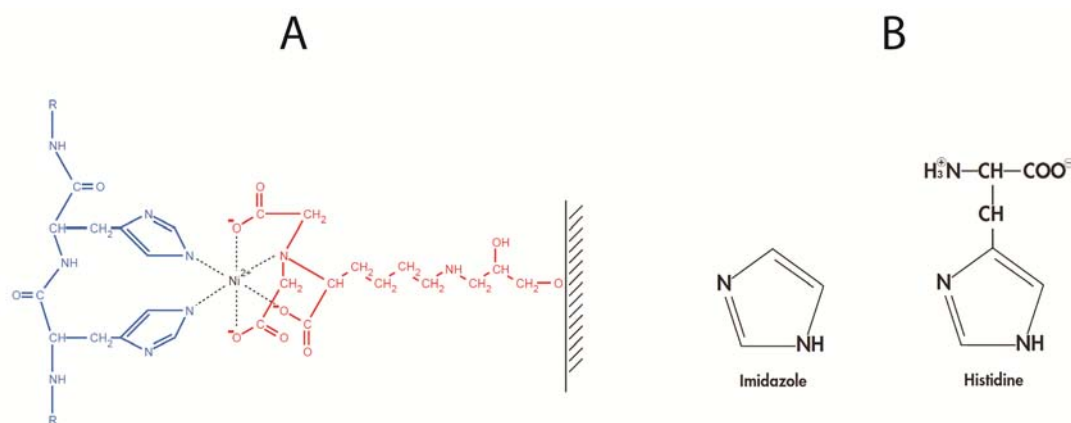
Figure 2.2. Basis principals of Ni^{2+}-affinity chromatography. **A** - Interaction between neighboring residues in the 6xHis tag and Ni^{2+}-NTA matrix (Qiagen, Germany). Histidine residues are shown in blue. Ni^{2+}-NTA matrix is shown in red. **B** - Chemical structures of histidine and imidazole.

Ni^{2+}-NTA superflow resin (3 ml resin per 50 ml tube of solubilized protein) was added to the solubilized membrane fraction and incubated for 90 min in the cold room on a rotational shaker. 20 mM imidazole was added in order to prevent nonspecific protein binding, because imidazole has a similar chemical structure to histidine and therefore they compete for the same Ni^{2+}-binding sites on the Ni^{2+}-NTA resin (Figure 2.2.B). After that the sample was placed in a 25 ml disposable column (Bio-Rad, Germany) and washed with 200 ml of wash buffer containing 30 mM imidazole to remove endogenous proteins with histidine residues that interact with the Ni^{2+}-NTA

matrix. Finally, protein was eluted with 10-20 ml of elution buffer (see page 28) containing 400 mM of imidazole. Purified proteins were analyzed by SDS-PAGE and the protein concentration was determined (see Chapter 2.3.3.4). The purified protein was kept at 4 ⁰C prior to proteoliposomal reconstitution (see Chapter 2.4).

2.3.3.3. SDS polyacrylamide gel electrophoresis (SDS-PAGE)

Pre-cast polyacrylamide NuPAGE 4–12% Bis-Tris gels (1.0-mm thick, 10-well) (Invitrogen, Germany) were used for the SDS-PAGE. Purified protein (10 µl) was mixed with SDS sample buffer (10 µl) and loaded into the gel after 20 min of boiling at 95 ⁰C (or without boiling). The gel was placed in an electrophoresis chamber (Invitrogen, Germany) and the electrophoresis was performed at 180 mV in running buffer for 50 min. Novex protein standard (Invitrogen, Germany) was used as a molecular weight reference. The gel was stained for 3 h in the staining buffer (SimplyBlue™ SafeStain, Invitrogen, Germany) at room temperature then destained in water.

2.3.3.4. Determination of the protein concentration

The concentration of purified protein was determined in two ways: by ultraviolet absorption spectroscopy at 280 nm and using Bradford`s assay (*Bradford, 1976*).

1) <u>Ultraviolet absorption spectroscopy at 280 nm</u>

Proteins display a characteristic ultraviolet (UV) absorption spectrum around 280 nm, predominantly from aromatic amino acids such as tyrosine and tryptophan (*Methods in Enzymology, 2009*). According to Beer-Lambert's law, the absorbance of the protein is a linear function of the protein molar concentration, path length, and also the protein extinction coefficient:

$$A = \varepsilon * c * l$$

where ε is the molar extinction coefficient, c the molar protein concentration and l is the path length in cm. The molar extinction coefficient at 280 nm of KcsA potassium channel is 34,850 $M^{-1} * cm^{-1}$ (*Marius et al., 2008*).

2) <u>Bradford`s assay</u>

The Bio-Rad protein assay kit (Bio-Rad, Germany), which is based on the method of Bradford, was used to estimate the protein concentration. A dye reagent was prepared by diluting one part of the dye reagent concentrate in four parts of water and filtered through 0.45 µm filter (Roth, Germany). The protein (50 µl) was mixed with the dye reagent (2.5 ml) and the mixture was incubated for 5 min at room temperature. The blank sample contained 50 µl of elution buffer with 4 mM DM. The absorbance was measured at 595 nm against a blank. In order to estimate the protein concentration a calibration curve was measured using several dilutions of bovine serum albumin (BSA) standards varying from 0.2 to 1.5 mg.

2.3.3.5. Solutions for protein purification

<u>Lysis buffer:</u>

150 mM KCl
50 mM MOPS
Complete (Protease inhibitor, Roche); 1 tablet/100 ml
Lysozyme (BioChemika); 10 mg/100 ml
DNAase (Benzonase, Merck), 20 µl/100 ml
pH 7.0

<u>Solubilization buffer:</u>

150 mM KCl
100 mM NaP buffer
40 mM DM
20 mM Imidazole
Lysozyme (BioChemika); 10 mg/100 ml
DNAase (Benzonase, Merck), 20 µl/100 ml
pH 7.8

<u>Wash buffer:</u>

150 mM KCl
100 mM NaP buffer
4 mM DM
30 mM Imidazole
pH 7.8

<u>Elution buffer:</u>

150 mM KCl
100 mM NaP buffer
4 mM DM
400 mM Imidazole
pH 7.8

_____

2.4. Reconstitution of KcsA, [^{13}C^{15}N]-KcsA and KcsA-Kv1.3

The protein was reconstituted into liposomes as follows. Imidazole was removed from the eluates using PD-10 desalting column (GE Health care) containing Sephadex G-25. The column was equilibrated with 6-7 column volumes of the reconstitution buffer (see page 30) and 2.5 ml of purified protein was placed into the column. The flow-through was discarded and the protein was eluted with 3.5 ml of the reconstitution buffer. The required phospholipids (Avanti Polar Lipids, USA) were dissolved in a solvent composed of chloroform and methanol at 2:1 v/v ratio. The phospholipid mixture (see page 30) was dried under the nitrogen stream and the remaining solvent was removed under vacuum for 2 h. The dried phospholipids were resuspended in the reconstitution buffer containing 4 mM DM and the solution was mixed on the vortexer and sonicated in a bath sonicator (Branson-1510, Bransonic, USA). When the phospholipids were homogeneously resuspended, protein was added to the phospholipid mixture to give a protein/lipid mass ratio of 1:100 and 1:1000 for macroscopic and single channel measurements, respectively, and a protein/lipid molar ratio of 1:100 for samples used in ssNMR experiments. The mixture was incubated for 2 h at room temperature on the rotation shaker. Proteoliposomes were formed upon detergent removal by addition of washed Bio-Beads (Merck, Germany) (1 ml of Bio-Beads per 33 mg of DM) and the mixture was incubated for 2 h at rotation conditions. The Bio-Beads were then removed by filtration of the suspension of proteoliposomes through a 25 ml disposable column (Bio-Rad, Germany). Proteoliposomes for the planar lipid bilayer experiments were split into 250 µl aliquots, flash frozen via liquid N$_2$ and stored at -80 ºC until usage. Proteoliposomes for the macroscopic current measurement and ssNMR experiments were centrifuged at 100,000 g at 4 ºC in the ultracentrifuge. The supernatant was discarded and proteoliposomes were resuspended in the required buffer and centrifuged again at the same conditions. This procedure was repeat twice. Pelleted proteoliposomes were stored at 4 ºC until use.

_____

Solutions for reconstitution:

Reconstitution buffer: 450 mM KCl
                                                          10 mM HEPES
                                                          pH 7.4

Chloroform-methanol solution: Chloroform
                                                          Methanol
                                                          2:1 v/v ratio

Phospholipids in chloroform-methanol solution: DOPC:DOPG = 7:3
                                                          DOPC:DOPG = 3:7
                                                          DOPC:DOPA = 3:7
                                                          DOPC:DOPS = 3:7
                                                          DOPC:CL = 3:7
                                                          molar ratio

2.5. Macroscopic recording of KcsA using patch clamp technique

Macroscopic recordings of KcsA were performed on giant proteoliposomes using standard patch clamp technique. An aliquot (10-30 µl) of proteoliposomes with KcsA was placed on glass slides pretreated with poly-l-lysine in small petri dish. The proteoliposome sample was dried in a desiccator under vacuum overnight at 4 $^\circ$C. Next morning, the dried proteoliposome sample was rehydrated by adding 20-30 µl of rehydration buffer (see page 31). The sample was kept at room temperature and giant proteoliposomes were formed in 2-3 h. The petri dish containing giant proteoliposomes was filled with recording buffer (see page 31) and placed under an inverted light microscope Axiovert 405M (Carl Zeiss MicroImaging, Germany). The gigaseal was formed using a borosilicate glass patch pipette (GB 150-10, Science products, Germany) connected to a micromanipulator Patchman (Eppendorf AG, Germany). After gigaseal formation, the pipette containing a patch of membrane was pulled out to establish the *inside-out* mode. The KcsA was activated by fast change of pH (from 7 to 4) using a piezzo-driven double barrel perfusion system (SF-77B, Warner Instrument Corporation, USA). Macroscopic currents were recorded under symmetrical 150 mM KCl solutions. All measurements were performed at room temperature. Pipette resistances were 1–2 MΩ. Sampling rates were 1 kHz. Recordings and data acquisition were performed using an EPC-9 patch clamp

amplifier (HEKA Electronics, USA) and Patch Master software (HEKA Electronics, USA). Data analyses were performed with Igor Pro (Wave Metrics, USA). A schematic representation of the patch clamp set-up is shown on the Figure 2.3.

Figure 2.3. The scheme of the patch clamp set-up for the macroscopic recordings of KcsA in *inside-out* mode. The basic components, such as double barrel perfusion system, patch pipette, recording electrode and voltage-clamp amplifier are indicated. R_f - feedback resistance. H - headstage (pre-amplifier). The membrane patch containing KcsA potassium channel is shown inside of the patch pipette.

The compositions of the rehydration and recording buffers are shown below:

Rehydration buffer: 150 mM KCl
                                                     0.1 mM EDTA
                                                     0.01 mM CaCl2
                                                     5 mM HEPES
                                                     pH 7.0

Recording buffer pH 7.0:   150 mM KCl
                                                     10 mM HEPES

Recording buffer pH 4.0:   150 mM KCl
                                                     10 mM Succinic acid

2.6. Planar lipid bilayer electrophysiology

Planar lipid bilayer electrophysiology allows investigation of the purified ion channel proteins in artificial lipid membranes at the single molecule level, which provides information about ion channel function and its role in membrane transport and cell physiology (*Miller, 1986*). In this method, ion channel proteins are

reconstituted into the artificially formed planar bilayer composed of required lipids, allowing electrophysiological measurements to be conducted in a precisely controlled environment *(Miller, 1986)*.

2.6.1. Planar lipid bilayer set-up

In this study, single channel recordings of KcsA and KcsA-Kv1.3 potassium channels were performed on a planar lipid bilayer set-up. The set-up consists of several parts including a patch clamp amplifier (EPC10USB, HEKA Electronics, USA) for a signal acquisition, computer with a software for the data acquisition and processing and lipid bilayer control unit (Ionovation Compact, Ionovation, Germany), which has an integrated Faraday chamber, perfusion system to control precisely solution environment both inside and outside of the ion channel and some other essential components, such as a recording chamber where the lipid bilayer is formed and recording electrodes. The simplified electrical scheme of the planar lipid bilayer set-up in shown on the Figure 2.4.
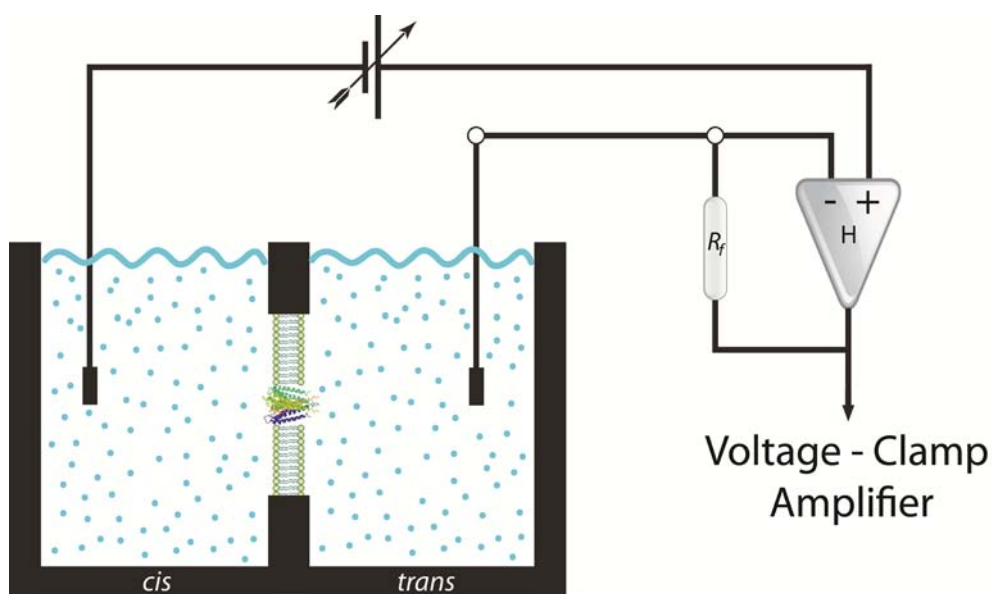

Figure 2.4.The scheme of the planar lipid bilayer set-up. The basic components are shown. Recording chamber (black) contains *cis* and *trans* compartments, filled by recording solutions (blue). The lipid bilayer containing KcsA potassium channel is located in the orifice between *cis* and *trans* sides. The electrodes are placed into recording chamber. The reference electrode is inserted into *cis* compartment. The recording electrode is placed into *trans* compartment. The electrodes are connected to the voltage-clamp amplifier (EPC10USB HEKA Electronics, USA) via headstage (pre-amplifier) (H). R_f - feedback resistance.

2.6.2. Formation of the lipid bilayer

The required phospholipids were dissolved in chloroform and methanol at a 2:1 v/v ratio to give a final phospholipid concentration of 100 mg/ml. This stock phospholipid solution was kept at -20 °C unlit use. In order to prepare a lipid bilayer sample, required amount of stock phospholipid solutions was mixed at the desired molar ratio (the phospholipid composition of the lipid bilayer samples is shown in the Table 2.1). 50 µl of the phospholipid mixture was placed in 200 µl glass tube and dried under vacuum for 30 min. Dried phospholipids were dissolved in 100 µl of *n*-decane and mixed on a vortexer. The final phospholipid concentration in the lipid bilayer sample was 50 mg/ml. The sample was kept at room temperature throughout the experiment. The compositions of the phospholipid mixtures are shown in Table 2.1.

The phospholipid composition of the lipid bilayers at molar ratio
DOPC : DOPG = 7 : 3
DOPC : DOPG = 3 : 7
DOPC : DOPA = 3 : 7
DOPC : DOPS = 3 : 7
DOPC : CL = 3 : 7

Table 2.1. The phospholipid composition used for the preparation of the lipid bilayer sample. DOPC - 1,2-dioleoyl-*sn*-glycero-3-phosphocholine; DOPG - 1,2-dioleoyl-*sn*-glycero-3-phospho-(1'-*rac*-glycerol); DOPA - 1,2-dioleoyl-*sn*-glycero-3-phosphate; DOPS - 1,2-dioleoyl-*sn*-glycero-3-phospho-L-serine; CL - bovine heart cardiolipin.

The formation the lipid bilayer was performed according to the *painting technique* (*Mueller et al., 1962*). Both *cis* and *trans* chambers (Figure 2.4) were filled with saline solutions. The surface around the hole was first pretreated by a drop of *n*-decane and dried. The lipid bilayer sample (1-3 µl) was applied on top of the solution in the *cis* chamber and the level of the solution in the *cis* chamber was lower and raised and the lipid bilayer was formed.

The formation of the lipid bilayer was monitored by the optic control system (Figure 2.5) and electrically by observation of the high resistance gigaseal formation with characteristic transient capacitance currents. The quality of the lipid bilayer was estimated visually by the optic control system and by means of the capacitance measurement. Lipid bilayers with irregular shape or/and with capacitance outside the range of 50-80 pF were not used in the experiments.
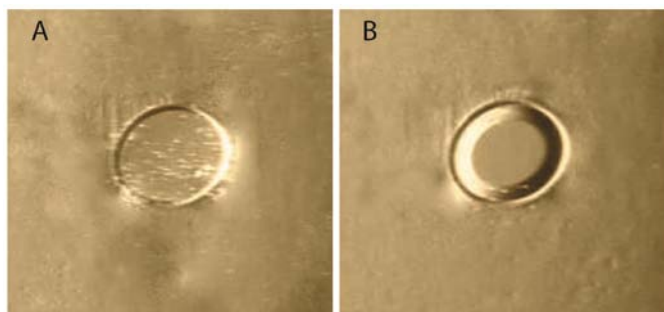
_____

Figure 2.5. Visual control of the lipid bilayer formation. A - unordered lipid across the 200 μm microhole (left); **B** - the planar lipid bilayer (right)

2.6.3. Incorporation of the channel into the lipid bilayer

The incorporation of the ion channel into lipid bilayer membrane is one of the limiting step in the planar lipid bilayer electrophysiology. Several parameters may affect the incorporation procedure. Moreover, conditions which are perfectly suitable for a particular type of the ion channel may be unsuitable for another once. Therefore conditions for successful incorporation of the particular ion channel need to be optimized.

It this study the incorporation of KcsA and KcsA-Kv1.3 into lipid bilayers was obtained by fusion of proteoliposomes carrying the channel into the planar lipid bilayer under osmotic gradient conditions (*Miller, 1986*).

A sample of frozen proteoliposomes with the channel was thawed at room temperature and mixed on the vortexer. The sample was passed through an extruder with a 200 nm polycarbonate membrane in order to form small unilamellar proteoliposomes. The sample was kept on ice until use and discarded after experiment.

After bilayer formation, proteoliposomes (5-10 μl) were added into *cis* compartment. To promote the fusion of proteoliposomes with the lipid bilayer, an osmotic gradient between the *cis* and *trans* compartments was established. The *trans* and *cis* chambers contained 20 mM KCl and 250 mM KCl, respectively. In this case, water flows into vesicles which come close to lipid bilayer and contact it. As a result of the water flow, the vesicles swell and fuse with the lipid bilayer (Figure 2.6). The fusion process was further enhanced by intensive stirring of the *cis* compartment via a small magnetic stirrer. Since the proteoliposomes and planar lipid bilayer contained

negatively charged anionic phospholipids, addition of micromolar levels of Ca^{2+} also increased the rate of fusion. When the channel was successfully incorporated in the lipid bilayer the fusion process was stopped by addition of EDTA to immobilize Ca^{2+}, with subsequent removal of the osmotic gradient by the perfusion system. The combination of the conditions described above allowed keeping well controlled rate of fusion proteoliposomes with the planar lipid bilayer in the experiment.
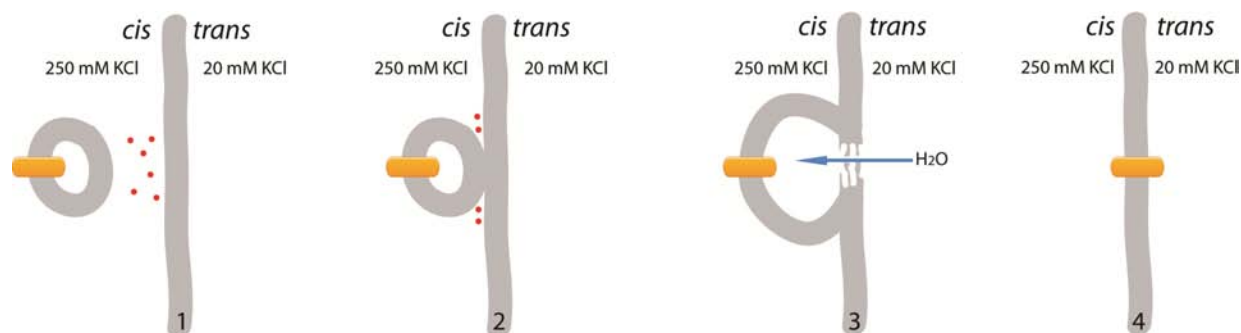

Figure 2.6. Schematic diagram of the fusion of proteoliposomes with the planar lipid bilayer. **1** - proteoliposome close to lipid bilayer, **2** - proteoliposome in contact with lipid bilayer; **3** - proteoliposome swelling and fusion; **4** - protein incorporated into the lipid bilayer. Lipid bilayer and proteoliposomes are drawn in grey. The protein is indicated in orange. Red dots - Ca^{2+} ions. Water flow is indicated by blue arrow.

2.6.4. Recording of KcsA and KcsA-Kv1.3 in planar lipid bilayer

After channel insertion, symmetric recording conditions were established by perfusion the *cis* and *trans* compartments with the required buffer (the composition of recording buffers is shown on the page 36). Although the majority of KcsA channels incorporate into the membrane with sensitivity to *trans* pH, there are some minor fraction of the channels with opposite orientation in the lipid bilayer (*Heginbotham et al, 1999*). Channels oriented in the opposite manner may complicate the interpretation of the data obtained in the experiment. In order to ensure that all channels observed in the experiment have a single orientation; pH asymmetry between *cis* and *trans* sides were established. That is why in all planar lipid bilayer experiments, the *trans* compartment was buffered to pH 4.0 with 10 mM succinic acid, and the *cis* compartment was buffered to pH 7.0 with 10 mM HEPES.

The recordings were performed on KcsA and KcsA-Kv1.3 channels incorporated in different mixtures of phospholipids (Table 2.1). As a general rule in

_____

this study, the phospholipid composition of the proteoliposomes and planar lipid bilayer were identical. The solution environment in a particular experiment can be quickly modified by the perfusion system integrated in the planar lipid bilayer set-up as required.

2.6.5. Solutions for the planar lipid bilayer experiments

Agar salt bridge solution: Agar 2%

3M KCl

Lipid bilayer solution: Phospholipids 50 mg/ml

in *n*-decane

Liposome fusion solution (*cis* side):   250 mM KCl

10 mM HEPES

pH 7.0

Liposome fusion solution (*trans* side):   KCl 20 mM,

10 mM Succinic acid

pH 4.0

Recording solution pH 4.0 (*trans* side):   150 mM KCl

10 mM Succinic acid

Recording solution pH 7.0 (*cis* side):   150 mM KCl

10 mM HEPES

CaCl$_2$ stock solution: 0.5 M CaCl$_2$

EDTA stock solution: 0.5 M EDTA

Tetraethylammonium (TEA) stock solution: 3M TEA

_____

2.6.6. Data acquisition and processing

All measurements were performed at room temperature (23 - 25 ºC). Data were sampled at 40 kHz and filtered at 1 kHz. The amplitudes of the single channel currents and chord conductance values were calculated from a double Gaussian fit of all-point histograms plotted for raw current traces. All kinetic analyses were done using the QuB software for single channel analysis (*www.qub.buffalo.edu*). Single channel currents were first idealized into noise free open and close transitions using a half-amplitude threshold algorithm. Closed and open intervals were compiled into dwell time histograms with logarithmic abscissa and square root ordinate (*Sigworth and Sine, 1987*) and were fitted by sums of exponentials (Figure 3.6) according following equations:

Equ. 2.1 $$f(t) = \sum_{i=1}^{n} a_i \lambda_i e^{-\lambda_i t} \quad \text{with} \quad \sum_{i=1}^{n} a_i = 1$$

where and λ_i is the reciprocal of the time constant of the ith component; n - number of exponential components; a_i is the fractional area occupied by the ith component; t is decay constant

The kinetic models of KcsA gating were made using a maximum likelihood criteria after imposing a dead time of 100 µs. P_O values were calculated according the following equation:

Equ. 2.2. $$P_o = \frac{\text{mean open time}}{\text{mean open time} + \text{mean closed time}}$$

Data acquisition was performed using Patch Master software (HEKA Electronics, USA). Data analysis were performed using Fit Master (HEKA Electronics), Igor Pro (Wave Metrics, USA), QuB software (State University of New York at Buffalo, USA) and Origin Pro 8.0 (Origin Lab, USA).

2.7. SsNMR spectroscopy under Magic Angle Spinning

SsNMR spectroscopy permits determination of the structure of membrane proteins in a non-crystalline lipid bilayer environment *(Renault et al., 2010)*. In addition to structural information, ssNMR spectroscopy also provides information on protein dynamics (*Ader et al., 2010*). Moreover, this approach gives a great freedom in terms of sample preparation. Many different parameters can be tested such as ionic strength, temperature, pH and lipid composition.

NMR spectroscopy is based on the principle that depending on the subatomic composition, certain nuclei posses a spin (spin quantum number *I*), which is a quantum mechanical property (*Keeler, 2010*). Those nuclei, and only those nuclei, are amenable to NMR spectroscopy. Those nuclei feature a magnetic dipole moment $\boldsymbol{\mu}$

Equ. 2.3
$$\mu = \gamma I \hat{h}$$

where γ is a nuclei-specific constant called the gyromagnetic ratio; $\hat{h}$ is Planck's constant. Spin quantum number *I* can adapt integer and half integer numbers. In this thesis, I exclusively dealt with spin = ½ nuclei. In this case, if a spin-half nucleus has an interaction with an external magnetic field $\boldsymbol{B_0}$, this gives rise to two energy levels, which become separated by

Equ. 2.4
$$\Delta E = \gamma \hat{h} B_0 = \hat{h} \omega_0$$

where, the resonance frequency ω_0 is called the *Larmor frequency*, which is characteristic of each type of nuclear species. However, usually, resonance frequencies slightly differ from ω_0. This difference is called the *chemical shift δ*, which is based on secondary fields generated by electrons surrounding the nuclei (δ is usually expressed in parts per million (*ppm*) by frequency). Nuclei resonate with chemical shifts characteristic for their chemical environment, which renders NMR a formidable analytical tool.

The spin ½ nuclei ^{1}H,[13]C,[15]N and ^{31}P are most commonly studied in biological ssNMR spectroscopy. Some of these nuclei (^{13}C,[15]N) occur only marginally at natural abundance and hence have to be incorporated into the sample by labeling techniques. This can be achieved during protein expression by introducing isotope-

_____

enriched sugars and ammonium salts in the minimal medium as exclusive nutrition source.

A serious problem in ssNMR spectroscopy is that the spectra are influenced by the anisotropic nature of relevant spin interactions, such as the chemical shift anisotropy, dipolar, scalar and quadrupolar couplings (*Renault et al., 2010*). These anisotropic effects can be eliminated by rotating the sample at an angle 54.7° with respect to the external magnetic field. This specific angle is called the Magic angle. Magic angle Spinning (MAS) exploits the orientational dependence of the anisotropic interactions, which varies with $(3\cos2\theta-1)/2$ and averages to zero at the magic angle, $\theta = 54.7°$ (*Renault et al., 2010*).

A number of experiments can be used in ssNMR to transfer the magnetization from one particular isotope to another. In my study I used several experimental protocols: ^{13}C-^{13}C spin diffusion, NCA, NCACX and NCOCX experiments (Figure 2.7).

In ^{13}C-^{13}C spin diffusion experiments, after an initial ^{1}H to ^{13}C nuclei cross-polarization step, longitudinal magnetization is transferred to other ^{13}C nuclei which are close in space. In this type of experiment, ^{13}C atoms within a certain distance of one another are correlated by cross peaks in the spectrum. Since the magnetization transfer efficiency is correlated to the inter-^{13}C distances, intra-residue correlations (at short mixing times of 30 ms) and inter-residue correlation (at long mixing time ~150 ms) can be distinguished or at least promoted by a proper choice of the mixing time.

In the NCA(NCACX) and NCOCX experiments the magnetization is transferred from ^{1}H to ^{15}N via cross-polarization and then selectively to the ^{13}CA or ^{13}CO, in NCA (NCACX) or NCOCX experiments, respectively, using a specific cross-polarization (*Baldus et al., 1998; Pauli et al., 2001*). Additionally, in the NCACX and NCOCX experiments the magnetization is transferred to other carbons using a ^{13}C-^{13}C spin diffusion step, thereby providing sequential correlations (*Seidel et al., 2004; Weingarth et al., 2009*). In this thesis, I used a PARIS spin diffusion mixing step (*Weingarth et al., 2009*). The chemical shift is evolved on the ^{15}N nuclei in the indirect dimension and detected on the ^{13}C nuclei.
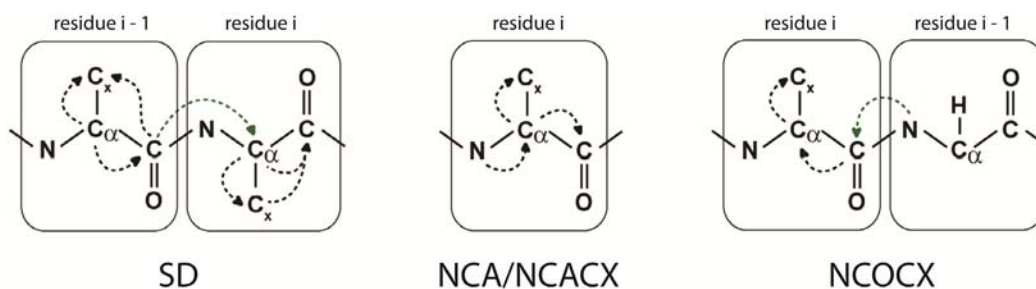
_____

Figure 2.7. Schematic representation of the magnetization transfer in different ssNMR experiments under MAS conditions. Spin diffusion (SD), NCA/NCACX and NCOCX experiments are shown. This figure is adapted from *Nand, 2011.*

In this study all ssNMR experiments were performed on [^{13}C^{15}N]-labeled KcsA reconstituted in liposomes composed of DOPC and DOPG (DOPA or CL) at 3/7 molar ratio in the presence of 150 mM KCl at pH 4.0. The experiments were conducted at 500-700 MHz ^{1}H resonance frequency on NMR spectrometers (Bruker Biospin, USA) equipped with a 3.2 mm triple resonance (^{1}H, ^{13}C, ^{15}N) MAS probe. All experiments were carried out at effective sample temperature of 273 K. Pelleted proteoliposomes containing [^{13}C^{15}N]-labeled KcsA were transferred to a 3.2 mm MAS rotor. The MAS frequency was set to 12, 11.4 kHz and 15 kHz for ^{13}C-^{13}C PDSD, NCA(CX) and NCOCX experiments, respectively. ^{13}C-^{13}C PDSD spectra were recorded using a longitudinal mixing time of 30 and 150 ms, respectively. NCA(CX) and NCOCX spectra were acquired by using ^{13}C-^{13}C magnetization transfer via 30 ms PARIS ^{13}C-^{13}C mixing step. ^{13}C and ^{15}N resonances were calibrated using adamantane and the tripeptide AGG as an external reference. The data acquisition and analysis were performed with Topspin 3.1 (Bruker Biospin, USA).

2.8. Molecular dynamics simulations

Coarse-grained Molecular Dynamics (CGMD) simulations were carried out using the GROMACS simulations package version 4.5.3 (*Hess et al., 2008*) and the MARTINI (*Marrink et al., 2007; Monticelli et al., 2008*) force field, together with an integration step of 25 fs and the standard settings for non-bonded interactions in a NPT ensemble with periodic boundary conditions. Simulation times were multiplied by a factor 4 to account for the smoothness of the CG potentials. The system was semi-isotropically coupled to a pressure bath at 1 bar (τ_p = 3 ps) and coupled (τ_T = 0.3 ps) to a heat bath. A solvated mixed DPPC:DPPG (3:1 molar ratio) bilayer, consisting of 1536 DPPC lipids, 512 DPPG lipids, 25,088 water and 512 sodium GC-beads, was self-assembled and equilibrated over 4.4 μs at 323 K, which resulted in a large membrane patch with dimensions of 25.2 x 25.2 nm^2. A frame of this system was extracted after 4.4 μs and the closed-conductive KcsA-Kv1.3 channel inserted while keeping the PC:PG 3:1 ratio. This system was equilibrated over 20 μs while keeping the channel core comprising the filter (backbone- and side chain-beads) and the intracellular side (backbone-beads only), corresponding to residues 22-49, 67-82 and 91-115, rigid throughout all simulations. Position restraints on the backbone-beads of the residues at the membrane/water interface (residues 50-66 and 83-90) of the extracellular side were gradually reduced during equilibration and very light position restraints of 10 kj/mol*nm^2 were applied during the final runs. KcsA was inserted in two different mixed bilayers extracted after 4.0 and 4.4 μs to minimise the influence of the initial lipid distribution.

3. Results

3.1. Expression, purification and reconstitution of KcsA

KcsA potassium channel were expressed in *E. coli* cells. Purification and reconstitution followed the protocol described in "Materials and Methods". Briefly, the channel protein was solubilized in detergent (DM) and purified using Ni^{2+}-affinity chromatography. At the final step of protein purification, KcsA was eluted in the elution buffer (see "Materials and Methods"), and was analyzed by SDS-PAGE (Fig. 3.1A). Under these conditions a single protein band was observed at ~52kDa, representing the KcsA tetramer. This finding agrees well with previously reported data. The KcsA tetramer is very stable, and can be disrupted only under harsh denaturing conditions like prolonged heating at 95 °C (*Heginbotham et al., 1997; Irizarry et al., 2002; Rotem et al., 2010; Valiyaveetil et al., 2002*). Incubating the KcsA sample at 95 C° for 20 minutes indeed produced KcsA monomers of about 17 kDa (Figure 3.1A). KcsA reconstituted into proteoliposomes was similarly analyzed. Untreated and heated samples ran as tetramer and monomers, respectively, indicating a successful reconstitution of purified KcsA (Figure 3.1B).
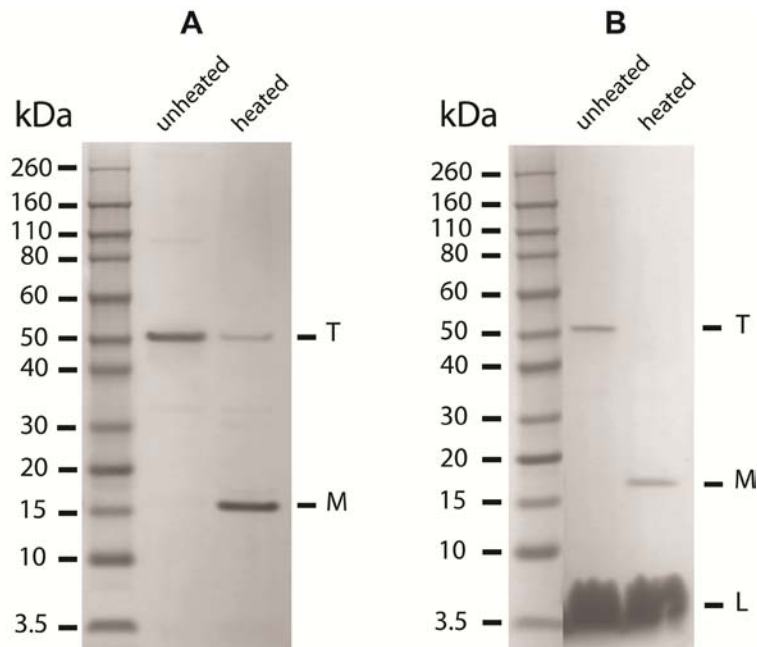

Figure 3.1. SDS-PAGE of purified and reconstituted KcsA potassium channel: **A** - purified KcsA and **B** - proteoliposomes containing KcsA before and after heating to 95 °C for 20 min. Samples were separated on a 4–12% Bis-Tris polyacrylamide gels and stained with Coomassie blue. Tetrameric (T), monomeric (M) and lipid (L) fractions are indicated accordingly.

_____

3.2. Functional studies with KcsA proteoliposomes

Following successful reconstitution of KcsA into proteoliposomes, I performed electrophysiological measurements of the channel in planar lipid bilayer and giant proteoliposomes. Upon a pH-jump from 7.0 to 4.0 I observed in giant KcsA proteoliposome preparations a transient KcsA mediated currents. It demonstrated that an increase in H^+ concentration activates KcsA. In agreement with the data in the literature, the KcsA mediated current rapidly decayed within a few seconds, reaching a steady state level corresponding to 11.6 ± 0.9 % (n=6, s.e.m.) of the maximum current amplitude *(Chakrapani et al., 2007a, b; Heginbotham et al., 1999; Hille, 2001; LeMasurier et al., 2001; Schrempf et al., 1995*) (Figure 3.2A). Single channel KcsA current at steady-state conditions was investigated in planar lipid bilayer (Figure 3.2B). The current was sensitive to TEA (Figure 3.2B), a well known K^+- channel blocker (*Hille, 2001*).
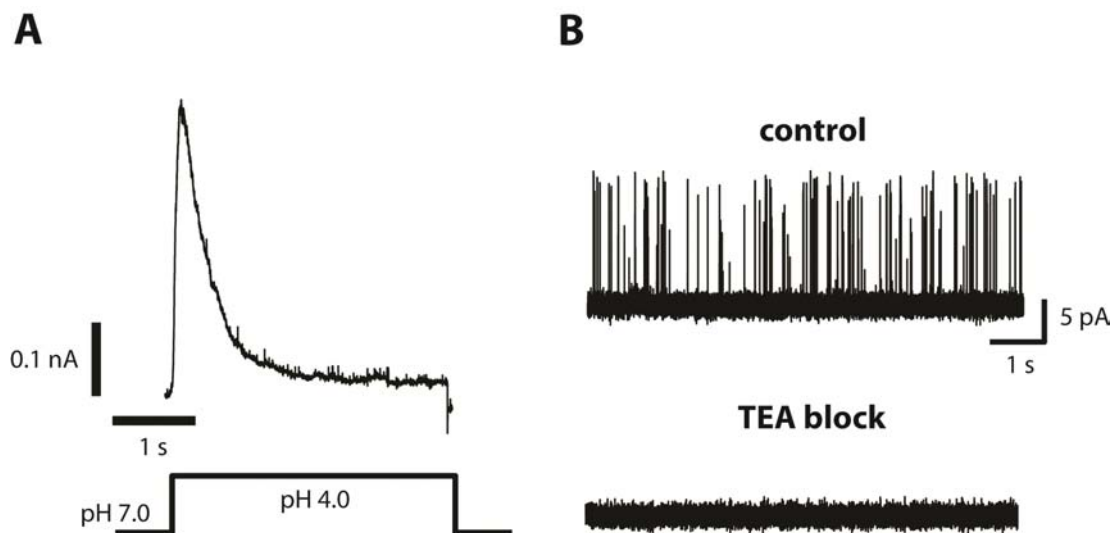

Figure 3.2. Macroscopic and single channel currents of KcsA reconstituted in proteoliposomes: **A** - recording of KcsA during a pH jump experiment. **B** - a single channel current of KcsA at steady-state conditions. Macroscopic activity of KcsA was recorded at symmetrical 150 mM KCl in an inside-out patch. KcsA was activated by pH jumps from 7.0 to 4.0 using a rapid solution exchanger with simultaneous application of a voltage of +100 mV. Single channel currents of KcsA were recorded in the planar lipid bilayer setup at +100 mV in symmetrical 150 mM KCl solution. The *cis* side of the chamber was buffered at pH 7.0 by 10 mM HEPES and the *trans* side was maintained at pH 4.0 using 10 mM succinic acid. TEA at final concentration of 30 mM was added to the *cis* chamber to ensure complete blockage of the single channel currents of KcsA channel as depicted in the lower panel of figure 3.2B.

3.3. Influence of different anionic phospholipid environments on KcsA

KcsA was reconstituted into liposomes composed of different types of anionic phospholipids. The liposomes were fused to planar lipid bilayers composed of 70 % of the respective anionic phospholipid and 30% of neutral DOPC (for details see chapter 2.6.2. in "Materials and Methods"). Four types of anionic phospholipids were used: DOPG, DOPA, DOPS and cardiolipin (CL). Phospholipid composition of KcsA proteoliposomes and planar lipid bilayers were identical in all experiments. Representative KcsA current traces recorded under different anionic phospholipid conditions are shown in Figure 3.3.
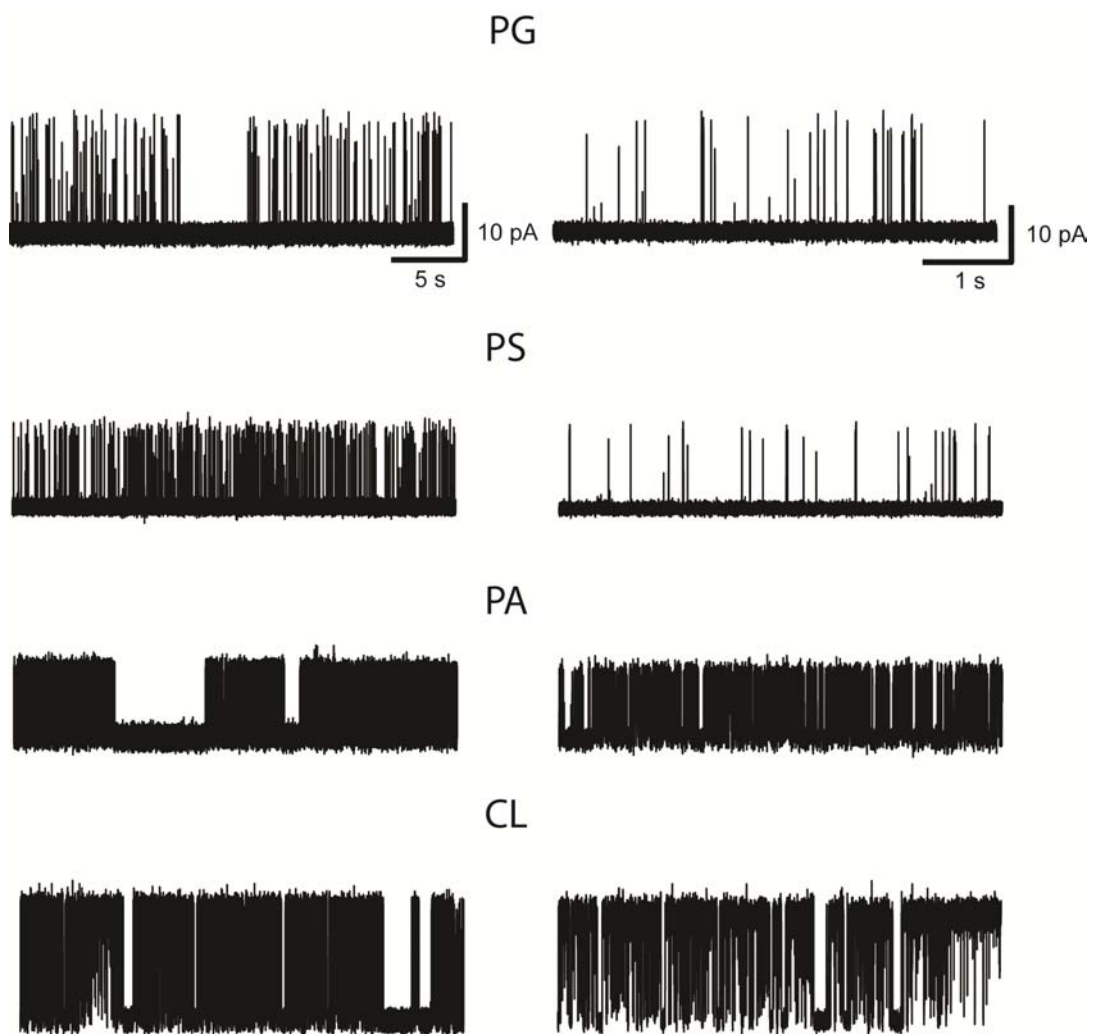

Figure 3.3. Representative current traces of KcsA recorded at different anionic phospholipid environments. The specific anionic phospholipid is indicated above the current traces. On the left part of the figure long 30 s traces are presented and on the right part of the figure 5 s traces are shown. All experiments were performed at +100 mV in symmetrical 150 mM KCl solution at pH = 7.0 on the *cis* side and pH 4.0 on the *trans* side. Lipid bilayers were composed of 70 % anionic phospholipid and 30 % neutral DOPC.

3.3.1. Effect of anionic phospholipids on KcsA single channel conductance

The data indicated that anionic phospholipid conditions differentially affected KcsA single channel properties. The chord conductance measured at + 100 mV was significantly higher in the presence of DOPG (174.7 ± 2.2 pS, n = 13, s.e.m.) and CL (169.0 ± 2.7 pS, n = 11, s.e.m.) in comparison to the channel incorporated into lipid bilayers composed of DOPA (118.4 ± 3.1 pS, n = 12, s.e.m.) and DOPS (132.5 ± 4.2 pS, n = 6, s.e.m.) (Figure 3.4A). The effect of the anionic phospholipids on the KcsA conductance was observed only at positive potentials > 20 mV, meaning that the phospholipids affected outward rectification properties of KcsA (Figure 3.4B). The phospholipids had identical acyl chain lengths to eliminate any possible effects of acyl chain variation on channel function. Also, the phospholipid effect on the current rectification showed no significant correlation to the charge of the phospholipid headgroup: both DOPG having one negative charge, and CL having two negative charges at neutral pH, shifted KcsA conductance to the high conductance mode (Figure 3.4). Boltzmann fits to single channel KcsA current-voltage (I-V) curves showed that in the presence of DOPG and CL, the KcsA I-V relation was slightly shifted to more depolarized potentials ($V_{1/2}$[PG] = 42.4 ± 1.5 mV; $V_{1/2}$[CL] = 39.9 ± 0.9 mV; $V_{1/2}$[PS] = 53.4 ± 1.8 mV; $V_{1/2}$[PA] = 52.6 ± 4.0 mV). This shift is probably due to a surface charge effect of the negatively charged phospholipids. More important is the observation that I-V relations are significantly steeper in the presence of DOPG and CL (K^{PG} = 40.2 ± 1.6 mV; K^{CL} = 40.9 ± 0.9 mV) than in the presence of DOPS and DOPA (K^{PS} = 57.9 ± 2.0 mV; K^{PA} = 68.1 ± 4.2 mV), combined with a gradual increase of single channel conductance at positive potentials. The data, therefore, suggests that charge of phospholipid headgroup plays a minor role and the structure of the phospholipid headgroup a major role in the observed KcsA conductance increase.
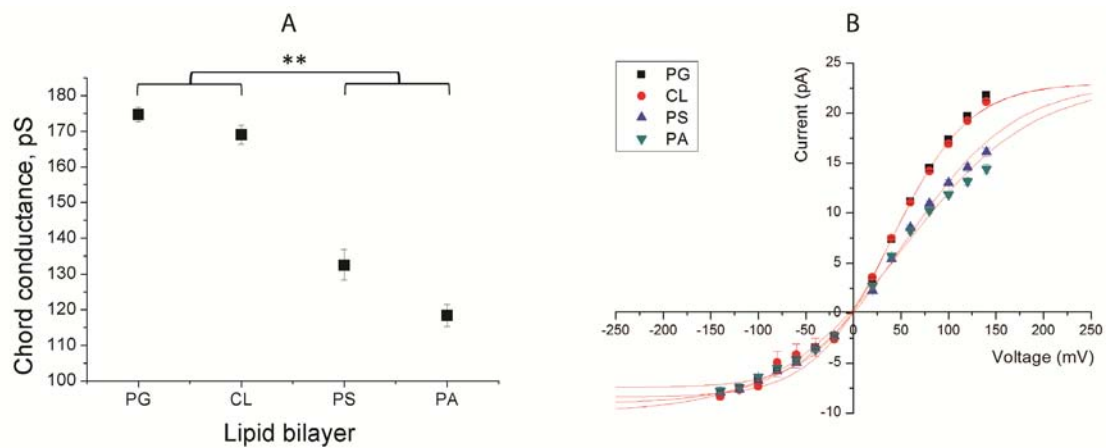
Figure 3.4. Effect of anionic phospholipid environment on the single channel conductance of KcsA : A – KcsA chord conductance at + 100 mV in different anionic phospholipid environments; **B** – current-voltage relationship of KcsA recorded in different anionic phospholipids. DOPG - black, DOPA - green, DOPS - blue, CL - red. All experiments were performed in symmetrical 150 mM KCl solution at pH = 7.0 on the *cis* side and pH 4.0 on the *trans* side. Lipid bilayers were composed of 70 % anionic lipid and 30% neutral DOPC. The graphs represent data from 6-13 independent experiments. Chord conductance values are given in pS as mean ± s.e.m. Current-voltage relationship were fit by a Boltzmann function ($y=[(A_1-A_2)/(1+e^{(V-V_{1/2})/K})]+A_2$, where A_1 - initial value of the current, A_2 - final value of the current, $V_{1/2}$ - the voltage of half-maximal current, K - the slope factor for I-V curve). The curves were fit from -250 to 250 mV. ** - p < 0.01.

3.3.2. Effect of anionic phospholipids on KcsA open probability

In addition to an effect on single channel conductance described above, anionic phospholipids modulated the open probability (P_O) of the KcsA channel. All-point histograms of KcsA recorded under different anionic phospholipid conditions revealed that KcsA has a significantly higher P_O if the channel is incorporated in the lipid bilayer composed of DOPA or CL in comparison to DOPG or DOPS lipid bilayers (Figure 3.5). Thus, the conductance and rectification properties of KcsA current are uncorrelated with an increase in P_O.
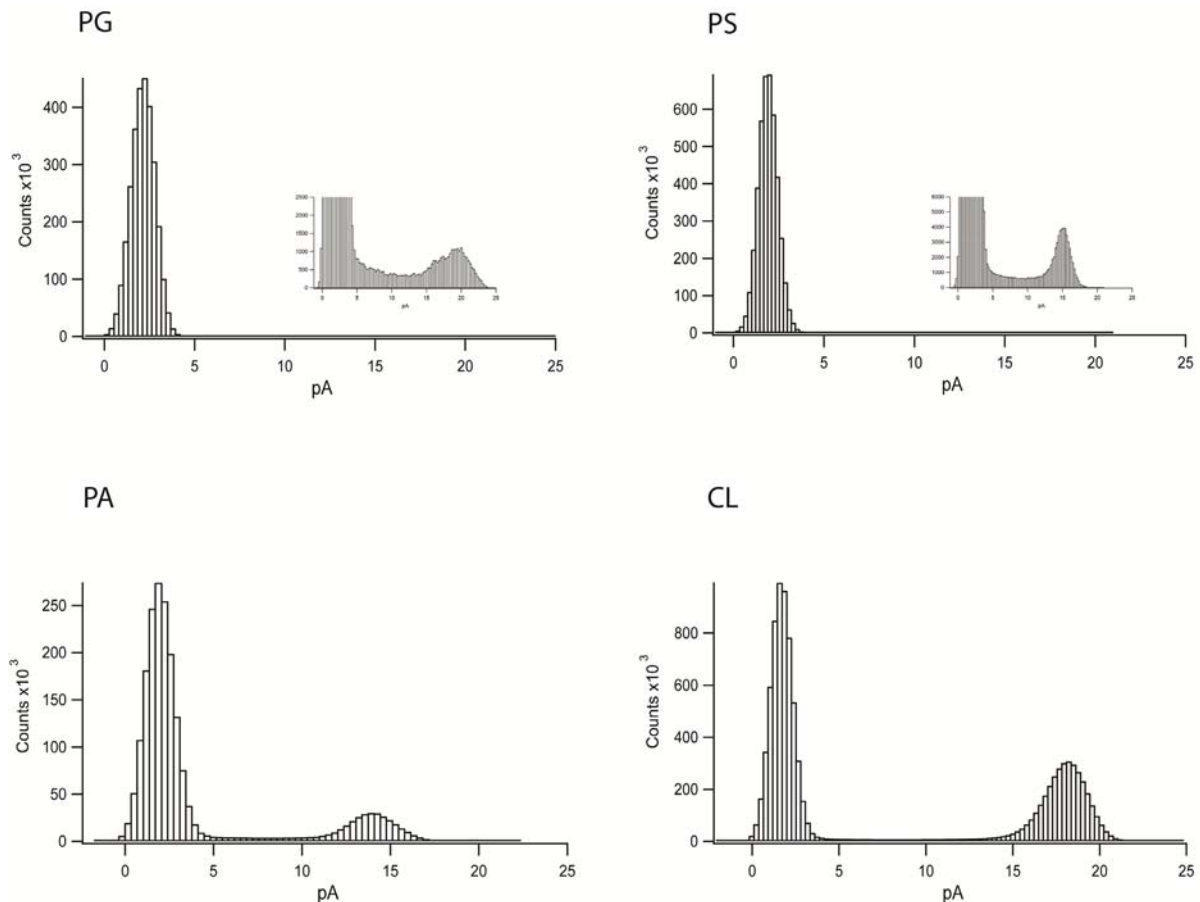
Figure 3.5. Representative illustrations of all-points histograms for KcsA recorded in different anionic phospholipid environment. All experiments were performed in symmetrical 150 mM KCl solution at pH = 7.0 on the *cis* side and pH 4.0 on the *trans* side. Lipid bilayers were composed of 70 % anionic lipid and 30 % neutral DOPC. All-points histograms were plotted for entire recordings of the single channel currents conducted by KcsA, including long closed periods, and thus represent the overall P_O of KcsA potassium channels in the particular phospholipid membrane. The insets in the histograms show the KcsA potassium channel recorded in the presence of DOPG and DOPS and illustrate the paucity of open events. KcsA open probability (P_O) values are given in the text as mean ± s.e.m.

In contrast to the effect of anionic phospholipids on single channel conductance, KcsA P_O correlated with the charge of the phospholipid headgroup. P_O was high in a lipid environment with more negatively charged headgroups DOPA (-1.3) (P_O=0.19 ± 0.02, n=10, s.e.m.) and CL (-2) (P_O=0.37 ± 0.09, n=8, s.e.m.) and comparably low in a lipidic environment with less negatively charged head groups, for example in DOPG (-1) (P_O=0.010 ± 0.002, n=9, s.e.m.) and in DOPS (-1) (P_O=0.013 ± 0.003, n=6, s.e.m.), respectively. Maximal P_O was observed in the presence of CL (0.37 ± 0.09, n=8, s.e.m.), which has the highest headgroup charge of the anionic phospholipids tested (Figure 3.5).

3.3.3. Kinetic analysis of KcsA gating under different anionic phospholipid environment

It has been shown previously that KcsA closed times at steady-state conditions mainly correspond to an inactivated-opened equilibrium of the channel (*Chakrapani et al., 2007a; Cordero-Morales et al., 2006)*. Thus, I considered that closed times in my study correspond to inactivated states. Therefore, at steady-state conditions P_O of KcsA mainly reflects the sum of transitions between open and inactivated states. This situation simplifies equation 1.1 (see Introduction, page 16) to equation 3.1,

Equ. 3.1
$$P_o = \frac{\sum_{i=1}^{n}[O_i]}{\sum_{i=1}^{n}[O_i] + \sum_{j=1}^{n}[I_j]}$$

where **O** means open state duration, *i* - number of open states, **I** - nonconductive inactivated state duration, *j* - number of nonconductive inactivated states.

Based on these general considerations, a detailed analysis of KcsA gating kinetics was carried out in order to find out more about the mechanism(s) by which anionic phospholipids modulate KcsA gating.

All kinetic analyses were done using the QuB software for single channel analysis and modulation (*www.qub.buffalo.edu*). Single channel currents of KcsA recorded in different anionic phospholipid environments were first idealized into noise free open and close transitions using a half-amplitude threshold algorithm. Closed and open intervals were compiled into dwell time histograms with logarithmic abscissa and square root ordinate (*Sigworth and Sine, 1987*) and were fitted by a 3 - exponential fit (Figure 3.6) according to equation 3.2:

Equ. 3.2
$$f(t) = \sum_{i=1}^{n} a_i \lambda_i e^{-\lambda_i t} \qquad \text{with} \qquad \sum_{i=1}^{n} a_i = 1$$

where λ_i is the reciprocal of the time constant of the ith component; *n* is the number of exponential components; a_i is the fractional area occupied by the ith component; *t* is the decay constant.
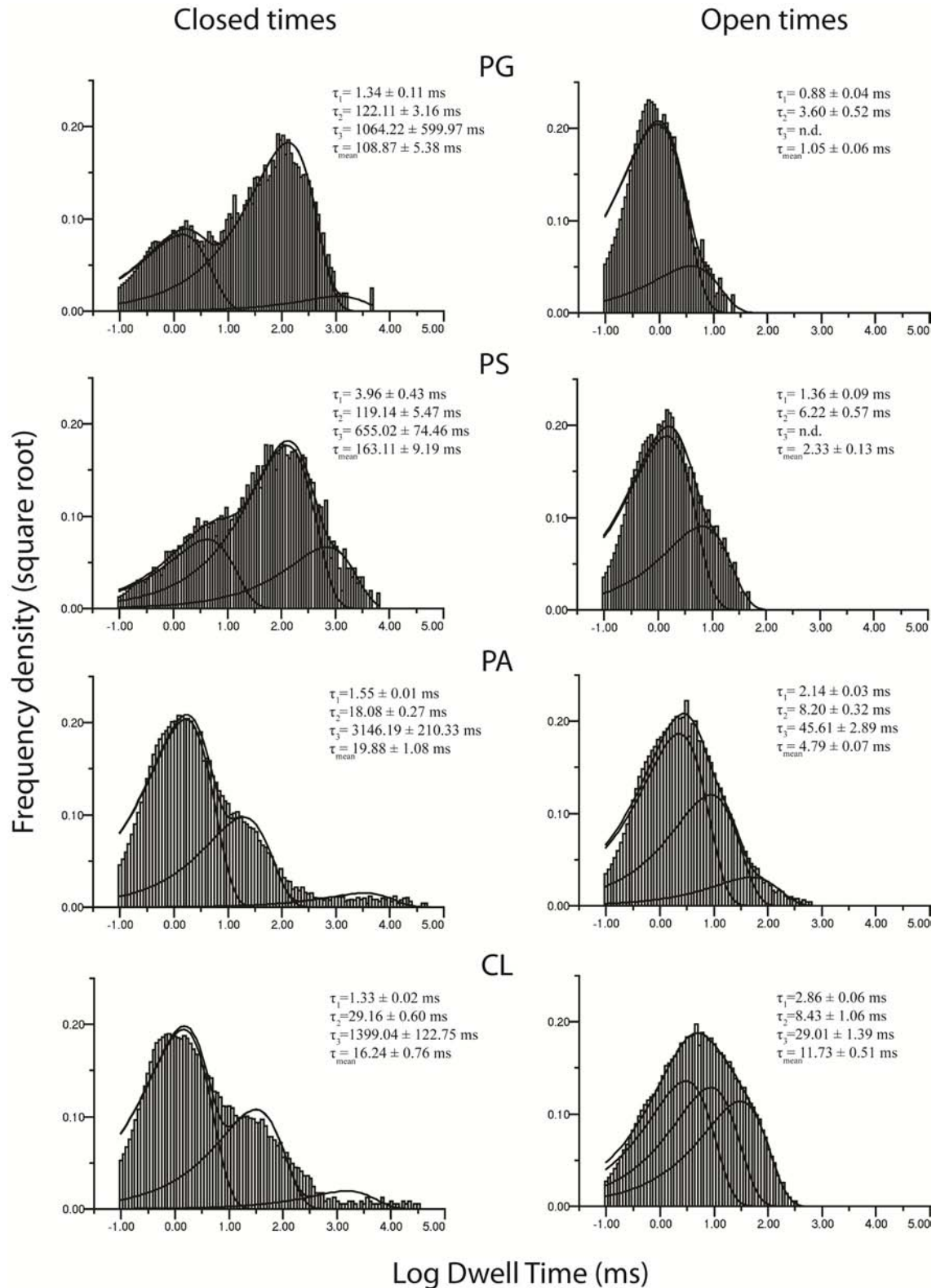
Figure 3.6. Representative dwell time histograms of KcsA recorded in different anionic phospholipids. All experiments were performed in symmetrical 150 mM KCl solution at pH = 7.0 on the *cis* side and pH 4.0 on the *trans* side. Lipid bilayers were composed of 70 % anionic lipid and 30 % neutral DOPC. Time constants (τ) were calculated from a three exponential fits (see equations on the page 48) to log dwell time distributions. Time constants (τ) are given in ms as mean ± std (see Table 3.1).

_____

Analysis of the dwell time histograms revealed that both open and closed durations are composed of multiple kinetic components, which is in good agreement with previous studies (*Chakrapani et al., 2007b; Irizarry et al., 2002*). Under all experimentally tested phospholipid conditions, dwell time histograms for closed durations were best fit with three exponentials corresponding to three non-conductive states of the KcsA channel (Figure 3.6). Closed times, which represent inactivated states, were sensitive to changes in anionic phospholipid environment. The total mean closed time (τ_{mean}) was ~ 8 fold shorter in the presence of DOPA and CL (19.88 ± 1.08 ms (n=10, std) and 16.24 ± 0.76 ms (n=8, std), respectively) in comparison to DOPG (108.87 ± 5.38 ms; n=9, std) and DOPS (163.11 ± 9.2 ms; n=6, std) (Figure 3.6 and Table 3.1).

This effect of DOPA and CL was due to reduction of the most prevalent second closed state in the presence of DOPG (τ_2 = 122.11 ± 3.16 ms, a_2 = 0.83 ± 0.01, n=9, std) and DOPS (τ_2 = 119.14 ± 5.47 ms, a_2 = 0.76 ± 0.05, n=6, std). In the presence of DOPA and CL, the second closed state was greatly reduced (τ_2 = 18.08 ± 0.27 ms, a_2 = 0.20 ± 0.01 (n=10, std) and τ_2 = 29.16 ± 0.60 ms, a_2 = 0.25 ± 0.02 (n=8, std) for DOPA and CL, respectively) and the first short-lived closed state became the predominate one (τ_1 = 1.55 ± 0.01 ms, a_1 = 0.80 ± 0.01 (n=8, std) in DOPA and τ_1 = 1.33 ± 0.02 ms, a_1 = 0.75 ± 0.02 (n=10, std) in CL) (Figure 3.6 and Table 3.1). Taken together, analysis of closed time distributions indicates a significant effect of the anionic phospholipids on KcsA channel C-type inactivation, which is decreasing by phospholipids with more negatively charged headgroup such as DOPA and CL. This effect accounts for the observed increase in P_O in the presence of more negatively charged DOPA and CL (page 47, Figure 3.5).

The three exponential fit of dwell time histograms for open durations has revealed that KcsA mean open time in the presence of DOPA (τ_{mean} = 4.79 ± 0.07 ms, n=10, std) and CL (τ_{mean} = 11.73 ± 0.51 ms, n=8, std) was higher than in presence of DOPG (τ_{mean} = 1.05 ± 0.06 ms, n=9, std) and DOPS (τ_{mean} = 2.33 ± 0.13 ms, n=6, std). Two factors have contributed to this effect. First, the duration and impact of the second open state were higher in the presence of DOPA (τ_2 = 8.20 ± 0.32 ms, a_2 = 0.30 ± 0.06, n=10, std) and CL (τ_2 = 8.43 ± 1.06 ms, a_2 = 0.35 ± 0.03, n=8, std), in comparison to DOPG (τ_2 = 3.60 ± 0.52 ms, a_2 = 0.06 ± 0.02, n=9, std) and DOPS (τ_2 = 6.22 ± 0.57 ms, a_2 = 0.20 ± 0.02, n=6, std). Second, in the presence of DOPA and CL, the third long-lived open state of KcsA was observed in the dwell time

_____

distributions (τ_3 = 45.61 ± 2.89 ms, a_3 = 0.02 ± 0.01 % (n=10, std) and τ_3 = 29.01 ± 1.39 ms, a_3 = 0.28 ± 0.04 (n=8, std) for DOPA and CL, respectively) (Figure 3.6 and Table 3.1), while in the DOPG and DOPS, the third long-lived open state was not detectable (τ_3 for KcsA recorded in the DOPG and DOPS lipid bilayers is marked as *n.d.* (not detectable) in Figure 3.6 and Table 3.1).

My findings suggest that the effect of anionic phospholipids on KcsA closed and opened durations depends on phospholipid headgroup charge. More negatively charged headgroups reduce the mean closed (inactivated) time of the channel and, thereby, increase its mean open time, which then results in an overall increase in channel P_O (page 47, Figure 3.5). The maximal mean open time of KcsA was observed in CL which was the most negatively charged phospholipid among the tested phospholipids. The variation in the number of open states might be associated with the modulation of the modal gating of KcsA by anionic phospholipids.

		PG		PS		PA		CL	
		τ, ms	a*i*	τ, ms	a*i*	τ, ms	a*i*	τ, ms	a*i*
open times	τ_1	0.88 ± 0.04	0.94 ± 0.02	1.36 ± 0.09	0.80 ± 0.02	2.14 ± 0.03	0.69 ± 0.07	2.86 ± 0.06	0.38 ± 0.07
	τ_2	3.60 ± 0.52	0.06 ± 0.02	6.22 ± 0.57	0.20 ± 0.02	8.20 ± 0.32	0.30 ± 0.06	8.43 ± 1.06	0.35 ± 0.03
	τ_3	n.d.	< 0.001	n.d.	< 0.001	45.61 ± 2.89	0.02 ± 0.01	29.01 ± 1.39	0.28 ± 0.04
	τ_{mean}	1.05 ± 0.06		2.33 ± 0.13		4.79 ± 0.07		11.73 ± 0.51	
closed times	τ_1	1.34 ± 0.11	0.16 ± 0.01	3.96 ± 0.43	0.13 ± 0.04	1.55 ± 0.01	0.80 ± 0.01	1.33 ± 0.02	0.75 ± 0.02
(inactivated)	τ_2	122.11 ± 3.16	0.83 ± 0.01	119.14 ± 5.47	0.76 ± 0.05	18.08 ± 0.27	0.20 ± 0.01	29.16 ± 0.60	0.25 ± 0.02
	τ_3	1064.22 ± 599.97	0.01 ± 0.002	655.02 ± 74.46	0.11 ± 0.05	3146.19 ± 210.33	0.01 ± 0.001	1399.04 ± 122.75	0.01 ± 0.001
	τ_{mean}	108.87 ± 5.38		163.11 ± 9.19		19.88 ± 1.08		16.24 ± 0.76	

Table 3.1. Dwell times for open and closed (inactivated) states of KcsA recorded in different anionic phospholipid environments. Mean open and closed (inactivated) times were calculated from a three exponential fit (see equations on the page 48) to log dwell time distributions (Figure 3.6.). Open and closed times (τ) are given in ms as mean ± std. Area values (a) are given as mean ± std. These values were calculated from 6 to 10 experiments. *n.d.* - not detectable.

_____

3.3.4. Kinetic models of KcsA gating in different anionic phospholipids

In order to describe quantitatively the observed anionic phospholipid modulation of KcsA, kinetic models of single channel behavior were generated. Taking into consideration the previous analysis of the dwell time distributions described above, it has been assumed that KcsA channel has three discrete nonconductive closed states, which according to the literature correspond to the inactivated-opened equilibrium of the channel under stationary conditions *(Chakrapani et al., 2007b; Cordero-Morales et al., 2006*). It has been also assumed that the KcsA channel potentially displays up to three distinct gating modes under steady state conditions. This property is referred to as modal gating. The gating modes differ in their mean open times. The channel is able to switch spontaneously from one mode to another (*Chakrapani et al., 2011; Chakrapani et al., 2007b).* Based on these assumptions, kinetic models were generated for all four phospholipid conditions using maximum interval likelihood algorithm in the QUB software for a single channel analysis and modulation (*www.qub.buffalo.edu*). The kinetic models are represented on the Figure 3.7. In Table 3.2 the statistics of the kinetic models are shown.

A model with three closed (inactivated) states well described the observed lipid effects. The number of opened states varies in the models depending on lipid environment: 2 open states for KcsA in DOPG and DOPS and 3 open states in DOPA and CL. The models showed that the KcsA channel stays inactivated longer in the presence of DOPG and DOPS, consistent with an observed smaller Po (page 47, Figure 3.5). In summary, the data suggests that changes in lipid environment are associated with a modulation of open KcsA states and hence affect modal gating behavior of the KcsA channel.
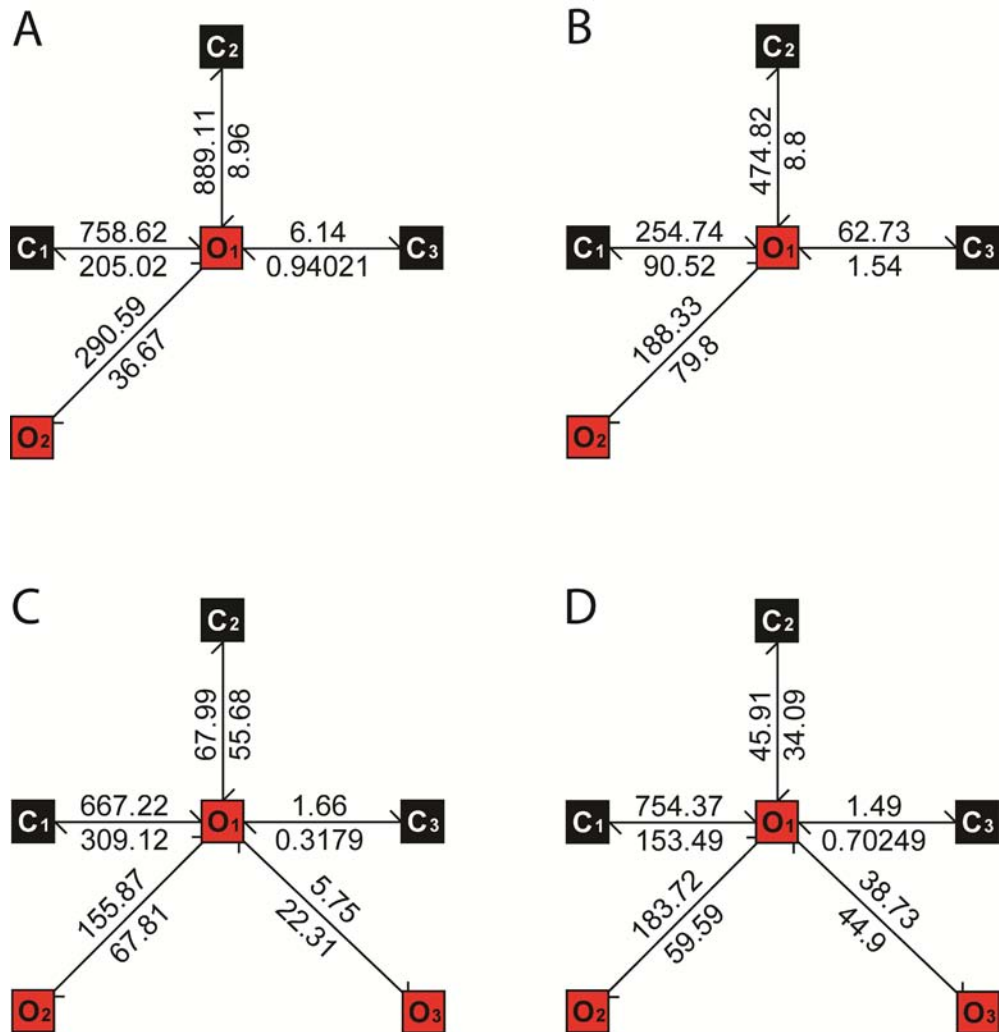
_____

Figure 3.7. Kinetic model of KcsA gating in different anionic phospholipids. **A** - DOPG lipid bilayer, **B** - DOPS lipid bilayer, **C** - DOPA lipid bilayer, **D** - CL lipid bilayer. Nonconductive closed (inactivated) states are shown as black boxes with the respective state number. Open states are indicated as red boxes with the corresponding state number. Transition rate constants were calculated using maximal likelihood-based method (see "Material and Methods"). The lines connecting states represent transitions from one state to another with corresponding transition rate constants, which are expressed in units of frequency, s^{-1}.

PG

From	To	Transition rate constants, s^{-1}
C2	O1	8.96 ± 0.23
O1	C2	889.11 ± 21.83
C3	O1	0.94 ± 0.53
O1	C3	6.14 ± 5.25
C1	O1	758.62 ± 59.34
O1	C1	205.02 ± 12.17
O1	O2	36.67 ± 8.11
O2	O1	290.59 ± 41.74

PS

From	To	Transition rate constants, s^{-1}
C2	O1	8.80 ± 0.41
O1	C2	474.82 ± 17.72
C3	O1	1.54 ± 0.17
O1	C3	62.73 ± 11.33
C1	O1	254.74 ± 29.22
O1	C1	90.52 ± 7.70
O1	O2	79.80 ± 10.09
O2	O1	188.33 ± 16.84

PA

From	To	Transition rate constants, s^{-1}
C2	O1	55.68 ± 0.83
O1	C2	67.99 ± 1.12
C3	O1	0.32 ± 0.02
O1	C3	1.66 ± 0.11
C1	O1	667.22 ± 4.69
O1	C1	309.12 ± 2.56
O1	O2	67.81 ± 2.71
O2	O1	155.87 ± 6.07
O1	O3	5.75 ± 0.57
O3	O1	22.31 ± 1.41

CL

From	To	Transition rate constants, s^{-1}
C2	O1	34.09 ± 0.73
O1	C2	45.91 ± 0.89
C3	O1	0.70 ± 0.06
O1	C3	1.49 ± 0.15
C1	O1	754.37 ± 7.67
O1	C1	153.49 ± 2.29
O1	O2	59.59 ± 5.82
O2	O1	183.72 ± 23.61
O1	O3	38.73 ± 3.63
O3	O1	44.90 ± 1.96

Table 3.2. Transition rate constants calculated for the kinetic models of KcsA gating in different anionic phospholipids. Transition rate constants are given in s^{-1} as mean ± std. C - closed (inactivated) states; O - open states. The type of the anionic phospholipid is indicated on the left panel.

3.4. Structural investigation of KcsA in anionic phospholipid environment by ssNMR spectroscopy

SsNMR spectroscopy has been used extensively to probe membrane protein structure in a lipidic environment (*Renault et al., 2010*). This holds especially for the KcsA-related KcsA-Kv1.3 chimera, where the loop sequence is harboring a scorpion toxin-binding site from Kv1.3 potassium channel (*Legros et al., 2000; Legros et al., 2002*). Conformational changes of key residues were identified in the selectivity filter and activation gate of the KcsA-Kv1.3 channel (see "Introduction", Chapter 1.5.), which are involved in scorpion toxin-binding and in transitions between closed-conductive and opened-inactivated states *(Ader et al., 2008; Schneider et al., 2008)*.

3.4.1. Effect of different anionic phospholipids on KcsA structure

To gain insight into the structural basis of phospholipid modulation of the KcsA channel, ssNMR spectroscopical experiments were performed with proteoliposomes containing KcsA in a phospholipid environment similar to the ones used in my electrophysiological experiments. Uniformly [^{13}C,^{15}N]-labelled KcsA was reconstituted into liposomes composed of 3 to 7 molar ratios of DOPC:DOPG, DOPC:DOPA, and DOPC:CL. As in the electrophysiological experiments, I shall henceforth abbreviate the phospholipid compositions that I used, as DOPG, DOPA and CL liposomes. All experiments were performed under conditions as close as possible to the electrophysiological experiments. Two-dimensional (2D) spectra of KcsA obtained at 500 and 700 MHz (^{1}H-frequency) spectrometers were assigned, based on the known chemical shifts of closed-conductive and open-inactivated conformations of KcsA-Kv1.3 (*Ader et al., 2008; Schneider et al., 2008*) and chemical shifts of closed-conductive state of KcsA (data not published).

^{13}C-^{13}C Proton Driven Spin Diffusion (PDSD) experiments were performed with a 30 ms mixing time in order to identify intraresidue ^{13}C spin systems. ^{13}C-^{13}C 2D PDSD correlation spectra recorded on KcsA enabled me to identify ^{13}C chemical shifts of key residues (T72CG2-CA/CB, T74CA-CB, T74CG2-CA/CB; T75CA-CB, T75CG2-CA) within the KcsA selectivity filter. In DOPG and DOPA the conformation of these residues corresponded to a collapsed (inactivated) conformation of the KcsA selectivity filter (Figure 3.8). Surprisingly, in CL ^{13}C-^{13}C 2D PDSD correlation spectra revealed a peak doubling at T72CG2-CA/CB, T74CA-CB, T74CG2-CB, T75CA-CB

_____

and T75CG2-CA indicating both collapsed (inactivated) and conductive conformations of the selectivity filter (Figure 3.8). At the same time the conformation of KcsA activation gate was identified as open by detecting corresponding signals at I100CG2-CA and T101CG2-CA (Figure 3.8). These results are in well agreement with my electrophysiological data that showed that the effect of CL on the decrease of the C-type inactivation of KcsA was more profound among other anionic phospholipids.
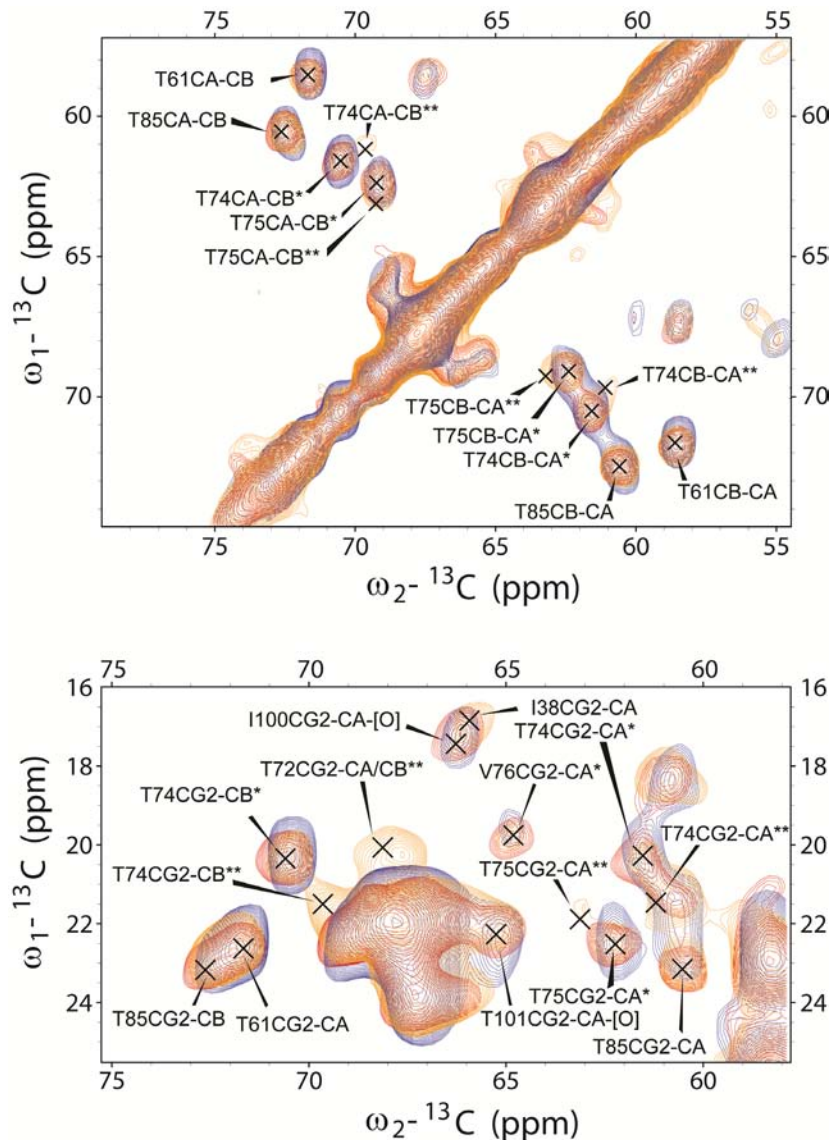

Figure 3.8. ^{13}C-^{13}C 2D PDSD correlation spectrum of KcsA recorded in the presence of 150 mM KCl at pH 4.0 in different anionic phospholipid environment with a mixing time of 30 ms at 500 MHz ^{1}H-frequency. Effective sample temperature - 273 K and MAS frequency - 12 kHz. KcsA was reconstituted into proteoliposomes composed of DOPC and DOPG (DOPA or CL) at 3/7 molar ratio. Blue - DOPA, red - DOPG; orange - CL. * - chemical shifts corresponding to the collapsed (inactivated) conformation of the selectivity filter; ** - chemical shifts corresponding to the conductive conformation of the selectivity filter; [O] - chemical shifts corresponding to the open conformation of the activation gate.

3.4.2. Investigation of KcsA potassium channel in CL lipid bilayers

To gain further insight into CL effect on KcsA structure, several additional ssNMR experiments were performed.

In the Figure 3.9 the NCA and NCACX spectra of KcsA potassium channel recorded in CL lipid bilayer at pH 4.0 are shown. In the NCA and NCACX experiments the magnetization was transferred from ^{1}H to ^{15}N via cross-polarization and then selectively to the ^{13}CA using a specific cross-polarization (*Baldus et al., 1998; Pauli et al., 2001*). Additionally, in the NCACX experiment the magnetization was transferred to other carbons (CB, CG, CD) using a ^{13}C-^{13}C PARIS mixing step (*Weingarth et al., 2009*). This enabled detection of residues in the selectivity filter including glycines which are part of the highly conserved selectivity filter signature of K$^+$ channels *(Doyle et al., 1998; Hille, 2001; Morais-Cabral et al., 2001)*. Peak doubling was observed for signals corresponding to T74-CA/CB/CG2, T75-CA/CG2, G77-CA and G79-CA, which confirmed the presence of both conductive and collapsed conformation of the KcsA selectivity filter. (Figure 3.9).
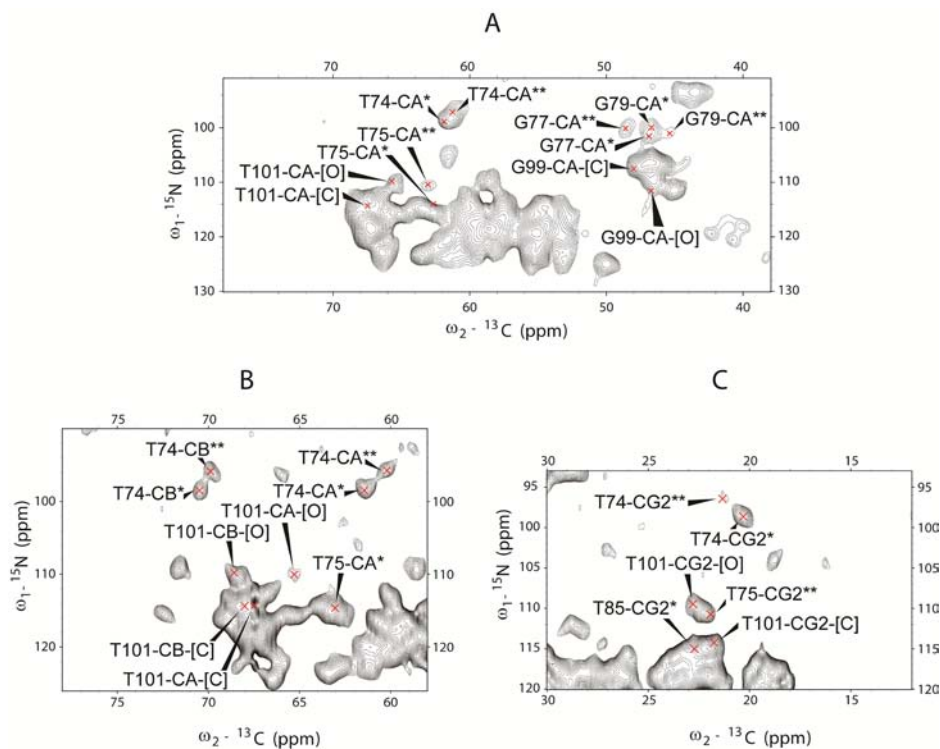

Figure 3.9. NCA (A) and NCACX (B and C) spectra of KcsA recorded at 500 MHz ^{1}H-frequency in CL in the presence of 150 mM KCl at pH 4.0. Effective sample temperature - 273 K and MAS frequency - 11.4 kHz. KcsA was reconstituted in proteoliposomes composed of DOPC and CL at 3/7 molar ratio. * - chemical shifts corresponding to the collapsed conformation of the selectivity filter; ** - chemical shifts corresponding to the conductive conformation of the selectivity filter; [O] - chemical shifts corresponding to the open conformation of the activation gate; [C] - chemical shifts corresponding to the closed conformation of the activation gate.

_____

In NCA and NCACX spectra the peaks, that correspond to the open conformation of KcsA activation gate have been detected at T101CA/CB/CG2, which was expected for pH 4.0 conditions when activation gate is protonated. However the intensity and resolution in these experiments were not sufficient to describe precisely the conformation of KcsA activation gate in the presence of CL. Therefore, an additional NCOCX experiment was performed on KcsA in CL lipid bilayer.

Similar to the above mentioned scheme, in an NCOCX experiment, the magnetization was specifically transferred to ^{13}CO, and then to other carbons via ^{13}C-^{13}C PARIS spin diffusion. Through the transfer to the neighboring carbons (i-1), sequential correlations are provided (*Seidel et al., 2004; Weingarth et al., 2009*).

The NCOCX spectrum of KcsA recorded in a CL lipid bilayer is shown on the Figure 3.10. As in the experiments described above, the selectivity filter of the KcsA had two conformations in the NCOCX spectrum: collapsed and conductive. The signals, that correspond to the open conformation of the KcsA activation gate were detected for T101N-I100CA and G99N-A98CB (Figure 3.10). However, some ambiguous peaks for the same residues were present that may be related to closed conformation, and, further, some signals which correspond to the open conformation of the KcsA were absent in the NCOCX spectrum.
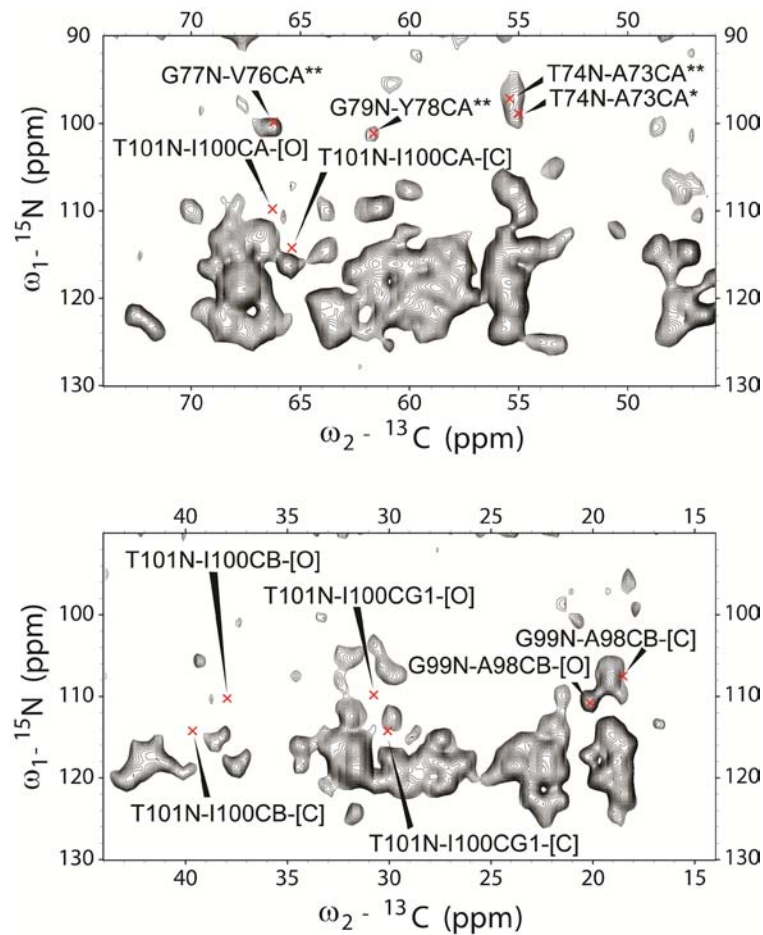
Figure 3.10. NCOCX spectrum of KcsA recorded at 700 MHz [1]H-frequency in CL in the presence of 150 mM KCl at pH 4.0. Effective sample temperature - 273 K and MAS frequency - 15 kHz. KcsA was reconstituted in proteoliposomes composed of DOPC and CL at 3/7 molar ratio. * - chemical shifts corresponding to the collapsed conformation of the selectivity filter; ** - chemical shifts corresponding to the conductive conformation of the selectivity filter; [O] - chemical shifts corresponding to the open conformation of the activation gate; [C] - chemical shifts corresponding to the closed conformation of the activation gate.

In order to make a clear conclusion about the activation gate conformation of KcsA in the presence CL, I decided to conduct one additional [13]C-^{13}C PDSD experiment at long mixing time (150 ms) to be able to detect inter-residue contacts. The results of this experiment are represented in the Figure 3.11. In this experiment I observed signals corresponding to inter-residue contacts of I100CB-G99CA, I100CD1-T101CG2, T101CG2-I100CB, G99CA-I100CD1 and G99CA-A98CB which confirmed that activation gate of KcsA in its open conformation.

_____

Taken together, ssNMR results show a marked effect of CL on the selectivity filter conformation of KcsA potassium channel at pH 4.0 in maintaining the channel open and partially conductive. It seems that in the presence of CL, which is more negatively charged in comparison to other anionic phospholipids, the equilibrium within KcsA gating is shifted to the open-conductive state in comparison to other phospholipids. Therefore at steady state conditions the impact of the open-conductive state is sufficient to probe it using ssNMR. These results are in good agreement with my electrophysiological experiments that showed that the mean open time of KcsA is higher in the presence of CL in comparison to other anionic phospholipids (see Table 3.1).
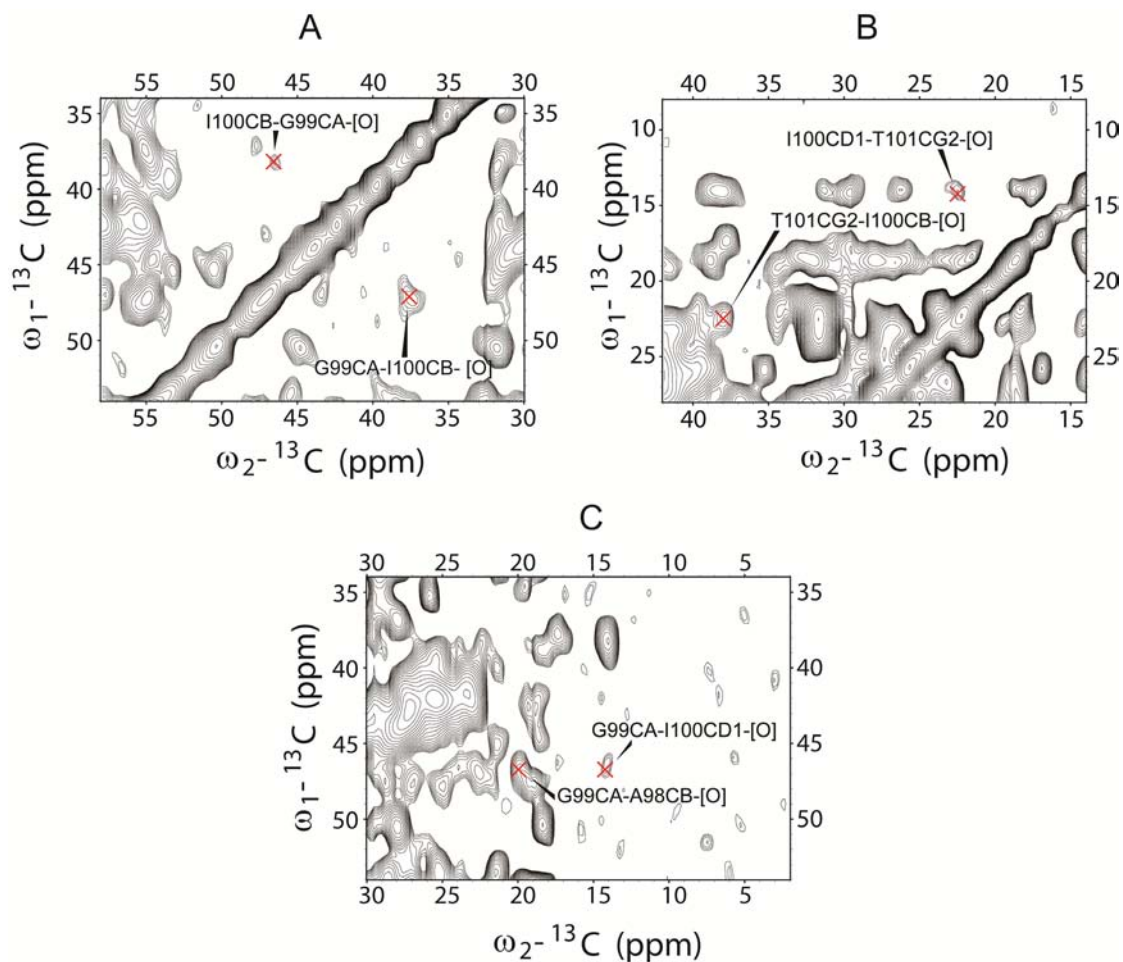

Figure 3.11.The conformation of the activation gate of the KcsA in CL lipid bilayer. [13]C-[13]C 2D PDSD correlation spectrum recorded on KcsA in the presence of 150 mM KCl at pH 4.0 in CL lipid bilayer with a mixing time of 150 ms at 500 MHz [1]H-frequency. Effective sample temperature - 273 K and MAS frequency - 12 kHz. KcsA was reconstituted in proteoliposomes composed of DOPC and CL at 3/7 molar ratio. [O] - chemical shifts corresponding to the open conformation of the activation gate.

Based on ssNMR experiments on KcsA in CL lipid bilayers a signal to noise analysis was performed to estimate the approximate ratio between opened-conductive and opened-collapsed conformations of KcsA. NCA and NCACX spectra have been chosen for this evaluation. The signal to noise analysis revealed that ratio between opened-collapsed and opened-conductive conformations of KcsA in CL is approximately 6/4, meaning that the opened-collapsed conformation is predominant (Figure 3.12). This result is in good agreement with the Po of 0.37 measured for KcsA in CL containing lipid bilayers in the electrophysiological experiments (page 47, Figure 3.5).
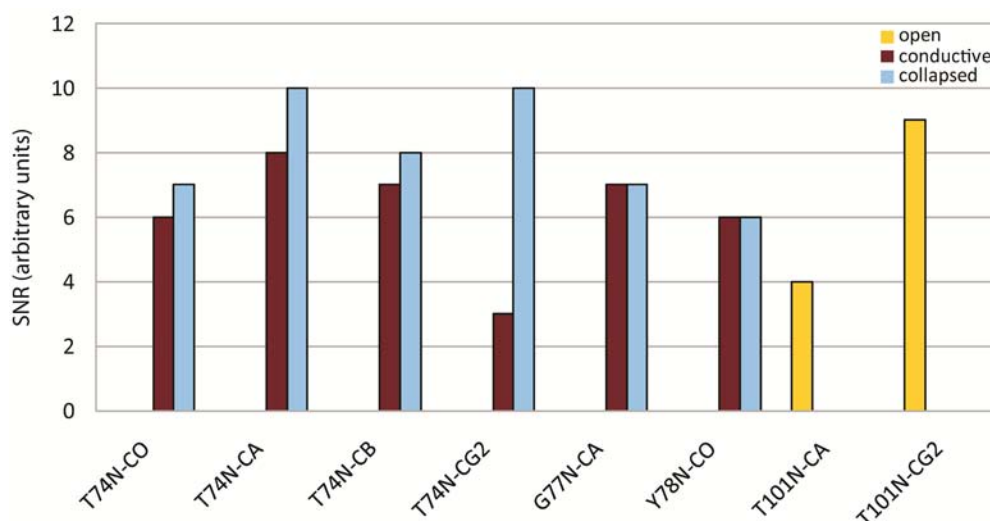

Figure 3.12. Signal to noise analysis of key residues corresponded to selectivity filter and activation gate of KcsA. NCA and NCACX spectra were used for the analysis. The collapsed (inactivated) and conductive conformations of the selectivity filter of the KcsA are indicated in blue and purple respectively. The residues corresponded to the activation gate is indicated in yellow. SNR - signal-to-noise ratio.

3.5. Role of the KcsA turret region in anionic phospholipid modulation of KcsA

3.5.1. Effect of the turret substitution on KcsA phospholipid sensitivity

The results reported above suggest that the headgroup of anionic phospholipids play an important role in modulation of KcsA channel activity. In general, modulation of channel gating and conductance can occur via interaction of anionic phospholipids with the extracellular or intracellular side of the channel. My data suggested that the phospholipids influence the activity of the KcsA inactivation gate. It is located in the part of the channel that is embedded in the membrane facing the extracellular side of the lipid bilayer. The turret region (between Ala 50 and Ala 65) which is located at the extracellular part of KcsA (see "Introduction", Figures 1.2 and 1.3) is one of the potential structures which might be involved in lipid-protein interaction. Therefore, I investigated whether the extracellular turret of KcsA plays a role in anionic phospholipid modulation.

I performed lipid bilayer experiments with varying molar ratios of DOPG anionic phospholipid on KcsA and KcsA-Kv1.3, a chimerical KcsA channel variant containing the turret region of the Kv1.3 channel (*Lange et al., 2006; Ader et al., 2008; Ader et al., 2009*). Representative KcsA and KcsA-Kv1.3 current traces recorded in the lipid bilayer with different DOPG contents are shown in the Figure 3.13.
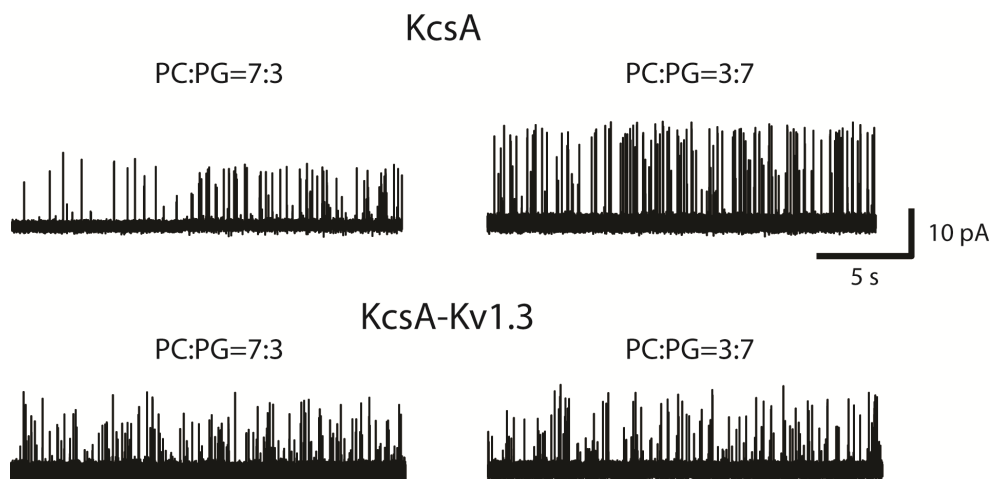

Figure 3.13. Representative current traces of KcsA and KcsA-Kv1.3 recorded at different DOPG molar ratio anionic phospholipid environments. The phospholipid composition is indicated above the current traces. All experiments were performed at +100 mV in symmetrical 150 mM KCl solution at pH = 7.0 on the *cis* side and pH 4 on the *trans* side. The sequence alignment of KcsA and KcsA-Kv1.3 channels are illustrated in the Figure 7.1 on the page 84 ("Appendix").

Comparison of the results showed that KcsA chord conductance significantly increased with increasing molar fraction of DOPG, which matches with previous measurements (*Marius et al., 2008*). In contrast, KcsA-Kv1.3 conductance changed only weakly with varying phospholipid composition (Figure 3.13 and 3.14). The data indicates that extracellular turret region (between Ala 50 and Ala 65) plays an important role for phospholipid sensitivity of the KcsA.
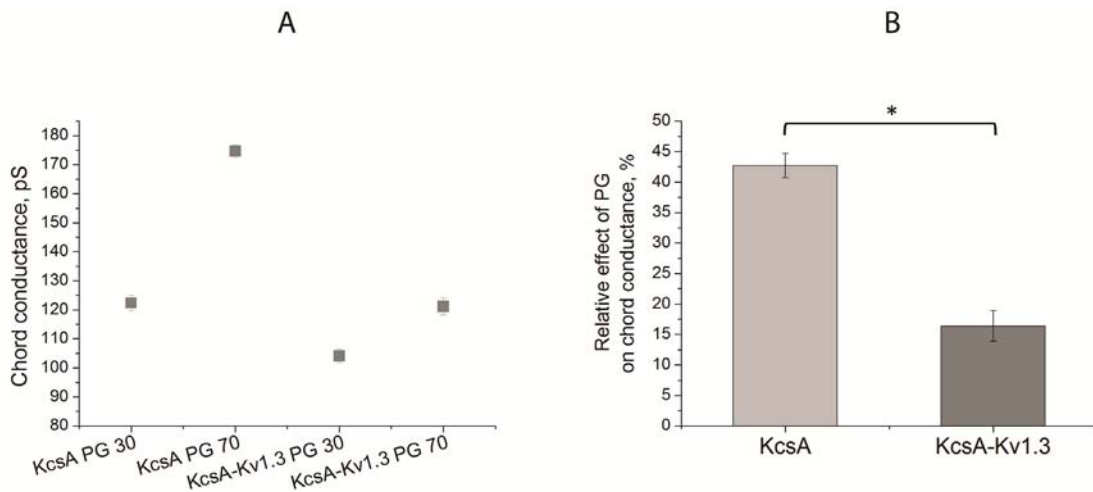

Figure 3.14. Chord conductance calculated for KcsA and KcsA-Kv1.3 recorded at different DOPG molar ratios. **A** - absolute values of chord conductance of KcsA and KcsA-Kv1.3, **B** - relative effect of DOPG on chord conductance of KcsA and KcsA-Kv1.3 potassium channels. All experiments were performed at +100 mV in symmetrical 150 mM KCl solution at pH = 7.0 on the *cis* side and pH 4 on the *trans* side. The graphs represent data from 3-5 independent experiments. * - p < 0.05.

3.5.2. Specific phospholipid binding in KcsA probed by MD simulations

To gain further insight into the nature of differential anionic phospholipid sensitivity of KcsA and KcsA-Kv1.3, coarse grain molecular dynamics (CGMD) simulations using the MARTINI force field (*Marrink et al., 2007*) were performed on the two channels. The CGMD simulations revealed considerable differences in specific phospholipid binding between KcsA and KcsA-Kv1.3. In line with previous experimental studies (*Marius et al., 2008*), the results showed for both channels specific phospholipid binding on the µs timescale. Lifetimes of bound phospholipids, however, differed by approximately one order of magnitude, especially for PG binding, being significantly longer in the case of KcsA in comparison to KcsA-Kv1.3 (Figure 3.15).
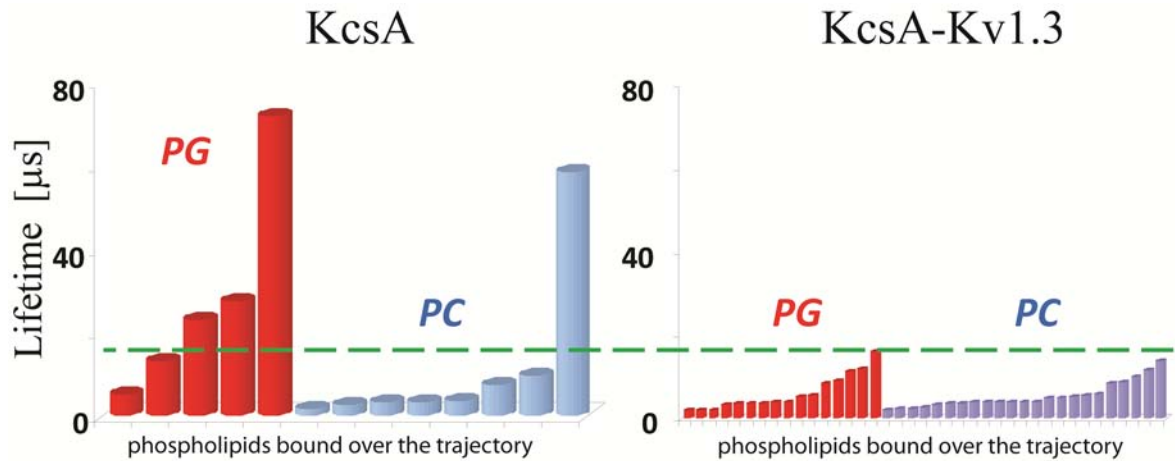
Figure 3.15. Specific phospholipid binding in KcsA probed by CGMD simulations Evaluation of the lifetimes of bound PG (red) and PC (blue) for lipid binding sites of KcsA and KcsA-Kv1.3 over trajectories of 100 μs. The first 10 μs were considered as equilibration period. The type of the K^+ channel is indicated on the upper panel.

3.5.3. Effect of anionic phospholipids on KcsA turret probed by ssNMR

It has been shown previously by combining ssNMR spectroscopical and electrophysiological studies that the KcsA-Kv1.3 turret region is involved in C-type inactivation. The signal for Ala 50 (A50CA-CB), which is one of the residues in the turret region, was observed only for the closed-conductive channel (pH 7.5, in asolectin), while it was too broad to be detected in the ^{13}C-^{13}C 2D PDSD correlation spectrum in asolectin at pH 4.0, which represented the opened-inactivated conformation of the channel (*Nand, 2011*). In my study, in the ^{13}C-^{13}C 2D PDSD correlation spectrum Ala 50 signal (A50CA-CB) also was observed for the closed-conductive conformation of KcsA in asolectin at pH 7.5 (gray spectrum in Figure 3.16). When KcsA was reconstituted in DOPG and DOPA at pH 4.0, the A50CA-CB signal on the ^{13}C-^{13}C 2D PDSD correlation spectrum was undetectable (Figure 3.16: red and blue spectra for DOPG and DOPA, respectively). By contrast, in presence of CL at pH 4.0, the A50CA-CB signal was observed (orange spectrum in Figure 3.16).

Thus, the effect of CL on KcsA channel activity was correlated with structural changes in the turret region, which confirms, in agreement with my functional and CGMD simulation experiments, the importance of the turret region in anionic phospholipid modulation of KcsA channel.
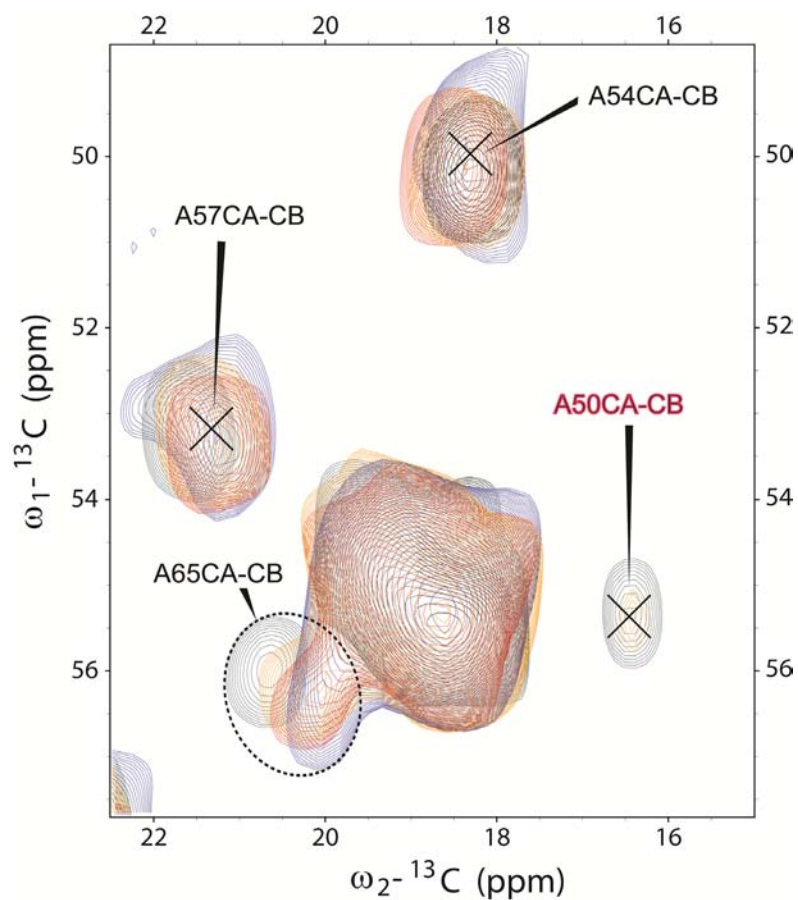
_____

Figure 3.16. The Ala-region of KcsA in ^{13}C-^{13}C 2D PDSD correlation spectrum recorded on in the presence of 150 mM KCl at pH 4.0 in different anionic phospholipid environment with a mixing time of 30 ms at 500 MHz ^{1}H-frequency. Effective sample temperature - 273 K and MAS frequency - 12 kHz. KcsA was reconstituted in proteoliposomes composed of DOPC and DOPG (DOPA or CL) at 3/7 molar ratio. Grey - asolectin pH 7.5, blue - DOPA pH 4.0, red - DOPG pH 4.0; orange - CL pH 4.0.

4. Discussion

The purpose of my study was to investigate structural and functional aspects of KcsA potassium channel modulation by anionic phospholipids, utilizing a combination of functional and structural tools including electrophysiology, ssNMR spectroscopy and MD simulations.

4.1. Functional modulation of KcsA by anionic phospholipids

Single channel recordings of KcsA, reconstituted in planar lipid bilayers revealed that KcsA single channel properties are affected by anionic phospholipids. I observed that anionic phospholipids modulate both single channel conductance and gating. Previously, it has been shown that PG, which is negatively charged, increases both P_O and single channel conductance of KcsA (*Marius et al., 2008*). It was proposed that the effect of PG on KcsA single channel properties is associated with charge-specific binding of negatively charged anionic phospholipids with *non-annular* lipid binding sites located between two adjacent KcsA subunits (*Marius et al., 2012; Marius et al., 2008).* My study shows that the mechanism of anionic phospholipid influence on KcsA might be more complex. I observed a correlation between phospholipid headgroup charge and KcsA P_O. P_O was high in a lipidic environment with more negatively charged headgroups, such as DOPA (-1.3) and CL (-2), and comparably low in a lipidic environments with less negatively charged head groups, such as DOPG (-1) and in DOPS (-1). Maximal P_O was observed in the presence of CL, which has the highest headgroup charge among the anionic phospholipids tested (page 47, Figure 3.5). However, the effect of anionic phospholipids on single channel conductance showed no significant correlation with phospholipid headgroup charge: both DOPG having one negative charge, and CL having two negative charges, shifted the KcsA to the high conductance mode (page 46, Figure 3.4). The data, therefore, suggests that not the charge, but the structure of the lipid headgroup affects KcsA conductance. Note that the effect of the anionic phospholipids on KcsA conductance was observed only at positive potentials, significantly affecting the outward rectification properties of the KcsA (page 46, Figure 3.4B). The rectification is generally linked to a voltage-dependent block of the conduction pathway. For K_{ir}

_____

channels it has been shown that strong inward rectification is associated with voltage-dependent block of the channel by multivalent ions of the cytoplasm, Mg^{2+} and polyamines, such as spermine, spermidine and putrescine (*Hille, 2001*). For KcsA potassium channels, Ba^{2+} and Na^+ voltage-dependent blocks were shown (*Cheng et al., 2011; Nimigean and Miller, 2002; Piasta et al., 2011*). I always used ultra-pure chemicals in the experiments. Most likely, this rules out contaminating effects of Na^+ although I used lipids as sodium salts. Previously, it was shown that KcsA outward rectification is a very robust phenomenon, being identical if the channel was recorded in solutions made of reagent-grade or ultra-pure KCl, or solutions containing different types of pH buffers (*LeMasurier et al., 2001*).

The analysis of single channel KcsA current-voltage curves revealed that in the presence of DOPG and CL, the KcsA current-voltage relation was slightly shifted to more depolarized potentials. This shift is probably due to a surface charge effect of the negatively charged lipids. More important is the observation that current-voltage relations are significantly steeper than in the presence of DOPA and DOPS, combined with a gradual increase of single channel conductance at positive potentials.

Analysis of the dwell time histograms revealed that both opened and closed durations of KcsA are comprised of multiple kinetic components, which corroborates previous studies (*Chakrapani et al., 2007; Irizarry et al., 2002*). My findings suggest that the effect of anionic phospholipids on closed and opened durations of the KcsA depends on phospholipid headgroup charge. More negatively charged headgroups reduce the mean closed (inactivated) time of the channel and, thereby, increase its mean opened time, resulting in an overall increase in channel P_O (page 47, Figure 3.5). Moreover, I observed a variation in the number of opened states. In the presence of less negatively charged headgroups, such as DOPG (-1) and in DOPS (-1) KcsA exhibited two opened states. While in the lipidic environment with more negatively charged headgroups DOPA (-1.3) and CL (-2), respectively, three distinct opened states were detected (page 49, Figure 3.6; page 51, Table 3.1 and page 53, Figure 3.7). The variation in the number of opened states suggests that anionic phospholipids influence modal gating of the KcsA channel.

The modal gating behavior of KcsA has been previously demonstrated (*Chakrapani et al., 2011; Chakrapani et al., 2007*). Modal gating is not unique to KcsA. It has been also observed with other K^+ channels, in which time-dependent

_____

single channel activity can switch abruptly between periods of high and low P_O, under fixed experimental conditions (*Cooper and Shrier, 1989; Dreyer et al., 2001; Singer-Lahat et al., 1999; Stuhmer et al., 1988*). The modal gating behavior of the channel represent an effective regulatory mechanism by which ion channels control the ionic fluxes (*Chakrapani et al., 2011*). My data shows that K^+ channel modal gating behavior can be modulated by anionic phospholipids.

Taking together, my functional data shows that modulation of KcsA single channel properties involves at least two different pathways: one, which is sensitive to phospholipid headgroup charge, and another one, which depends on headgroup structure. The latter pathway probably involves a specific interaction of phospholipid headgroup with the KcsA channel (Figure 4.1).
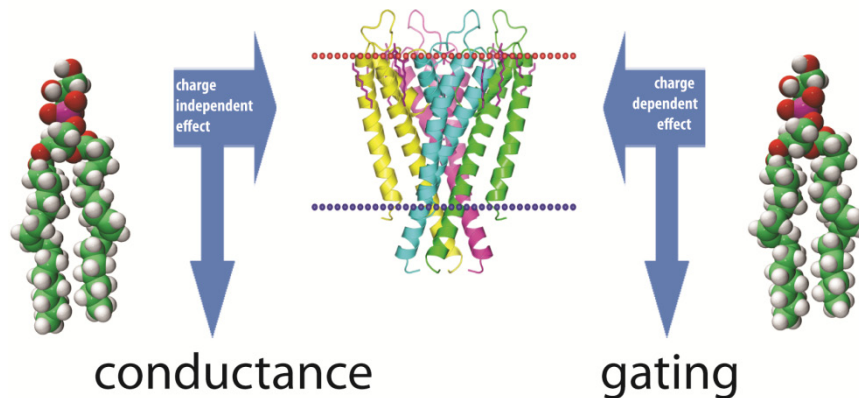

Figure 4.1. The proposed mechanism of anionic phospholipid modulation of the KcsA potassium channel. KcsA is shown in the middle of the figure as ribbon diagram. Anionic phospholipids are indicated in the left and right panels. The red and blue dashed lines represent approximate limits of the membrane.

_____

4.2. Structural basis of KcsA modulation by anionic phospholipids

It is still difficult to study the structure of membrane proteins in their native environment. So far, it has been impossible to obtain crystal structures of proteoliposomes, for example. At present, ssNMR spectroscopy is the method of choice to characterize the structure of membrane proteins in a lipid environment (*Renault et al., 2010*). Fortunately, it has been shown that the structure of KcsA related KcsA-Kv1.3 chimera is amenable to detailed ssNMR spectroscopic analysis (*Ader et al., 2010; Ader et al., 2009; Ader et al., 2008; Legros et al., 2000; Legros et al., 2002*). The data showed two distinct conformations of K^+ channel pore domain: i) a closed-conductive conformation where the activation gate of the channel is closed and the inactivation gate is opened; ii) open-inactivated (collapsed) conformation where the activation gate is open, but the selectivity filter is collapsed (closed inactivation gate), so that the channel is inactivated and cannot conduct ions (*Ader et al., 2009; Ader et al., 2008*).

Importantly, the conformation of the opened-conductive state of KcsA in the lipid bilayer is still unknown. This is most likely due to the very short lifetime of this state during KcsA gating (*Cordero-Morales et al., 2006*) reflected by low P_O of KcsA at steady-state conditions. Determination of the structure of the open-conductive state of KcsA in lipid environment, where activation gate and inactivation gate are open, is, however, crucial for a detailed understanding of the molecular mechanism of K^+ channel gating.

My data shows that the conformation of the KcsA selectivity filter is modulated by anionic phospholipid environment. I observed opened-collapsed conformation of KcsA in the presence of DOPG and DOPA at pH 4.0. In the presence of CL both, opened-collapsed and opened-conductive conformations were detected. CL is more negatively charged than the other anionic phospholipids, that I investigated. Possibly, CL markedly reduces KcsA C-type inactivation enabling a detection of the open-conductive conformation of the selectivity filter of KcsA. The interpretation of the ssNMR results is consistent with results of the electrophysiological experiments that showed a significant attenuation of inactivation in CL in comparison to DOPA and DOPG.
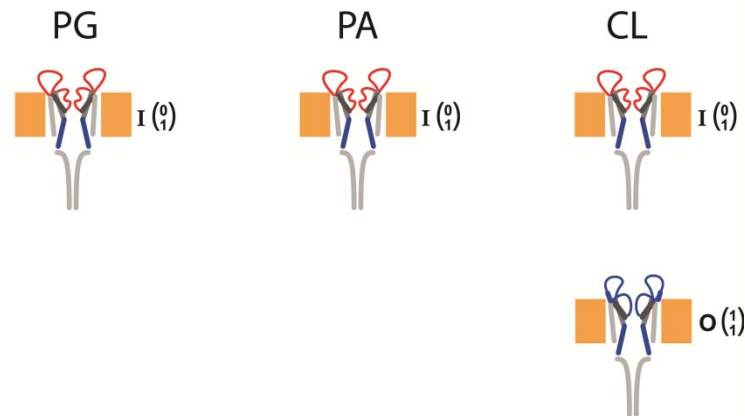
Figure 4.2. The cartoon representation of anionic phospholipids influence on the conformation of the selectivity filter of KcsA. Two conformations of the channel are shown. I - open-inactivated (collapsed) state (0 - inactivation gate is closed; 1- activation gate is open). O - open-conductive state (1 - inactivation gate is open; 1- activation gate is open). Lipid bilayer is indicated in orange. Conductive conformation of the selectivity filter is shown in blue. Collapsed (inactivated) conformation of the selectivity filter is indicated in red.

In summary, the ssNMR results showed a marked effect of CL on the selectivity filter conformation of KcsA. Obviously, CL stabilizes at pH 4.0 the opened-conductive state of the channel (Figure 4.2).

4.3. Role of the turret region in functional KcsA-lipid interactions

The turret region of KcsA faces the extracellular side (page 6, Figure 1.3B). This localization predestines the turret region to interact with the surrounding lipids, especially with lipid headgroups. It has been shown that mutations introduced in the turret region have a profound effect on the K$^+$ channel C-type inactivation and K:Na selectivity (*Liu et al., 2002*). Taking into consideration that the turret region interacts with some residues of KcsA within the P-helix and P-loop (*Broomand et al., 2007*), this structure is well suited to play a role in anionic phospholipid modulation of KcsA. Indeed, my data show that KcsA turret (A50-A65) region is involved in phospholipid modulation of the channel. In contrast to KcsA, where, as discussed above, chord conductance increases with increasing concentration of negatively charged DOPG, KcsA-Kv1.3 which has modified turret region (page 84, Figure 7.1), chord conductance is relatively insensitive to changes in lipid environment (page 62, Figure 3.13 and page 63, Figure 3.14). The data indicate that the extracellular turret region (between Ala 50 and Ala 65) plays an important role for phospholipid sensitivity of the KcsA.

It was shown previously that at pH 4.0 when the channel is at open-collapsed conformation, the cross-correlation between Ala 50-CA and Ala 50-CB in the ^{13}C, ^{13}C-correlation spectra is attenuated, which shows that upon transition from closed-conductive to opened-collapsed state the turret region undergoes a structural change (*Ader et al., 2008; Nand, 2011*). I observed in ssNMR ^{13}C, ^{13}C-corelation spectra of CL-containing proteoliposomes that the opened-conductive conformation was correlated with appearance of a defined Ala 50CA-CB correlation (page 65, Figure 3.16). It suggests that CL stabilizes via an interaction with the turret an opened-conductive conformation of the selectivity filter of KcsA.

Furthermore, MD simulation confirms that the turret region plays an important role in KcsA modulation by anionic phospholipids. The CGMD simulations revealed considerable differences in specific phospholipid binding between KcsA and KcsA-Kv1.3. While specific lipid binding to the inter-subunit binding site was observed for both channels on the μs timescale, lifetimes of bound phospholipids were about one order of magnitude longer for KcsA, in particular for negatively charged PG, than for KcsA-Kv1.3 (page 64, Figure 3.15).

Thus, functional, structural and MD simulation data signify a role of the turret region in phospholipid modulation of KcsA. There are several possible explanations for the importance of this region in channel modulation by anionic phospholipids. First, this region contains the Arg 64 residue, which together with Arg 89 forms a specific *non-annular* binding site for anionic phospholipids (*Deol et al., 2006; Marius et al., 2008*). A [^{31}P]-ssNMR study conducted on liposomes with and without KcsA provided direct evidence of anionic phospholipid binding to the Arg 64-Arg 89 *non-annular* binding site (*Marius et al., 2012*). It was shown also that substitution of Arg 64 and Arg 89 by neutral Leu appears to act synergistically to reduce the P_O of KcsA (*Marius et al., 2012*). However, other positively charged residue(s) of the turret region might also be involved in the phospholipid modulation, for example Arg 52 (*Raja, 2011*). Indeed, in KcsA-Kv1.3 Arg 52 is replaced by Ala. It has been shown that the KcsA turret forms close connections with the conserved Trp68 of the P-helix and Pro83 of the P-loop (*Broomand et al., 2007; Elinder and Arhem, 1999*). Therefore, conformational rearrangements within the turret induced by its interaction with anionic phospholipids may affect gating of the KcsA potassium channel. In this case, the charge of the entire turret region might be important for anionic phospholipid modulation of the K$^+$ channel. This, however, needs further investigation.

5. Conclusion

KcsA single channel properties are modulated by the surrounding phospholipids. The modulation involves the charge of the phospholipid headgroup as well as the structure of the phospholipid headgroup. Taking into consideration that KcsA is a prototype of the K^+ channel pore, phospholipid influence on KcsA properties may be a common feature in the K^+ channel family.

SsNMR data revealed that anionic phospholipids affect the conformation of the KcsA selectivity filter. In particular, CL, which was the most negatively charged phospholipid among the tested phospholipids, renders the selectivity filter conformation of KcsA at pH 4.0 opened and conductive. The data suggest that the conductive conformation of the KcsA selectivity filter is stabilized by CL, because the observed structural changes lead to a marked reduction of KcsA C-type inactivation. In agreement with this notion, electrophysiological experiments showed a significant reduction of C-type inactivation in CL in comparison to other anionic phospholipids such as DOPA and DOPG.

A combination of functional, structural and MD simulation data indicated that the turret region of KcsA plays a significant role in phospholipid – channel interaction. Hence, I propose that interaction of negatively charged anionic phospholipids with the KcsA turret region evokes structural rearrangements within the selectivity filter affecting KcsA single channel properties.

6. References

Adelman, J.P., Shen, K.Z., Kavanaugh, M.P., Warren, R.A., Wu, Y.N., Lagrutta, A., Bond, C.T., and North, R.A. (1992). Calcium-activated potassium channels expressed from cloned complementary DNAs. Neuron *9*, 209-216.

Ader, C., Pongs, O., Becker, S., and Baldus, M. (2010). Protein dynamics detected in a membrane-embedded potassium channel using two-dimensional solid-state NMR spectroscopy. Biochimica et biophysica acta *1798*, 286-290.

Ader, C., Schneider, R., Hornig, S., Velisetty, P., Vardanyan, V., Giller, K., Ohmert, I., Becker, S., Pongs, O., and Baldus, M. (2009). Coupling of activation and inactivation gate in a K+-channel: potassium and ligand sensitivity. EMBO J *28*, 2825-2834.

Ader, C., Schneider, R., Hornig, S., Velisetty, P., Wilson, E.M., Lange, A., Giller, K., Ohmert, I., Martin-Eauclaire, M.F., Trauner, D*., et al.* (2008). A structural link between inactivation and block of a K$^+$ channel. Nature structural & molecular biology *15*, 605-612.

Aidley, D.J., and Stanfield, P.R. (1996). Ion channels : molecules in action (Cambridge ; New York: Cambridge University Press).

Aldrich, R.W. (2001). Fifty years of inactivation. Nature *411*, 643-644.

Alexander, S., Mathie, A., and Peters, J. (2008). Guide to Receptors and Channels (GRAC), 3rd edition. British journal of pharmacology *153 Suppl 2*, 209.

Armstrong, C.M. (1969). Inactivation of the potassium conductance and related phenomena caused by quaternary ammonium ion injection in squid axons. J Gen Physiol *54*, 553-575.

Armstrong, C.M. (2003). Voltage-gated K channels. Science's STKE : signal transduction knowledge environment *2003*, re10.

Atkinson, N.S., Robertson, G.A., and Ganetzky, B. (1991). A component of calcium-activated potassium channels encoded by the Drosophila slo locus. Science *253*, 551-555.

Baldus, M., Petkova, A.T., Herzfeld, J., and Griffin, R.G. (1998). Cross polarization in the tilted frame: assignment and spectral simplification in heteronuclear spin systems. Mol Phys *95*, 1197-1207.

Bertini I., McGreevy K., Parigi G.. (2012). NMR of biomolecules (Wiley-Blackwll).

Blunck, R., Cordero-Morales, J.F., Cuello, L.G., Perozo, E., and Bezanilla, F. (2006). Detection of the opening of the bundle crossing in KcsA with fluorescence lifetime spectroscopy reveals the existence of two gates for ion conduction. J Gen Physiol *128*, 569-581.

Broomand, A., Osterberg, F., Wardi, T., and Elinder, F. (2007). Electrostatic domino effect in the Shaker K channel turret. Biophysical journal *93*, 2307-2314.

References

Cahalan, M.D., Wulff, H., and Chandy, K.G. (2001). Molecular properties and physiological roles of ion channels in the immune system. Journal of clinical immunology *21*, 235-252.

Chakrapani, S., Cordero-Morales, J.F., Jogini, V., Pan, A.C., Cortes, D.M., Roux, B., and Perozo, E. (2011). On the structural basis of modal gating behavior in K^+ channels. Nature structural & molecular biology *18*, 67-74.

Chakrapani, S., Cordero-Morales, J.F., and Perozo, E. (2007a). A quantitative description of KcsA gating I: macroscopic currents. J Gen Physiol *130*, 465-478.

Chakrapani, S., Cordero-Morales, J.F., and Perozo, E. (2007b). A quantitative description of KcsA gating II: single-channel currents. J Gen Physiol *130*, 479-496.

Cheng, W.W., McCoy, J.G., Thompson, A.N., Nichols, C.G., and Nimigean, C.M. (2011). Mechanism for selectivity-inactivation coupling in KcsA potassium channels. Proceedings of the National Academy of Sciences of the United States of America *108*, 5272-5277.

Cooper, E., and Shrier, A. (1989). Inactivation of A currents and A channels on rat nodose neurons in culture. J Gen Physiol *94*, 881-910.

Cordero-Morales, J.F., Cuello, L.G., and Perozo, E. (2006a). Voltage-dependent gating at the KcsA selectivity filter. Nature structural & molecular biology *13*, 319-322.

Cordero-Morales, J.F., Cuello, L.G., Zhao, Y., Jogini, V., Cortes, D.M., Roux, B., and Perozo, E. (2006b). Molecular determinants of gating at the potassium-channel selectivity filter. Nature structural & molecular biology *13*, 311-318.

Cordero-Morales, J.F., Jogini, V., Chakrapani, S., and Perozo, E. (2011). A multipoint hydrogen-bond network underlying KcsA C-type inactivation. Biophysical journal *100*, 2387-2393.

Cortes, D.M., Cuello, L.G., and Perozo, E. (2001). Molecular architecture of full-length KcsA: role of cytoplasmic domains in ion permeation and activation gating. J Gen Physiol *117*, 165-180.

Cuello, L.G., Jogini, V., Cortes, D.M., Pan, A.C., Gagnon, D.G., Dalmas, O., Cordero-Morales, J.F., Chakrapani, S., Roux, B., and Perozo, E. (2010a). Structural basis for the coupling between activation and inactivation gates in K^+ channels. Nature *466*, 272-275.

Cuello, L.G., Jogini, V., Cortes, D.M., and Perozo, E. (2010b). Structural mechanism of C-type inactivation in K^+ channels. Nature *466*, 203-208.

Cuello, L.G., Romero, J.G., Cortes, D.M., and Perozo, E. (1998). pH-dependent gating in the Streptomyces lividans K^+ channel. Biochemistry *37*, 3229-3236.

Deol, S.S., Domene, C., Bond, P.J., and Sansom, M.S. (2006). Anionic phospholipid interactions with the potassium channel KcsA: simulation studies. Biophysical journal *90*, 822-830.

References

Doyle, D.A., Morais Cabral, J., Pfuetzner, R.A., Kuo, A., Gulbis, J.M., Cohen, S.L., Chait, B.T., and MacKinnon, R. (1998). The structure of the potassium channel: molecular basis of K+ conduction and selectivity. Science *280*, 69-77.

Dreyer, I., Michard, E., Lacombe, B., and Thibaud, J.B. (2001). A plant Shaker-like K^+ channel switches between two distinct gating modes resulting in either inward-rectifying or "leak" current. FEBS Lett *505*, 233-239.

Dunn, K.M., and Nelson, M.T. (2010). Potassium channels and neurovascular coupling. Circulation journal : official journal of the Japanese Circulation Society *74*, 608-616.

Elinder, F., and Arhem, P. (1999). Role of individual surface charges of voltage-gated K channels. Biophysical journal *77*, 1358-1362.

Escriba, P.V., Gonzalez-Ros, J.M., Goni, F.M., Kinnunen, P.K., Vigh, L., Sanchez-Magraner, L., Fernandez, A.M., Busquets, X., Horvath, I., and Barcelo-Coblijn, G. (2008). Membranes: a meeting point for lipids, proteins and therapies. Journal of cellular and molecular medicine *12*, 829-875.

Fanger, C., Ghanshani, S., Logsdon, N., Rauer, H., Kalman, K., Zhou, J., Beckingham, K., Chandy, K., Cahalan, M., and Aiyar, J. (1999). Calmodulin mediates calcium-dependent activation of the intermediate conductance KCa channel, IKCa1. The Journal of biological chemistry *274*, 5746-5800.

Félétou, M. (2009). Calcium-activated potassium channels and endothelial dysfunction: therapeutic options? British journal of pharmacology *156*, 545-607.

Fink, M., Duprat, F., Lesage, F., Reyes, R., Romey, G., Heurteaux, C., and Lazdunski, M. (1996). Cloning, functional expression and brain localization of a novel unconventional outward rectifier K+ channel. EMBO J *15*, 6854-6862.

Goudreau, P.N., and Stock, A.M. (1998). Signal transduction in bacteria: molecular mechanisms of stimulus-response coupling. Current opinion in microbiology *1*, 160-169.

Gross, A., Columbus, L., Hideg, K., Altenbach, C., and Hubbell, W.L. (1999). Structure of the KcsA potassium channel from Streptomyces lividans: a site-directed spin labeling study of the second transmembrane segment. Biochemistry *38*, 10324-10335.

Gutman, G., Chandy, K., Adelman, J., Aiyar, J., Bayliss, D., Clapham, D., Covarriubias, M., Desir, G., Furuichi, K., Ganetzky, B.*, et al.* (2003). International Union of Pharmacology. XLI. Compendium of voltage-gated ion channels: potassium channels. Pharmacological reviews *55*, 583-589.

Heginbotham, L., Kolmakova-Partensky, L., and Miller, C. (1998). Functional reconstitution of a prokaryotic K^+ channel. J Gen Physiol *111*, 741-749.

Heginbotham, L., LeMasurier, M., Kolmakova-Partensky, L., and Miller, C. (1999). Single streptomyces lividans K^+ channels: functional asymmetries and sidedness of proton activation. J Gen Physiol *114*, 551-560.

References

_____

Heginbotham, L., Lu, Z., Abramson, T., and MacKinnon, R. (1994). Mutations in the K^+ channel signature sequence. Biophysical journal *66*, 1061-1068.

Heginbotham, L., Odessey, E., and Miller, C. (1997). Tetrameric stoichiometry of a prokaryotic K^+ channel. Biochemistry *36*, 10335-10342.

Hille, B. (2001). Ion channels of excitable membranes, 3rd edn (Sunderland, Mass.: Sinauer).

Ho, K., Nichols, C.G., Lederer, W.J., Lytton, J., Vassilev, P.M., Kanazirska, M.V., and Hebert, S.C. (1993). Cloning and expression of an inwardly rectifying ATP-regulated potassium channel. Nature *362*, 31-38.

Hodgkin, A.L., and Huxley, A.F. (1952). A quantitative description of membrane current and its application to conduction and excitation in nerve. The Journal of physiology *117*, 500-544.

Hoffmann, E.K. (2011). Ion channels involved in cell volume regulation: effects on migration, proliferation, and programmed cell death in non adherent EAT cells and adherent ELA cells. Cellular physiology and biochemistry : international journal of experimental cellular physiology, biochemistry, and pharmacology *28*, 1061-1078.

Hoshi, T., Zagotta, W.N., and Aldrich, R.W. (1990). Biophysical and molecular mechanisms of Shaker potassium channel inactivation. Science *250*, 533-538.

Hoshi, T., Zagotta, W.N., and Aldrich, R.W. (1991). Two types of inactivation in Shaker K^+ channels: effects of alterations in the carboxy-terminal region. Neuron *7*, 547-556.

Huopio, H., Shyng, S.L., Otonkoski, T., and Nichols, C.G. (2002). K(ATP) channels and insulin secretion disorders. American journal of physiology Endocrinology and metabolism *283*, E207-216.

Irizarry, S.N., Kutluay, E., Drews, G., Hart, S.J., and Heginbotham, L. (2002). Opening the KcsA K^+ channel: tryptophan scanning and complementation analysis lead to mutants with altered gating. Biochemistry *41*, 13653-13662.

Jiang, Y., Lee, A., Chen, J., Cadene, M., Chait, B.T., and MacKinnon, R. (2002). The open pore conformation of potassium channels. Nature *417*, 523-526.

Joiner, W., Wang, L., Tang, M., and Kaczmarek, L. (1997). hSK4, a member of a novel subfamily of calcium-activated potassium channels. Proceedings of the National Academy of Sciences of the United States of America *94*, 11013-11021.

Kamb, A., Iverson, L.E., and Tanouye, M.A. (1987). Molecular characterization of Shaker, a Drosophila gene that encodes a potassium channel. Cell *50*, 405-413.

Kamnesky, G., Shaked, H., and Chill, J. (2012). The distal C-terminal region of the KcsA potassium channel is a pH-dependent tetramerization domain. Journal of molecular biology *418*, 237-284.

Keeler, J. (2010). Understanding NMR spectroscopy, 2nd edn (Chichester, U.K.: John Wiley and Sons).

References

_____

Ketchum, K.A., Joiner, W.J., Sellers, A.J., Kaczmarek, L.K., and Goldstein, S.A. (1995). A new family of outwardly rectifying potassium channel proteins with two pore domains in tandem. Nature *376*, 690-695.

Kew, J.N.C., and Davies, C.H. (2010). Ion channels : from structure to function, 2nd edn (Oxford ; New York: Oxford University Press).

Kim, J., and Hoffman, D.A. (2008). Potassium channels: newly found players in synaptic plasticity. The Neuroscientist : a review journal bringing neurobiology, neurology and psychiatry *14*, 276-286.

Kiss, L., LoTurco, J., and Korn, S.J. (1999). Contribution of the selectivity filter to inactivation in potassium channels. Biophysical journal *76*, 253-263.

Kurachi, Y., and Ishii, M. (2004). Cell signal control of the G protein-gated potassium channel and its subcellular localization. The Journal of physiology *554*, 285-294.

Lang, F. (2007). Mechanisms and significance of cell volume regulation. Journal of the American College of Nutrition *26*, 613S-623S.

Lange, A., Giller, K., Hornig, S., Martin-Eauclaire, M.F., Pongs, O., Becker, S., and Baldus, M. (2006a). Toxin-induced conformational changes in a potassium channel revealed by solid-state NMR. Nature *440*, 959-962.

Lange, A., Giller, K., Pongs, O., Becker, S., and Baldus, M. (2006b). Two-dimensional solid-state NMR applied to a chimeric potassium channel. Journal of receptor and signal transduction research *26*, 379-393.

Latorre, R., and Brauchi, S. (2006). Large conductance Ca^{2+}-activated K^+ (BK) channel: activation by Ca^{2+} and voltage. Biological research *39*, 385-401.

Lee, A.G. (2004). How lipids affect the activities of integral membrane proteins. Biochimica et biophysica acta *1666*, 62-87.

Legros, C., Pollmann, V., Knaus, H.G., Farrell, A.M., Darbon, H., Bougis, P.E., Martin-Eauclaire, M.F., and Pongs, O. (2000). Generating a high affinity scorpion toxin receptor in KcsA-Kv1.3 chimeric potassium channels. The Journal of biological chemistry *275*, 16918-16924.

Legros, C., Schulze, C., Garcia, M.L., Bougis, P.E., Martin-Eauclaire, M.F., and Pongs, O. (2002). Engineering-specific pharmacological binding sites for peptidyl inhibitors of potassium channels into KcsA. Biochemistry *41*, 15369-15375.

LeMasurier, M., Heginbotham, L., and Miller, C. (2001). KcsA: it's a potassium channel. J Gen Physiol *118*, 303-314.

Lesage, F., Guillemare, E., Fink, M., Duprat, F., Lazdunski, M., Romey, G., and Barhanin, J. (1996a). A pH-sensitive yeast outward rectifier K^+ channel with two pore domains and novel gating properties. The Journal of biological chemistry *271*, 4183-4190.

References

Lesage, F., Guillemare, E., Fink, M., Duprat, F., Lazdunski, M., Romey, G., and Barhanin, J. (1996b). TWIK-1, a ubiquitous human weakly inward rectifying K^+ channel with a novel structure. EMBO J *15*, 1004-1011.

Liu, Y., Jurman, M.E., and Yellen, G. (1996). Dynamic rearrangement of the outer mouth of a K^+ channel during gating. Neuron *16*, 859-867.

Liu, Y.S., Sompornpisut, P., and Perozo, E. (2001). Structure of the KcsA channel intracellular gate in the open state. Nature structural biology *8*, 883-887.

Longden, T.A., Dunn, K.M., Draheim, H.J., Nelson, M.T., Weston, A.H., and Edwards, G. (2011). Intermediate-conductance calcium-activated potassium channels participate in neurovascular coupling. Br J Pharmacol *164*, 922-933.

Loots, E., and Isacoff, E.Y. (1998). Protein rearrangements underlying slow inactivation of the Shaker K^+ channel. J Gen Physiol *112*, 377-389.

Lopez-Barneo, J., Hoshi, T., Heinemann, S.H., and Aldrich, R.W. (1993). Effects of external cations and mutations in the pore region on C-type inactivation of Shaker potassium channels. Receptors & channels *1*, 61-71.

MacKinnon, R. (2003). Potassium channels. FEBS letters *555*, 62-67.

MacKinnon, R. (2004). Potassium channels and the atomic basis of selective ion conduction (Nobel Lecture). Angewandte Chemie (International ed in English) *43*, 4265-4342.

Marius, P., Alvis, S.J., East, J.M., and Lee, A.G. (2005). The interfacial lipid binding site on the potassium channel KcsA is specific for anionic phospholipids. Biophysical journal *89*, 4081-4089.

Marius, P., de Planque, M.R., and Williamson, P.T. (2012). Probing the interaction of lipids with the non-annular binding sites of the potassium channel KcsA by magic-angle spinning NMR. Biochimica et biophysica acta *1818*, 90-96.

Marius, P., Zagnoni, M., Sandison, M.E., East, J.M., Morgan, H., and Lee, A.G. (2008). Binding of anionic lipids to at least three nonannular sites on the potassium channel KcsA is required for channel opening. Biophysical journal *94*, 1689-1698.

Markley, J.L., Bax, A., Arata, Y., Hilbers, C.W., Kaptein, R., Sykes, B.D., Wright, P.E., and Wuthrich, K. (1998). Recommendations for the presentation of NMR structures of proteins and Nucleic Acids (Reprinted from Pure and Applied Chemistry, vol 70, pgs 117-142, 1998). Journal of molecular biology *280*, 933-952.

Marrink, S.J., Risselada, H.J., Yefimov, S., Tieleman, D.P., and de Vries, A.H. (2007). The MARTINI force field: coarse grained model for biomolecular simulations. The journal of physical chemistry B *111*, 7812-7824.

Meuser, D., Splitt, H., Wagner, R., and Schrempf, H. (1999). Exploring the open pore of the potassium channel from Streptomyces lividans. FEBS Lett *462*, 447-452.

Miller, C. (1986). Ion channel reconstitution (New York: Plenum Press).

Miller, C. (2000). An overview of the potassium channel family. Genome biology *1*, REVIEWS0004.

Molina, M.L., Encinar, J.A., Barrera, F.N., Fernandez-Ballester, G., Riquelme, G., and Gonzalez-Ros, J.M. (2004). Influence of C-terminal protein domains and protein-lipid interactions on tetramerization and stability of the potassium channel KcsA. Biochemistry *43*, 14924-14931.

Morais-Cabral, J.H., Zhou, Y., and MacKinnon, R. (2001). Energetic optimization of ion conduction rate by the K+ selectivity filter. Nature *414*, 37-42.

Mueller, P., Rudin, D.O., Tien, H.T., and Wescott, W.C. (1962). Reconstitution of cell membrane structure in vitro and its transformation into an excitable system. Nature *194*, 979-980.

Nand D. (2011). Solid-state NMR on complex biomolecules: Novel methods and applications. (Doctoral thesis, ISBN 978-90-393-5635-7)

Nerbonne, J.M. (2000). Molecular basis of functional voltage-gated K^+ channel diversity in the mammalian myocardium. The Journal of physiology *525 Pt 2*, 285-298.

Niemeyer, M.I., Cid, L.P., Barros, L.F., and Sepulveda, F.V. (2001). Modulation of the two-pore domain acid-sensitive K^+ channel TASK-2 (KCNK5) by changes in cell volume. The Journal of biological chemistry *276*, 43166-43174.

Nimigean, C.M., and Miller, C. (2002). Na^+ block and permeation in a K^+ channel of known structure. J Gen Physiol *120*, 323-335.

Noda, M., Shimizu, S., Tanabe, T., Takai, T., Kayano, T., Ikeda, T., Takahashi, H., Nakayama, H., Kanaoka, Y., Minamino, N.*, et al.* (1984). Primary structure of Electrophorus electricus sodium channel deduced from cDNA sequence. Nature *312*, 121-127.

Noulin, J.F., Brochiero, E., Coady, M.J., Laprade, R., and Lapointe, J.Y. (2001). Molecular identity and regulation of renal potassium channels. The Japanese journal of physiology *51*, 631-647.

Papazian, D.M., Schwarz, T.L., Tempel, B.L., Jan, Y.N., and Jan, L.Y. (1987). Cloning of genomic and complementary DNA from Shaker, a putative potassium channel gene from Drosophila. Science *237*, 749-753.

Pauli, J., Baldus, M., van Rossum, B., de Groot, H., and Oschkinat, H. (2001). Backbone and side-chain 13C and 15N signal assignments of the alpha-spectrin SH3 domain by magic angle spinning solid-state NMR at 17.6 Tesla. Chembiochem : a European journal of chemical biology *2*, 272-281.

Perozo, E., Cortes, D.M., and Cuello, L.G. (1998). Three-dimensional architecture and gating mechanism of a K+ channel studied by EPR spectroscopy. Nature structural biology *5*, 459-469.

Perozo, E., Cortes, D.M., and Cuello, L.G. (1999). Structural rearrangements underlying K^+ channel activation gating. Science *285*, 73-78.

References

___

Piasta, K.N., Theobald, D.L., and Miller, C. (2011). Potassium-selective block of barium permeation through single KcsA channels. J Gen Physiol *138*, 421-436.

Pluger, S., Faulhaber, J., Furstenau, M., Lohn, M., Waldschutz, R., Gollasch, M., Haller, H., Luft, F.C., Ehmke, H., and Pongs, O. (2000). Mice with disrupted BK channel beta1 subunit gene feature abnormal Ca^{2+} spark/STOC coupling and elevated blood pressure. Circulation research *87*, E53-60.

Pongs, O. (1999). Voltage-gated potassium channels: from hyperexcitability to excitement. FEBS Lett *452*, 31-35.

Pongs, O., Kecskemethy, N., Muller, R., Krah-Jentgens, I., Baumann, A., Kiltz, H.H., Canal, I., Llamazares, S., and Ferrus, A. (1988). Shaker encodes a family of putative potassium channel proteins in the nervous system of Drosophila. EMBO J *7*, 1087-1096.

Pongs, O., and Schwarz, J.R. (2010). Ancillary subunits associated with voltage-dependent K+ channels. Physiological reviews *90*, 755-796.

Raja, M. (2010a). The role of extramembranous cytoplasmic termini in assembly and stability of the tetrameric K^+ channel KcsA. The Journal of membrane biology *235*, 51-61.

Raja, M. (2010b). The role of phosphatidic acid and cardiolipin in stability of the tetrameric assembly of potassium channel KcsA. The Journal of membrane biology *234*, 235-240.

Raja, M. (2011). The potassium channel KcsA: a model protein in studying membrane protein oligomerization and stability of oligomeric assembly? Archives of biochemistry and biophysics *510*, 1-10.

Raja, M., Spelbrink, R.E., de Kruijff, B., and Killian, J.A. (2007). Phosphatidic acid plays a special role in stabilizing and folding of the tetrameric potassium channel KcsA. FEBS Lett *581*, 5715-5722.

Reid, J.D., Lukas, W., Shafaatian, R., Bertl, A., Scheurmann-Kettner, C., Guy, H.R., and North, R.A. (1996). The S. cerevisiae outwardly-rectifying potassium channel (DUK1) identifies a new family of channels with duplicated pore domains. Receptors & channels *4*, 51-62.

Remedi, M.S., and Koster, J.C. (2010). K(ATP) channelopathies in the pancreas. Pflugers Archiv : European journal of physiology *460*, 307-320.

Renault, M., Cukkemane, A., and Baldus, M. (2010). Solid-state NMR spectroscopy on complex biomolecules. Angew Chem Int Ed Engl *49*, 8346-8357.

Rotem, D., Mason, A., and Bayley, H. (2010). Inactivation of the KcsA potassium channel explored with heterotetramers. J Gen Physiol *135*, 29-42.

Sandhiya, S., and Dkhar, S.A. (2009). Potassium channels in health, disease & development of channel modulators. The Indian journal of medical research *129*, 223-232.

Schmidt, D., Jiang, Q.X., and MacKinnon, R. (2006). Phospholipids and the origin of cationic gating charges in voltage sensors. Nature *444*, 775-779.

Schmidt, D., and MacKinnon, R. (2008). Voltage-dependent K^+ channel gating and voltage sensor toxin sensitivity depend on the mechanical state of the lipid membrane. Proceedings of the National Academy of Sciences of the United States of America *105*, 19276-19281.

Schneider, R., Ader, C., Lange, A., Giller, K., Hornig, S., Pongs, O., Becker, S., and Baldus, M. (2008). Solid-state NMR spectroscopy applied to a chimeric potassium channel in lipid bilayers. Journal of the American Chemical Society *130*, 7427-7435.

Schrempf, H., Schmidt, O., Kummerlen, R., Hinnah, S., Muller, D., Betzler, M., Steinkamp, T., and Wagner, R. (1995). A prokaryotic potassium ion channel with two predicted transmembrane segments from Streptomyces lividans. EMBO J *14*, 5170-5178.

Seidel, K., Lange, A., Becker, S., Hughes, C.E., Heise, H., and Baldus, M. (2004). Protein solid-state NMR resonance assignments from (C-13, C-13) correlation spectroscopy. Physical Chemistry Chemical Physics *6*, 5090-5093.

Sheng, M., and Kim, E. (1996). Ion channel associated proteins. Current opinion in neurobiology *6*, 602-608.

Shieh, C.C., Coghlan, M., Sullivan, J.P., and Gopalakrishnan, M. (2000). Potassium channels: molecular defects, diseases, and therapeutic opportunities. Pharmacological reviews *52*, 557-594.

Sigworth, F.J., and Sine, S.M. (1987). Data transformations for improved display and fitting of single-channel dwell time histograms. Biophysical journal *52*, 1047-1054.

Singer-Lahat, D., Dascal, N., and Lotan, I. (1999). Modal behavior of the Kv1.1 channel conferred by the Kvbeta1.1 subunit and its regulation by dephosphorylation of Kv1.1. Pflugers Archiv : European journal of physiology *439*, 18-26.

Splitt, H., Meuser, D., Borovok, I., Betzler, M., and Schrempf, H. (2000). Pore mutations affecting tetrameric assembly and functioning of the potassium channel KcsA from Streptomyces lividans. FEBS Lett *472*, 83-87.

Stuhmer, W., Stocker, M., Sakmann, B., Seeburg, P., Baumann, A., Grupe, A., and Pongs, O. (1988). Potassium channels expressed from rat brain cDNA have delayed rectifier properties. FEBS Lett *242*, 199-206.

Thompson, A.N., Posson, D.J., Parsa, P.V., and Nimigean, C.M. (2008). Molecular mechanism of pH sensing in KcsA potassium channels. Proceedings of the National Academy of Sciences of the United States of America *105*, 6900-6905.

Tillman, T.S., and Cascio, M. (2003). Effects of membrane lipids on ion channel structure and function. Cell biochemistry and biophysics *38*, 161-190.

Uysal, S., Cuello, L.G., Cortes, D.M., Koide, S., Kossiakoff, A.A., and Perozo, E. (2011). Mechanism of activation gating in the full-length KcsA K^+ channel. Proceedings of the National Academy of Sciences of the United States of America *108*, 11896-11899.

References

_____

Uysal, S., Vasquez, V., Tereshko, V., Esaki, K., Fellouse, F.A., Sidhu, S.S., Koide, S., Perozo, E., and Kossiakoff, A. (2009). Crystal structure of full-length KcsA in its closed conformation. Proceedings of the National Academy of Sciences of the United States of America *106*, 6644-6649.

Valiyaveetil, F.I., Zhou, Y., and MacKinnon, R. (2002). Lipids in the structure, folding, and function of the KcsA K$^+$ channel. Biochemistry *41*, 10771-10777.

van Dalen, A., Hegger, S., Killian, J.A., and de Kruijff, B. (2002). Influence of lipids on membrane assembly and stability of the potassium channel KcsA. FEBS Lett *525*, 33-38.

van den Brink-van der Laan, E., Chupin, V., Killian, J.A., and de Kruijff, B. (2004a). Small alcohols destabilize the KcsA tetramer via their effect on the membrane lateral pressure. Biochemistry *43*, 5937-5942.

van den Brink-van der Laan, E., Chupin, V., Killian, J.A., and de Kruijff, B. (2004b). Stability of KcsA tetramer depends on membrane lateral pressure. Biochemistry *43*, 4240-4250.

Wang, Z.W., Kunkel, M.T., Wei, A., Butler, A., and Salkoff, L. (1999). Genomic organization of nematode 4TM K+ channels. Annals of the New York Academy of Sciences *868*, 286-303.

Watanabe, S., Hoffman, D.A., Migliore, M., and Johnston, D. (2002). Dendritic K$^+$ channels contribute to spike-timing dependent long-term potentiation in hippocampal pyramidal neurons. Proceedings of the National Academy of Sciences of the United States of America *99*, 8366-8371.

Weingarth, M., Demco, D.E., Bodenhausen, G., and Tekely, P. (2009). Improved magnetization transfer in solid-state NMR with fast magic angle spinning. Chem Phys Lett *469*, 342-348.

Weinreich, F., and Jentsch, T.J. (2000). Neurological diseases caused by ion-channel mutations. Current opinion in neurobiology *10*, 409-415.

Xia, X., Fakler, B., Rivard, A., Wayman, G., Johnson-Pais, T., Keen, J., Ishii, T., Hirschberg, B., Bond, C., Lutsenko, S.*, et al.* (1998). Mechanism of calcium gating in small-conductance calcium-activated potassium channels. Nature *395*, 503-510.

Xu, Y., Ramu, Y., and Lu, Z. (2008). Removal of phospho-head groups of membrane lipids immobilizes voltage sensors of K+ channels. Nature *451*, 826-829.

Zachariae, U., Schneider, R., Velisetty, P., Lange, A., Seeliger, D., Wacker, S.J., Karimi-Nejad, Y., Vriend, G., Becker, S., Pongs, O.*, et al.* (2008). The molecular mechanism of toxin-induced conformational changes in a potassium channel: relation to C-type inactivation. Structure *16*, 747-754.

Zhang, X.H., Zhang, Y.Y., Sun, H.Y., Jin, M.W., and Li, G.R. (2012). Functional ion channels and cell proliferation in 3T3-L1 preadipocytes. Journal of cellular physiology *227*, 1972-1979.

Zhou, M., Morais-Cabral, J.H., Mann, S., and MacKinnon, R. (2001a). Potassium channel receptor site for the inactivation gate and quaternary amine inhibitors. Nature *411*, 657-661.

_____

Zhou, X., Vaillant, B., Loukin, S., Kung, C., and Saimi, Y. (1995). YKC1 encodes the depolarization-activated K$^+$ channel in the plasma membrane of yeast. FEBS letters *373*, 170-176.

Zhou, Y., and MacKinnon, R. (2003). The occupancy of ions in the K$^+$ selectivity filter: charge balance and coupling of ion binding to a protein conformational change underlie high conduction rates. Journal of molecular biology *333*, 965-975.

Zhou, Y., Morais-Cabral, J.H., Kaufman, A., and MacKinnon, R. (2001b). Chemistry of ion coordination and hydration revealed by a K$^+$ channel-Fab complex at 2.0 A resolution. Nature *414*, 43-48.

Zimmerberg, J., and Gawrisch, K. (2006). The physical chemistry of biological membranes. Nature chemical biology *2*, 564-567.

7. Appendix

7.1. Sequence alignment of KcsA and KcsA-K$_v$1.3 channels

Figure 7.1. Sequence alignment of KcsA and KcsA-K$_v$1.3 channels. Gray boxes and lines above the alignment indicate the membrane topology of the channels. NTD - N-terminal cytoplasmic domain; TM1 - outer helix; P-loop - pore loop; TM2 - inner helix; CTD - C-terminal cytoplasmic domain. Selectivity filter residues are indicated in blue. Amino acid substitutions in KcsA-Kv1.3 are shown in red.

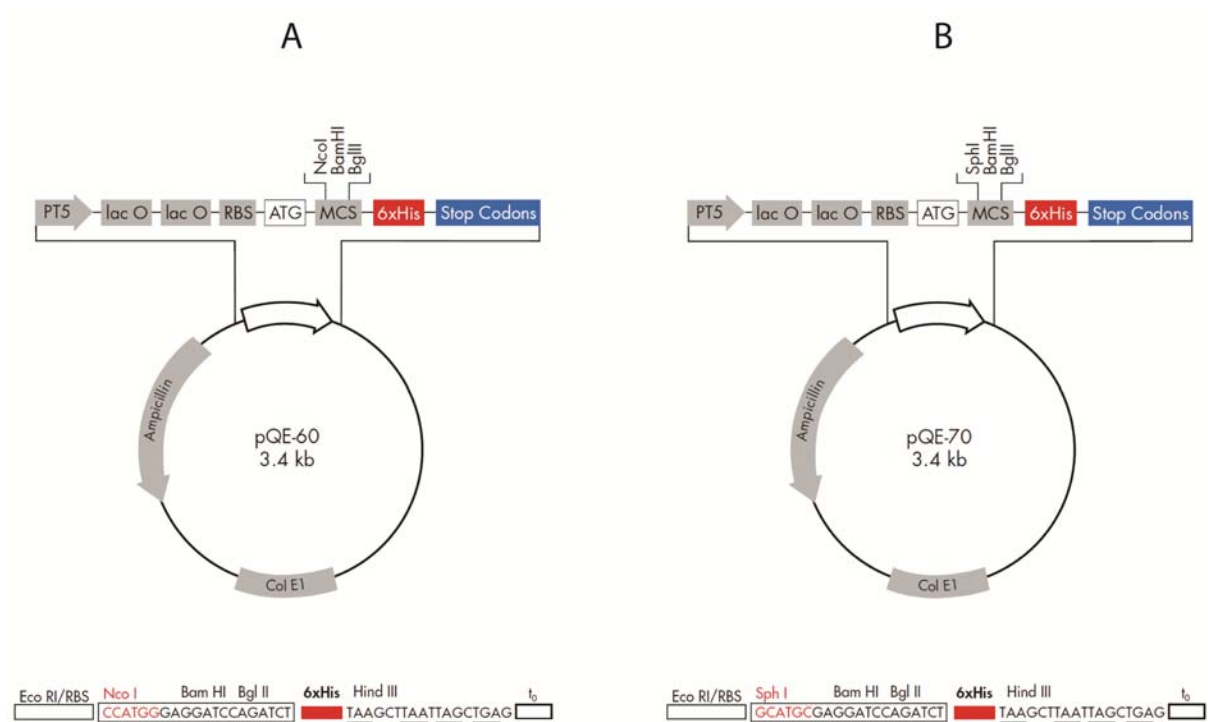## 7.2. Expression vectors used for the protein expression

Figure 7.2. pQE vectors used for protein expression. A - pQE60 vector used for the expression of KcsA. **B** - pQE70 vector used for the expression of KcsA and KcsA-K_v1.3. PT5 - T5 promoter; lac O - lac operon; RBS - ribosome binding site; ATG - start codon; 6xHis - His tag sequence; MCS - multiple cloning sites (restriction recognition sites are shown); Col E1 - Col E1 origin of replication; Ampicillin - ampicillin resistance gene; t_0 - lambda t_0 transcriptional termination region. This figure is adapted from Qiagen handbook for protein expression and purification.

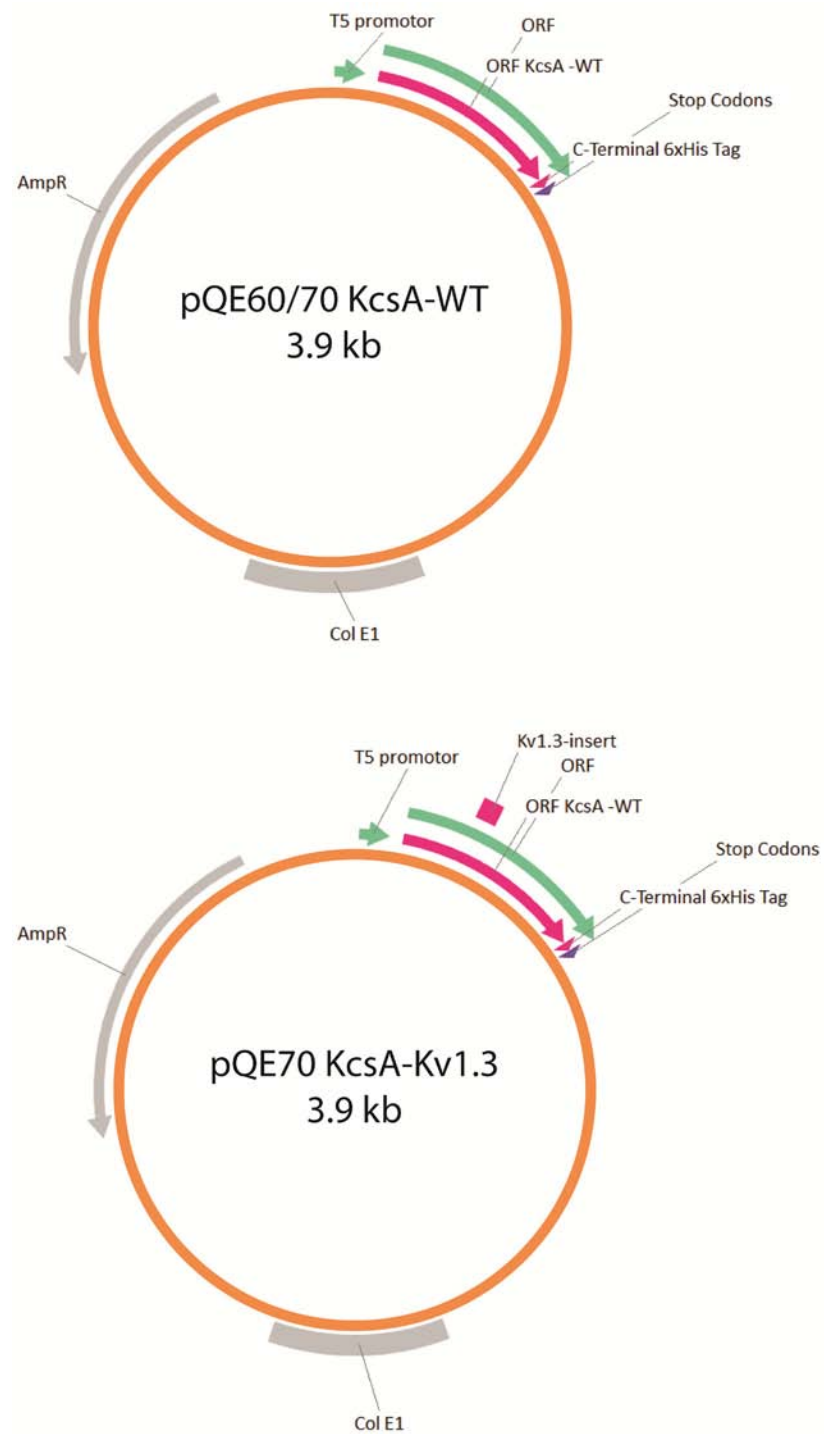_____

7.3. Clone cards of used plasmids

Figure 7.3. Clone cards of plasmids for KcsA and KcsA-K$_v$1.3 expression. ORF - open reading frame; AmpR - ampicillin resistance gene; Col E1 - Col E1 origin of replication.

_____

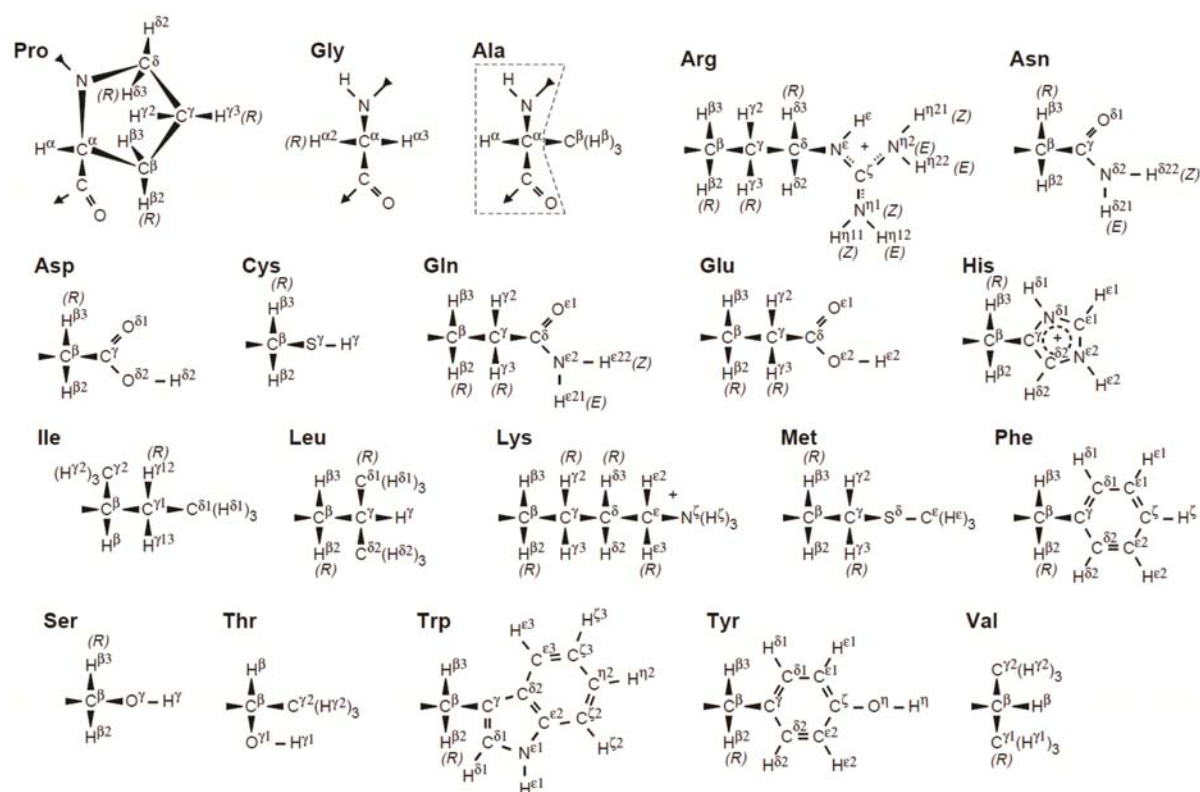## 7.4. The atom-naming conventions recommended for proteins by IUPAC

Figure 7.4. The atom-naming conventions recommended for proteins by IUPAC-IUB Commission on Biochemical Nomenclature. Atom identifiers for the amino acids follow the 1969 IUPAC-IUB guidelines. The Greek letters may be replaced by upper case Roman letters: α = A, β = B, γ = G, δ = D, ε = E, ζ = Z, η = H (*Markley et al., 1998*).

8. Abbreviations

τ	time constant
Å	Angstrom
Amp	ampicillin
B	magnetic field
BSA	bovine serum albumin
ºC	degrees Celsius
CGMD	Coarse Grain Molecular Dynamics
cm	centimeter
CP	cross polarization
Da	Dalton
DM	n-Decyl-β-D-Maltopyranoside
DNA	deoxyribonucleic acid
DNase	deoxyribonuclease
E.coli	*Escherichia coli*
EDTA	ethylenediaminetetraacetic acid
e.g.	for example
EPR	Electron Paramagnetic Resonance
g	gram (g-force)
h	hours
HEPES	4-(2-hydroxyethyl)-1-piperazineethanesulfonic acid
His	histidine
Hz	Hertz
I	current
i.e.	that is
IPTG	Isopropyl β-D-thiogalactopyranoside
K	Kelvin
k	kilo-
Kan	kanamycin
kDa	kilodalton
kHz	kilohertz
l	liter
LB	Luria-Bertani
m	meter
M	Molar
MES	2-(*N*-morpholino)ethanesulfonic acid
ml	milliliter
µg	microgram
µl	microliter
µM	micromole
µm	micrometer
µs	microsecond

MAS	Magic Angle Spinning
mg	milligram
MHz	megahertz
min	minute
mM	millimole
MΩ	megaohm
MP	membrane protein
ms	millisecond
M_W	molecular weight
nA	nanoampere
NaP	sodium phosphate
ng	nanogram
nm	nanometer
NMR	Nuclear Magnetic Resonance
OD	optical density
pA	pico ampere
PARIS	phase-alternated recoupling irradiation scheme
PAGE	polyacrylamide gel electrophoresis
PDSD	Proton Driven Spin Diffusion
P_O	open probability
pS	picosiemens
psi	pound-force per square inch
R_f	feedback resistance
RPM	revolutions per minute
s	seconds
s.e.m.	standard error of the mean
SB	Super Broth
SDS	sodium dodecyl sulfate
SsNMR	Solid-state Nuclear Magnetic Resonance
std	standard deviation
T	temperature
TEA	tetraethylammonium
TM	transmembrane
UV	ultraviolet
V	voltage
v/v	volume by volume
WT	wild type

Abbreviations for Amino acid residues

Alanine	A	Ala
Arginine	R	Arg
Asparagine	N	Asn
Aspartic acid	D	Asp
Cysteine	C	Cys
Glutamic acid	E	Glu
Glutamine	Q	Gln
Glycine	G	Gly
Histidine	H	His
Isoleucine	I	Ile
Leucine	L	Leu
Lysine	K	Lys
Methionine	M	Met
Phenylalanine	F	Phe
Proline	P	Pro
Serine	S	Ser
Threonine	T	Thr
Tryptophan	W	Trp
Tyrosine	Y	Tyr
Valine	V	Val

Acknowledgements

I would like to express my sincere gratitude to Prof. Olaf Pongs for giving me the great opportunity to work in his research group. His supervision and guidance during my PhD study were essential to the success of the project. It was an honor and a privilege to study under his tutelage.

I thank Prof. Marc Baldus for providing me an opportunity to carry out part of my PhD study in his NMR Spectroscopy Research Group, and for the additional insight provided by our collaboration.

I would like also to thank Dr. Vitya Vardanyan (ZMNH, Hamburg) for his great help with many aspects of electrophysiology and molecular biology. I am grateful to Prof. Jürgen Schwarz (ZMNH, Hamburg) and Dr. Sönke Hornig (ZMNH, Hamburg) for their help with electrophysiological questions and engaging scientific discussions. I thank Iris Ohmert (ZMNH, Hamburg) for her help in molecular biology methods.

I would like to thank Elwin A. W. van der Cruijsen (MSc), Dr. Markus Weingarth, Dr. Abhishek Cukkemane and Dr. Deepak Nand from NMR Spectroscopy Research Group for their active participation in my PhD project, their help with ssNMR experiments and for corrections of my PhD thesis. My special thanks to Dr. Markus Weingarth for performing MD simulations.

I would like to sincerely thank my co-adviser Prof. Christian Lohr for reviewing my thesis. I am grateful to Prof. Jörg Fromm, Prof. Stefan Hoth and Prof. Jürgen Schwarz who agreed to participate in the official defense of my PhD thesis.

A particular thank you to Dr. Lindsay Baker for the time dedicated to reading and correcting this thesis as a native English speaker.

I would like to thank Dr. Irm Hermans-Borgmeyer and Dr. Sabine Hoffmeister-Ullerich for providing me an opportunity to take part in the Graduate Study Program in Molecular Biology (Aufbaustudium Molekularbiologie) at ZMNH.

Many thanks to all of my colleagues in the Institute of Neural Signal Transduction (ZMNH, Hamburg, Germany): Vitya Vardanyan, Christian Mayer, Iris Ohmert,